KU LEUVEN

FACULTY OF SCIENCE

Evolving Biofilm Communities

Insights into Biofilm Evolutionary Dynamics and Ecological Succession through Adhesion Modeling

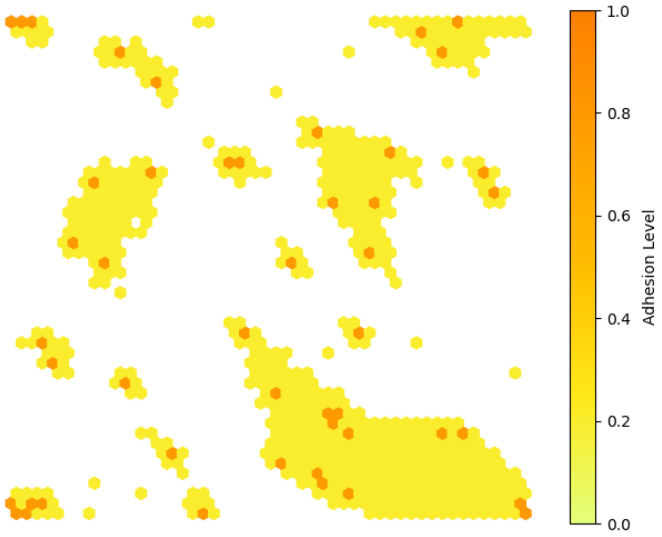

Nele GORISSEN

Thesis presented in
fulfillment of the requirements
for the degree of Master of Science
in Biology

Supervisor: Prof. P. van den Berg
KU Leuven, Research Group Evolutionary Modelling

Mentor: Alger Jorritsma
KU Leuven, Research Group Evolutionary Modelling

Academic year 2023-2024

Preface

In this thesis, I will introduce you to a field in full development: that of bacterial life cycles. Formerly, bacterial research focused on planktonic cells, yet the key to unraveling many ecological enigmas may be studying biofilm colonies instead. However, empirically investigating the fate of these cell conjunctions is challenging. By evolutionary modeling biofilm systems, we hope to shed light on the eco-evolutionary dynamics at play. As such, my personal goals for this work were two-sided. Firstly, I aimed to develop my modeling skills. As I was relatively new to programming, this came with challenges and, hence, with many growth opportunities for which I am grateful. My second personal goal was to become a better scientist and practice doing research in evolutionary biology. Conceptualizing the questions that had remained unanswered after a thorough literature review and molding them into a computational model helped me to gain a deeper understanding of biofilm communities and how their members interact. The main concepts discussed in this work include 1. the interaction of ecotypes and how they influence the niche, 2. stable coexistence and invasilibity of ecotypes, 3. diversity and priority effects, 4. system cyclicity and phenotypic plasticity, and 5. environmental instability and risk spreading. Puzzling the pieces of evolution and ecology together into a system has also fed my enthusiasm to delve further into theoretical biology. Related to this, I appreciate the learning opportunities I enjoyed in the evolutionary modeling lab. I would like to thank Alger Jorritsma for always making time to teach and guide me along the way. I am also grateful for the input and feedback provided by Prof. Piet van den Berg. Lastly, I would like to express my gratitude to the people close to me who have shown great support and to you as a reader; I hope you have a pleasant experience reading this.

Contribution statement

The idea for this thesis was developed and turned into a feasible plan by Alger Jorritsma and Nele Gorissen with the guidance of Prof. Piet van den Berg. Alger Jorritsma created the backbone of the model and provided daily supervision. Nele Gorissen performed the rest of the modeling, analyzed the data, and made the figures. Moreover, Nele Gorissen wrote the thesis with input and feedback from Alger Jorritsma and Prof. Piet van den Berg. Generative AI was used to solve coding errors.

Summary - English

Bacteria can grow planktonically or in a matrix-encased population, called a biofilm. They are typically attached to substrates or interfaces but can also be found solely in association with other cells. These communities can be surprisingly biodiverse, often formed by multiple species or even members of different domains (e.g., Archaea or Fungi). Despite being first described centuries ago, the predominance of biofilms has only gained recognition in the last fifty years. Hence, research on bacterial biofilm functioning lags in the scientific community. Yet, biofilms are a burden for society both in terms of health hazards and economic costs (mostly due to corrosion). They are especially persistent since the matrix provides an environment that is well-protected against antibiotics and removal products, such as antifouling. Therefore, bacteria can chronically infect all sorts of tissues and instruments. In contrast, when local conditions are unfavorable, bacteria can detach or form spores to initiate a biofilm elsewhere. As such, flexible attachment and detachment form the central aspects of the biofilm lifecycle.

To study this in more depth, we developed an individual-based model tracking the evolutionary dynamics of adhesion during ecological succession. Our first objective was to gain a deeper understanding of the characteristics of colonizers and successor ecotypes and how they interact with each other. That is brought into the bigger picture of eco-evolutionary dynamics shaping niches and cell traits. Secondly, we aimed to determine what ecotypes can coexist and towards which steady state the trait will converge. To this end, we performed an invasion analysis. Our third objective was to understand how demographic variables influence population dynamics. We analyzed this by quantifying the effect of surface growth rate, carrying capacity, and initial bulk population size on population diversification. Another goal of this study was to find how system cyclicity - an inherent aspect of succession - and phenotypic plasticity affect trait distribution, and temporal and spatial dynamics. Here, we included nutrient depletion as the driver of substrate renewal. Population sizes and nutrient levels were added as the environmental cues propelling the evolution of plasticity. Our last aim was to attain foundational insights into the impact of environmental instability on the trait distributions of adhesion and plasticity. To distinguish different types of stressors, we opted for a predictable change (i.e., varying initial resource levels to manipulate surface turnover indirectly) and chaotic fluctuations (i.e., disruption events where all cells are killed abruptly). The former can be mitigated by monitoring nutrient levels and reacting plastically, whereas the latter is unforeseeable.

To summarize, we found that highly adhesive cells are vital in the colonization stage, after which they gradually become swarmed and replaced by less adhesive individuals. That is, only highly adhesive cells have a high probability of remaining attached to an empty surface. From this point on, colonizers function as anchors for less adhesive cells to stick to, and as such, niches for successors are created. In other words, colonizers facilitate the rise of successors. In contrast, the first successors only manage to adhere to spots adjacent to colonizers, which imposes a severe growth limitation on the latter. Weakly adhesive cells also show faster growth, and consequently, the surface is rapidly covered by successors. Note, however, that the specific nature of interactions between two ecotypes depends on the adhesion levels of each. Yet, as we wanted to work towards a system with continuous trait levels, dynamics found among ecotypes with a discrete characterization are only discussed briefly. Instead, we continued by determining the evolutionarily stable strategy and running tests on the continuous model. We found that an adhesion level of around 0.225 was evolutionarily the optimal strategy. Moreover, we observed that diversity is influenced by the studied demographic parameters. This marks the importance of priority effects in models investigating ecological succession. When incorporating cyclicity, we found less inter-niche differentiation as colonizers from the bulk continuously reinitiate biofilm development. Furthermore, plasticity in response to population sizes and nutrient levels was preserved after 50000 generations of evolution. When demographics were perceivable, genetic adhesion was lost in the population. High surface turnover seemed to increase sensitivity to surface coverage as an environmental cue, while the plastic response to nutrient levels weakened. Importantly, when introducing high stress in the form of disruptions, populations adjusted their strategy: alleles encoding varying levels of adhesion became fixated in the population, while sensitivity to surface cues decreased due to unreliability.

Samenvatting - Nederlands

Bacteriën groeien zowel planktonisch als sessiel, in gemeenschap met andere. Samen vormen ze namelijk een biofilm, verenigd door een verstevigende matrix. Meestal zijn biofilms gebonden aan een oppervlak of scheidingsvlak, maar ook onthechte kolonies kunnen voorkomen. De biofilm gemeenschap kan verrassend biodivers zijn. Zo kan ze vertegenwoordigd worden door meerdere soorten. Ook leden van andere domeinen (bijvoorbeeld Archaea of Fungi) kunnen hun plaats vinden in de biofilm. Ondanks het feit dat ze reeds eeuwen geleden voor het eerst wetenschappelijk beschreven werden, worden ze slechts de laatste vijftig jaar erkend als een dominante levensvorm. Dat verklaart mede waarom wetenschappelijk onderzoek naar het functioneren van biofilms achterloopt. Nochtans is het belangrijk om biofilms te bestuderen, aangezien ze een zware last voor de maatschappij vormen, zowel op economisch vlak (voornamelijk ten gevolge van corrosie) als in de medische sector. Biofilms zijn zeer persistent. De matrix voorziet hen immers van een omgeving die antibiotica en verwijderingsproducten zoals ‘antifouling’ vaak succesvol afweert. Op die manier slagen bacteriën er dikwijls in om allerlei weefsels en materiaal chronisch te besmetten. Wanneer de condities ongunstig worden, daarentegen, kunnen bacteriën losbreken of sporen vormen om elders een nieuwe biofilm te starten. Dat illustreert het belang van flexibiliteit in het aanhechten en ontkoppelen als centrale aspecten van de biofilm-levenscyclus.

Om dit onderwerp in meer detail te bestuderen, ontwikkelden we een agent-gebaseerd model dat de evolutionaire dynamieken van adhesie volgt tijdens ecologische successie. Ons eerste doel was om de kenmerken van kolonisatoren en opvolgers, en hun manier van interageren met elkaar op te helderen. Dat wordt gelinkt aan de eco-evolutionaire dynamieken die typerend zijn voor zowel de celeigenschappen als de beklede niches. Vervolgens wilden we onderzoeken welke ecotypes naast elkaar kunnen evolueren op langere tijdschalen, en welke strategie evolutionair stabiel zou zijn. Om dit te bestuderen werd een invasie-analyse uitgevoerd. Het derde doel was om te begrijpen hoe demografische variabelen de gemeenschapsstructuur zouden beïnvloeden. We onderzochten dit door het effect van de groeisnelheid op het oppervlak, de draagkracht van de bulk, en de initiële bulk populatiegrootte op de biodiversiteit in de populatie te bepalen. Een volgende doelstelling was het begrijpen van de invloed van cycliciteit – hetgeen een inherent aspect is van ecologische successie – en fenotypische plasticiteit op de distributie van celeigenschappen. Ook de ruimtelijke en temporele dynamieken werden nagegaan. In het cyclische systeem kondigt de geleidelijke afname van nutriënten oppervlaktevernieuwing aan. Nutriëntenniveaus kunnen dus als omgevingssignaal dienen om een plastische respons uit te lokken, waarbij het adhesieve karakter van de cel wordt afgestemd op de omgeving. Daarnaast kunnen cellen ook sensitiviteit

ontwikkelen ten opzichte van populatiegroottes. Ten laatste wilden we de effecten van omgevingsverandering op distributie van adhesie en plasticiteit uiteenzetten. Om het type stressor te onderscheiden maakten we gebruik van een voorspelbare verandering (verschillende gradaties in nutriëntenrijkdom, hetgeen oppervlaktevernieuwing indirect manipuleert), en chaotische fluctuaties (disrupties waarbij alle cellen plots sterven). Schade ten gevolge van het eerste kan voorkomen worden door nutriëntenniveaus te controleren, terwijl het laatste onvoorspelbaar is.

Samengevat bevonden we dat sterk adhesieve cellen cruciaal zijn tijdens de kolonisatieperiode, waarna ze geleidelijk omsingeld en vervangen worden door minder adhesieve individuen. Meer bepaald, enkel sterk adhesieve cellen hebben een hoge kans om aan een leeg oppervlak gehecht te blijven. Eens vastgehecht, functioneren kolonisatoren als ankers voor minder adhesieve cellen. Bijgevolg creëren ze niches voor opvolgers. Met andere woorden, kolonisatoren faciliteren de opkomst van opvolgers. De eerste opvolgers kunnen zich echter enkel rondom de kolonisatoren vestigen, waardoor ze diens groei belemmeren. Bovendien groeien adhesieve cellen sneller, waardoor het oppervlak snel door opvolgers wordt overgenomen. Merk daarbij op dat de specifieke interacties tussen twee ecotypes afhankelijk zijn van ieders adhesieniveau. Echter, aangezien deze studie naar een systeem met continue adhesieniveaus toewerkt, worden dynamieken tussen ecotypes met discrete kenmerken slechts beknopt besproken. In plaats daarvan vervolgden we onze studie met de bepaling van de evolutionair stabiele staat en met testen op een systeem met continue adhesieniveaus. We bevonden dat een adhesieniveau rond 0.225 evolutionair gezien de optimale strategie is. Daarnaast observeerden we dat de diversiteit in de gemeenschap beïnvloed wordt door de bestudeerde demografische parameters. De resultaten onderstrepen het belang van prioriteitseffecten in modellen waarin ecologische successie verwerkt zit. Wanneer ook cycliciteit werd geïncorporeerd in de simulaties, stelden we vast dat inter-niche differentiatie verminderde, aangezien de biofilm steeds hernieuwd werd door stichters uit de bulkruimte. We constateerden ook dat plasticiteit als een reactie op populatiegrootte en nutriëntenniveaus niet verloren was gegaan na 50000 generaties. Wanneer de demografische variabelen waarneembaar waren voor de populatie, ging genetische adhesie verloren. Bovendien veranderde de populatie van strategie wanneer de populatie werd getroffen door disrupties. In dat geval werd een grote variëteit aan adhesieniveaus gefixeerd in de populatie, terwijl de gevoeligheid ten opzichte van omgevingssignalen komende van het oppervlak afnam. De effecten van oppervlakhernieuwing waren minder éénduidig.

List of abbreviations

AIC	Akaike's information criterion
c-di-GMP	cyclic diguanylate / cyclic di-GMP (i.e., guanosine monophosphate)
CI	confidence interval
ESS	evolutionarily stable strategy
PIP	pairwise invasibility plot

Table of contents

Introduction

Biofilm research

Since the first description of biofilms by Van Leeuwenhoek in the seventeenth century, the so-called animalcules have been examined diligently (Donlan & Costeron, 2002; Lane, 2015; McCarty et al., 2014). However, it was not until 1978 that the theory of biofilm predominance was advanced (Costeron et al., 1978). Even today, we often rely on extrapolated data from single-species laboratory cultures of planktonic cells when studying bacterial assemblages (Costeron et al., 1995). Yet, their sessile counterparts residing in multi-species biofilms play the lead in nearly all ecosystems except deep groundwater and abyssal oceans. In nutrient-rich aquatic ecosystems, over 99.9 % of the bacteria are estimated to grow in biofilms (Costeron et al., 1995; Geesey et al., 1978). Much like a forest constitutes a complex web of interacting species, biofilms are diverse ecosystems of matrix-enclosed micro-organisms attached to a substratum, interface, or each other (Costeron et al., 1995; Donlan & Costeron, 2002). Cross-linking effects between cells and between matrix components protect the biofilm against erosion (Klotz et al., 2019). The stability derived from living in a supportive population may, thus, have allowed prokaryotes to thrive in early Earth's hostile environments and to adapt to changing conditions. Indeed, the first fossil records of biofilm development date around 3.25 billion years back and include evidence for the prevalence of the growth form in a broad spectrum of species across Archaea and Bacteria domains (Hall-Stoodly et al., 2004).

Aside from being resilient, the flexibility of biofilm growth plays a central role in its existence. That is, cells can react to changing conditions by allocating energy to dispersal or growth. The interchange of planktonic and sessile life stages is mediated by species-specific environmental cues, ranging from nutrient availability to pH, osmolarity, and host factors, which activate regulatory circuits involved in biofilm development (reviewed by O'Toole et al., 2000 and Petrova & Sauer, 2012). Once a new habitat is colonized, proteins, intercellular signaling systems (e.g., quorum sensing), and regulating second messengers (e.g., c-di-GMP) drive the dynamic processes involved in the establishment of biofilms (Alotaibi, 2021). This ability to disperse and colonize new territories in response to specific stimuli underpins their success across countless settings (Costeron et al., 1995). Probably most notoriously, biofilms are associated with device-related and other chronic infections (Donlan & Costeron, 2002). Biofilm infections are typically a more severe threat compared to infections with planktonic pathogens due to the associated resilience against the host's immune system and medication. When unsuccessfully treated, infections cause chronic inflammation, indirectly offsetting the immune system and increasing the risk for numerous conditions such as cancer and heart disorders. Jointly, these chronic inflammatory diseases are the most

frequently occurring cause of death (Pahwa, 2023; Vestby et al., 2020). Biofilm research thus not only serves to strengthen our fundamental understanding of micro-organisms but also aids in strategy development to combat harmful outcomes in medical and industrial settings (Cámara et al., 2022; Donlan & Costeron, 2002; Galié et al., 2018).

The biofilm model

Biofilm development was formerly described as merely the grouping and attachment of bacterial cells. Presently, however, a growing body of research highlights both the dynamical behavior and the sophisticated composition exhibited by biofilms, ultimately revealing their role as a cornerstone of prokaryotic life history (Hall-Stoodly et al., 2004; Kostakioti et al., 2013). Yet, to conceptualize these dynamics, the biofilm life cycle is most famously presented in the 5-step model. That starts with the reversible attachment of planktonic cells that later attach irreversibly and go through maturation phases I and II to eventually disperse again as planktonic cells. This alternating cycle - of cells physiologically transitioning from free-living to attached cells and vice versa - is then reiterated (Berlanga & Guerrero, 2016; McDougald et al., 2012; Sauer et al., 2002; Figure 1.A). Note, however, that this model is restricting in terms of cell aggregation and detachment strategies, structural heterogeneity, and ecological succession. Therefore, Sauer et al., 2022 proposed a more inclusive 3-step model (Figure 1.B). Here, biofilms can be formed on a surface or in aggregation, and there is cell exchange between both growing mechanisms (Sauer et al., 2022). Also, the influx of new cells is included in the growth and accumulation phase. As such, *in vivo, in vitro,* and *in situ* biofilms can be described by this three-step model, regardless of their specific growing conditions and environment.

A world of difference

The biofilm life cycle is characterized by a pattern of shifts in growth rates and varying regulation of gene transcription (Donlan & Costeron, 2002). For instance, during the sessile stages, bacteria often show decreased metabolic activity and an upregulation of genes required for anaerobic growth (Li et al., 2014; Wan et al., 2018). Many stage transitions, e.g., biofilm formation, metabolic activity, and virulence, are directed by cell-to-cell communication or quorum sensing (Preda & Săndulescu, 2019). That all amounts to several apparent disparities between planktonic and sessile cells. Comparably to the dissemination processes in eukaryotes, the free-living bacteria are cyclically shed to colonize new sites but have lower survival rates (Costeron et al., 1995). The latter, on the other hand, can better resist (i.e., specific defense) attacks by the immune system (Jensen et al., 2010), disinfectants, or antibiotics due to increased production of protectants (e.g., chromosomal beta-lactamase or modified lipopolysaccharides) (Høiby et al., 2011). Moreover, they show increased tolerance (i.e., non-specific defense) for these stresses

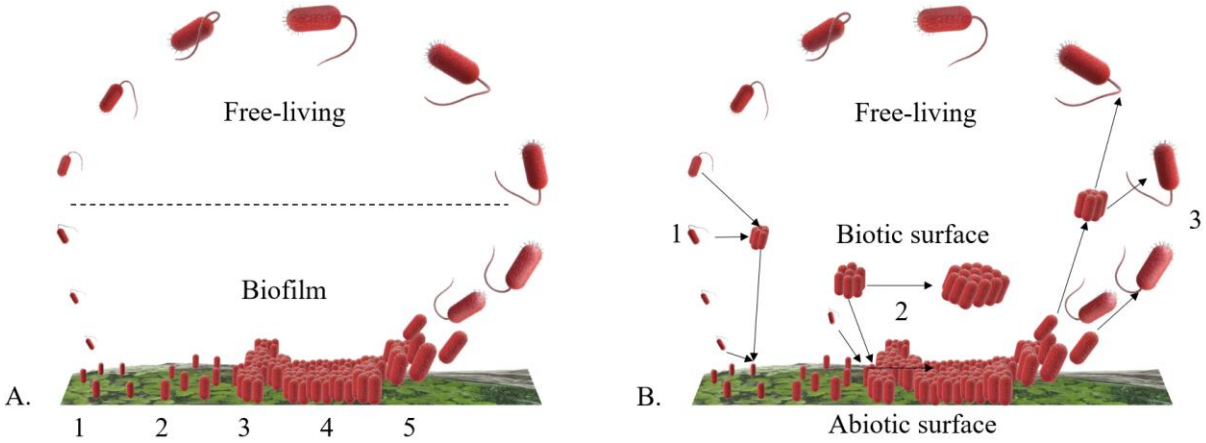

Figure 1: Systematic representation of the biofilm life cycle. A. The 5-step model is characterized by a free-living phase and five steps of biofilm formation (1: reversible attachment; 2: irreversible attachment; 3: maturation phase I; 4: mutation phase II; 5: dispersal). B. In addition, the 3-step model incorporates influx of individual cells at later stages, biofilm growth in aggregates (i.e., biotic surface), and exchange between biofilms formed on biotic and abiotic surfaces. The main steps include 1: aggregation to a biotic surface or attachment to an abiotic surface; 2: growth; 3: disaggregation from other cells or detachment from the surface.

resulting from matrix-mediated binding and because of the slower diffusion of drugs and the reduced metabolic rate in the inner biofilm layers (Høiby et al., 2011). In other words, biofilm cells are embedded in a defensive matrix that offers a form of safety renounced by planktonic cells (Costeron et al., 1995).

Biofilm composition and ecology

The encasing matrix is formed with extracellular polymeric substances (EPS), which are mainly composed of polysaccharides, proteins, and eDNA, forming a gel-like substance that retains high amounts of water (Flemming et al., 2007; Flemming & Wingender, 2010). Voids within the biofilm, possibly created by grazing protozoa, may enable liquid transport (McCarty et al., 2014; Wilking et al., 2013). As such, cells, nutrients, and oxygen can move through the water channels via simple diffusion, further nurturing the notion of a rudimentary circulation system in biofilms (Patel, 2005; Vasudevan, 2014). Evaporation from the surface may be a driving factor of the liquid flux, which again emphasizes the similarities with multicellular organisms, such as plants (Gelderblom et al., 2022; Patel, 2005; Wilking et al., 2013). The voids could also function as reservoirs of genes, enabling genetic exchange (McCarty et al., 2014). The functions of the biofilm matrix are manifold. Firstly, it extends the entropy gradient in space (Penesyan et al., 2021) and shields the cells against protozoan grazing, desiccation, chemicals, and abiotic fluctuations in the bulk phase (Costeron et al., 1995; Flemming et al., 2016; Matz & Kjelleberg, 2005; Ophir & Gutnick, 1994). Furthermore, the biofilm architecture forms a skeleton that allows

cells to pile up in mountain or mushroom-like structures, resulting in a structurally and functionally heterogeneous landscape of highly organized microcolonies (Costeron et al., 1995; Donlan & Costeron, 2002; Flemming et al., 2016; Lewandowski, 2000). The matrix also enhances digestive capacity, facilitates the development of steep gradients and high biodiversity, and promotes intercellular interactions (Flemming et al., 2016; Flemming & Wingender, 2010).

Drivers of diversification

Biofilms exhibit high diversification, both on a genotypic and a phenotypic level. Firstly, empirical evidence has found that mutation rates are increased in biofilm cells (Coenye et al., 2022). Under stress, both the horizontal gene transfer and the mutation rates rise, thus resulting in higher adaptation speed (Steenackers et al., 2016). The combined effects of the latter two and the decreased entropy gradient facilitate the formation of biodiversity hotspots, also labeled as diversity incubators by Penesyan et al. (2021). They state that the protective environment allows the population to generate a wide array of genetic variants before facing the filter of natural selection. In comparison, Costeron et al. suggested that a large part of this diversity is the result of nongenetic variation between cells closely matching their specific microenvironment within the biofilm through phenotypic plasticity (1995). Another mechanism by which a population of genetically identical cells can achieve phenotypic diversity is the stochastic pulsing of gene expression. Here, a low concentration of transcriptional regulators allows for their pulsed activity, where binding and release from the binding sites become probabilistic (Nijhout, 2013). Nadezhdin et al. have shown that stochastic gene expression strongly influences spatial patterns during biofilm formation (2020).

The advantages of increased variability in biofilms may be multifaceted. For instance, in environments where the optimal phenotype changes unpredictably, maintaining a diverse array of phenotypes in the population broadens the fitness landscape by insurance effects (Frank, 2011; Steenackers et al., 2016). This risk-spreading strategy is called bet-hedging (Morawska et al., 2021). Apart from the mechanisms driving diversification, a wide spectrum of ecological and evolutionary processes has been put forward as potential causes thereof (extensively reviewed by Steenackers et al., 2016). Here, we exclusively elaborate on the role of niche partitioning and modification.

Niche partitioning and diversification

Niche partitioning is the process in which natural selection causes the evolutionary paths of competitors to diverge (MacArthur, 1958). Individuals can, subsequently, coexist by specializing in distinct patch types (Bazzaz & Catovsky, 2001). Hence, this division of niches is associated with increased cooperation between ecotypes and enriched productivity (Brockhurst et al., 2006; Ellis et al., 2015). Importantly, niche partitioning relies on the environmental variation shaped by spatial and temporal

heterogeneity. Negative frequency-dependent selection (NFDS) can then promote the maintenance of genetic diversity by favoring rare genotypes, and thus, it stabilizes the coexistence of competitors. In the following, I will dissect how niche partitioning is interconnected with these three concepts.

Firstly, the degree of spatial heterogeneity sets a foundation for determining the number of obtainable niches. As previously discussed, the intrinsic properties of biofilm architecture lead to the development of environmental gradients (Flemming et al., 2016). This gradual spatial heterogeneity allows the bridging of adjacent fitness peaks, as molecular evolution can occur in small steps (Steenackers et al., 2016). Moreover, a study conducted by Fowler et al. showed that biofilm thickness affects population assembly and phylogenetic diversity (2023). More concretely, deterministic population assembly processes may be more pronounced in thin biofilms due to shear stress at the surface. Conversely, thick biofilms expose higher degrees of diversity, which may be due to drift and reduced gene flow, leading to stochastic historical contingency. An alternative explanation for the positive volume-diversity relationship is that environmental heterogeneity may cause more variable selection regimes (Fowler et al., 2023). In addition, Vallespir & Ursell studied how structural anisotropy affects population dynamics in microbial populations (2019). They found that environmental structure may facilitate the coexistence of two competing species by securing competition interfaces, whereas it may impede the stability of intransitive cycles of three species (Vallespir & Ursell, 2019), thus leading to an increase or decrease in diversity, respectively. Also, classic niche theory predicts that the relationship between spatial heterogeneity and diversity is strictly positive. However, as stochastic effects rise with increased heterogeneity, recent work suggests that unimodal relationships may be more likely to occur (Allouche et al., 2012; de Souza Júnior et al., 2014).

Secondly, niche partitioning has a temporal component. More specifically, the temporal variation in biofilm ecology can occur at different timescales, varying from diurnal variation and seasonality to long-term environmental shifts. This temporal variation affects population composition through species interactions and adaptation. As described by Brockhurst et al., the niche occupation at the time of arrival determines the ecological opportunity of invading species (2007), marking the importance of immigration history and diversification rate (Fukami et al., 2007; Gómez and Buckling, 2013). Similarly, Cheong et al. have shown how priority effects shape population structure (2021). In a broader sense, priority effects are described as the impacts of arrival timing and abundance of residents on succeeding colonizer establishment (Chappell et al., 2022). In this regard, though poorly studied, priority effects also incorporate both temporal and spatial dynamics. Several related predictions are

reviewed by Debray et al. (2021). To demonstrate, the early arrival of colonizers can yield priority effects by niche-pre-emption (i.e., reducing the availability of resources; Figure 2.A.ii.a) or niche modification (i.e., changing the local microhabitat; Figure 2.A.ii.b and further discussed in the next section) (Fukami, 2015). Notably, priority effects can also be the result of adaptation of colonizers to local conditions. This type of priority effect is called monopolization and can be further ranked based on the competitive dominance of the adapting colonizers over preadapted immigrants (De Meester et al., 2016; Figure 2.B.i). For this reason, an increased lag time between colonizers and successors strengthens the evolutionary potential of the former, increasing priority effects (Svoboda et al., 2018). When including spatial heterogeneity, not merely abundance but also distribution of residents affects colonizer population dynamics. Given this, high spatial structure predictably slows down the saturation rate of colonizing strains (Debray et al., 2021). Hence, more spare microhabitats will remain vacant when later-arriving strains are established. Moreover, the increased spatial structure may also hinder consistent arrival times among bacterial strains in the respective microhabitats, ultimately clouding the priority effects in place (Debray et al., 2021). Lastly, NFDS can maintain high genetic diversity by favoring rare genotypes (Steenackers et al., 2016). In other words, increases in relative abundance are associated with decreased per capita fitness as the own niche is becoming more populated. That can be mediated by competition, e.g., for resources, along with other interactions with adverse effects, e.g., parasitism (Christie & McNickle, 2023). Turner et al. showed that NFDS facilitates the coexistence of different genotypes under fluctuating conditions (2020). As such, NFDS can maintain multiple niche specialists in a population, and thus, the partitioning of niches gets preserved.

Niche modification and diversification

Cells also shape their environment, and this process is called niche modification. Depending on whether colonizers indirectly favor or hinder later-arriving organisms, this is called niche facilitative or niche inhibitory modification, respectively (Fukami, 2015). This interaction can take many different forms. For instance, Koza et al. have demonstrated that colonists establish steep oxygen gradients through respiration and, thus, shape the environment significantly (2010). That is to say, where colonists consume oxygen, niches are created for anaerobes to establish (Jo et al., 2022). Overall, the formation of oxygen gradients can cause metabolic heterogeneity through differential gene expression and stratified growth. Hence, niche modification boosts phenotypic diversification at both sides of the oxygen transition zone and results in ecological succession within the biofilm population (Koza et al., 2010). Moreover, other mechanisms, such as stress-induced mutagenesis, will allow a part of the cells to

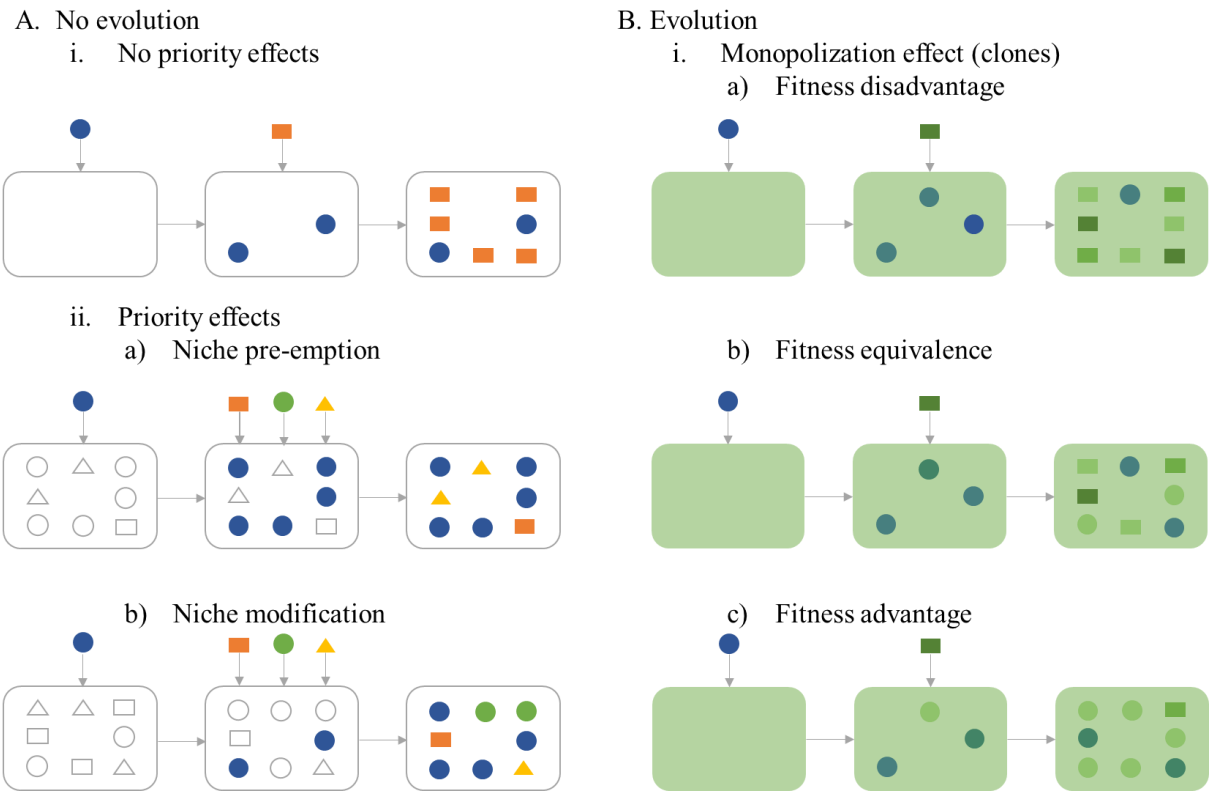

Figure 2: Competitive race between colonizers (the blue circle in each first patch) and following immigrants (each second patch).

Figure 2.A.: When there is no evolution at play, cells do not adapt to the local conditions. i. If the establishment of a late-arriving immigrant (orange rectangle) is not affected by a colonizer (blue circle), there are no priority effects. ii. a. Niche pre-emption: new immigrants with similar niches as the colonizer species cannot establish as they are occupied; new immigrants with different niches can still establish. b. Niche modification: the colonizer modifies multiple niches, and therefore, some immigrants no longer have compatible niches and cannot establish.

Figure 2.B: i. In the scenario where evolutionary processes are taken into account, species can adapt to their environment (blue circle turns green) and exert monopolization effects. a. Fitness disadvantage: a pre-adapted immigrant (i.e., lineages that have already undergone the evolutionary processes to adapt to a similar environment) wins the race from the initial colonizer as the latter cannot compete with a better-adapted invader if its own adaptation process is too slow. b. Fitness equivalence: adapting colonizer and immigrant can coexist, both having high population sizes. c. Fitness advantage: the colonizer adapts fast enough to hinder the establishment of a pre-adapted immigrant.

Adapted from "Evolving Perspectives on Monopolization and Priority Effects," by L. De Meester, J. Vanoverbeke, L. J. Kilsdonk, and M. C. Urban, 2016, *Trends in Ecology & Evolution, 31*(2), p. 136-146 (https://doi.org/10.1016/j.tree.2015.12.009) and "Historical Contingency in Population Assembly: Integrating Niches, Species Pools, and Priority Effects," by T. Fukami, 2015, *Annual Review of Ecology, Evolution, and Systematics, 46*(1), p. 1-23. (https://doi.org/10.1146/annurev-ecolsys-110411-160340).

adapt to the changing local conditions (Bjedov et al., 2003; Lee et al., 2015). Comparable dynamics take place along other chemical gradients, as broadly reviewed by Jo et al. (2022).

Biofilm formation, a special case of niche modification

A form of niche modification that is essential for the whole biofilm population is surface colonization, achieved by evolving adhesive properties. As for the development of oxygen gradients, adhesive colonists make the surface fit for other strains. Here, the establishment of less adhesive ecotypes is facilitated through biofilm production and enhanced attachment, and therefore, the arrival of colonists allows for population assembly and population diversification (Flynn et al., 2016). Being adhesive not only serves to strengthen attachment and form stable biofilms but also promotes green-beard-type cooperative interactions through preferential attachment (Schluter et al., 2015). Adhesion is, thus, vital for biofilm formation in terms of surface colonization and population support.

Whether adhesiveness evolves and spreads in a population depends on the balance of the cost-benefit ratio of adhesion. On the one hand, adhesin production has a bound energetic cost leading to reduced growth of the producer, and it brings the risk of immobility, risking adhesive cells to be buried under competing strains (Schluter et al., 2015). On the other hand, being adhesive enables cells to colonize surface territory and exploit an - as of yet - empty niche.

Interestingly, evolutionary experiments and simulations show that surface colonization repeatedly evolves *de novo* and sets the stage for less adhesive cells to proliferate (Rainey & Travisano, 1998; Spiers et al., 2002 van Gestel & Nowak, 2016). As such, an ecological succession unfolds as a result of niche construction where, upon colonization, individuals carrying the less adhesive climax genotype end up out-competing more adhesive early arrivers (Odling-Smee et al., 2013; Poltak & Cooper, 2011).

More generally speaking, early occupants can impose an environmental filter, either tolerating (cf. niche partitioning), facilitating (cf. niche modification), or inhibiting (cf. niche modification) the growth of later-arriving species (Brislawn et al., 2019; Connell & Slatyer, 1977). The system will reach a stable state when individuals are replaced by their own progeny. Yet the local circumstances often change, e.g., due to seasonal variations in temperature and light (Dmitrijs et al., 2022). As a result, the optimal phenotype modifies, favoring different genotypes or species and creating local instability (Connell & Slatyer, 1977). This successive dominance of genotypes indicates the manifestation of ecological succession. For example, elevated temperatures are associated with increased nutrient intake and growth rates of microbial populations, thus affecting population composition and succession patterns (Tilahun et al., 2016). Also fluctuations in other environmental parameters, such as nutrient levels, pH, oxygen, etc., have a

defining influence on the biofilm population through selective forces driving succession (i.e., distinctive survival and reproduction rates because of intrinsic biological properties; Jablonski, 2017; Pickett, 1976). If this process is not interrupted, the system will eventually reach a quasi-equilibrium state, where only minor modifications occur due to turnover. In field conditions, however, population development in biofilms is continually disturbed by changes in the direct environment, for instance, by intermittent antifouling pressure (Naik et al., 2023). When biofilms are removed, adhesive colonizers can initiate a biofilm elsewhere, and as such, the evolution of successor ecotypes is reiterated.

Interestingly, Callahan et al. have shown that adaptive niche construction can reevolve even after periodic disturbance and resetting of the environmental conditions (2014). That indicates that this process may be more ubiquitous than previously thought. These dynamics have also been studied extensively in the context of adhesion and surface colonization by, for example, Poltak and Cooper (2011), Ellis et al. (2015), Flynn et al. (2016), Traverse et al. (2013) and van Gestel and Nowak (2016). Similarly, the main interest of this thesis is the evolution of adhesive traits in biofilms during ecological succession.

Evolutionary dynamics of adhesion characteristics during ecological succession

Experiments conducted by the abovementioned authors have enhanced our understanding of how ecological diversity in adhesive properties evolves in biofilms. Notably, Poltak and Cooper developed a novel model of long-term evolution that allowed them to study ecological biofilm succession (2011). To elaborate, a plastic bead and one planktonic cell were added to a test tube. After 24 hours of growth, the bead was transferred to another test tube containing a new bead. The biofilm population had to disperse and colonize this new bead to succeed since only the most recently introduced bead was transferred to the next test tube. That resulted in a selection regime for cyclic biofilm colonization, growth, and dispersal. Using this bead transfer model and beginning in the absence of standing genetic variation, Poltak and Cooper have demonstrated the advent of successional stages resulting from changing selective forces for surface colonization (2011). In other words, selection within the population gives rise to a succession of genotypes adapted to different niches, thus differentiating ecotypes (Ellis et al., 2015).

When these types also differ morphologically, they are called morphotypes, as was the case in the experiments of Poltak and Cooper (2011). They found three ecologically distinguishable morphotypes - smooth,

ruffled, and wrinkly - that differed from the ancestor and emerged in a consistent sequence. In monoculture, the three morphotypes varied in fitness, biofilm production, growth rates, and territories. However, when grown together, biofilm output increased. Ecotype S was likely the first to emerge and was a better competitor for the medium than the ancestor, and it produced metabolites. Ecotypes R and W consumed these metabolites and colonized the empty bead surface. Henceforth, ecotype S was also able to attach to the surface, and all three lived in coexistence. In short, the three ecotypes interacted synergistically, where they benefit in the form of asymmetrical cross-feeding and through attachment facilitation.

As previously discussed, this ecotype diversification can arise as a result of niche partitioning or niche modification (Ellis et al., 2015). In the experiments of Poltak and Cooper, both the partitioning of biofilm space and niche facilitative modification in the form of asymmetrical cross-feeding were likely responsible for the productivity gains within the biofilm (2011). The authors then manipulated the environment by altering the number of available beads. Since diversity declined as environmental structure decreased, they reasoned that a structured biofilm environment facilitates functional and morphological diversification. It should, however, be noted that not all populations responded equally to structure manipulations, suggesting that depending on the specific (i) adaptive mechanisms, (ii) types of niche partitioning, and (iii) coevolutionary paths of ecotypes other eco-evolutionary feedback responses between ecological development and biodiversity are yielded.

Various studies have built further on the bead transfer model. Traverse et al. found remarkable mutational parallelism between independently evolving lineages under this selection regime promoting daily attachment and dispersal (2013). In line with the results of Flynn et al., they showed that, at the start of the experiment, the colonizing cells with high adhesion acquired mutations in genes regulating the levels of c-di-GMP (2016). This second messenger is used in signal transduction and is known to control the switch to a sessile lifestyle (Valentini & Filloux, 2016). As these initial colonists are relatively adhesive, they enable population assembly and facilitate the growth of climax ecotypes by allowing the adherence of less adhesive cells. In conclusion, these adaptive radiations likely drove the observed course of ecological succession. Hence, evolution was propelled along a predefined course (Flynn et al., 2016; Traverse et al., 2013).

Comparably, van Gestel and Nowak used an *in silico* experiment to study the evolution of adhesiveness (2016). To elaborate, they showed that an adhesive cell type can evolve and - as it can occupy a new niche (i.e., the surface) – it bypasses bulk competition. After initial surface colonization, non-adhesive phenotypes can also inhabit the surface by sticking to the adhesive

colonizers. Surface colonization, thus, occurs in two consecutive phases: colonization and climax. Low cell densities favor the colonizing genotype, whereas high cell densities promote the climax genotype (van Gestel and Nowak, 2016).

However, the specific dynamics of bacterial succession in biofilms and how each phase is influenced by environmental conditions (e.g., nutrient depletion) are not fully understood. Moreover, the nature of inter-ecotypic interactions and how this fuels ecological succession needs further research. Lastly, the specific mechanisms leading to biofilm population diversification and the effects of historical processes (e.g., priority effects) require more investigation.

Therefore, in this work, we will develop an individual-based model to study the evolutionary dynamics of an adhesion gene in a biofilm/bulk metapopulation undergoing ecological succession. In contrast to van Gestel and Nowak, we will treat adhesiveness as a continuous trait (cf. binary). As such, the model allows for the evolution of generalists and specialists. Also, as commented by Costeron et al., plasticity is a defining trait in biofilms (1995). Hence why, also the evolution of plasticity will be investigated. Moreover, surface turnover is included by allowing gradual nutrient depletion until all cells die and a new, replenished surface is set up. In the following, we will elaborate further on the study objectives and how the model functions to meet the research goals.

Objectives

As previously established, spatial heterogeneity has marked impacts on the ecology of the bacterial biofilm. This heterogeneity results in niches that can be occupied by distinct subpopulations, allowing the population to diversify through niche partitioning. In addition, the biofilm cells can actively modify their environment (i.e., niche construction), resulting in altered adaptive outcomes. Environmental gradients facilitate diversification as their spatial graduality allows the plastic and evolutionary shifts to proceed in small steps. The main mechanisms behind the genotypic and phenotypic heterogeneity include physiological adaptation through (i) altered gene expression and protein production, (ii) genetic adaptation through mutations and natural selection, and (iii) the stochastic pulsing of gene expression (Steenackers et al., 2016; Stewart & Franklin, 2008).

Here, we focus on the cyclic interplay between niche construction and the evolution of adhesiveness in the population during ecological succession. Both the spatial and temporal aspects of this eco-evolutionary feedback loop will be addressed, as well as the allele distribution in the population. Also, plasticity is included to investigate the competitiveness of plastic generalists and non-plastic specialists. Finally, we will study the effects of demographics and environmental stability on population diversity and trait distributions, respectively.

Niche modification and adhesion

The first objective of this study is to examine the fundamental population dynamics in biofilms and the role of adhesion in niche modification. As such, we aim to uncover what effect the adhesiveness of colonizers has on the biofilm ecology and the evolutionary trajectories followed by the population. To elaborate, when adhesive early colonizers attach to the surface, a new niche originates for less adhesive lineages to exploit. Will niche construction by colonizers result in population diversification? As found by Flynn et al., we hypothesize that selection for less adhesive phenotypes will prevail upon surface colonization by strongly adhesive lineages (2016). Furthermore, we expect an eco-evolutionary feedback loop where expanded intraspecific phenotypic variation allows other ecotypes to exploit newly created niches (Gómez et al., 2023).

Coexistence

Secondly, we will study the long-term evolution of adhesion in the population. More specifically, we will determine the model conditions (i.e., the adhesion level of the resident population and that of a rare mutant) that allow a mutant to replace the resident population, coexist with it, or go extinct. That will enable us to understand which strategies are evolutionary stable and which can be invaded by mutated cells. Negative frequency-dependent selection is the hypothesized mechanism behind a prolonged coexistence of distinct phenotypes in fluctuating conditions (Turner et al., 2020).

Diversification

Thirdly, we aim to study how demographic parameters affect the diversification process. That will shed light on how priority effects define the population structure. The effects of initial population size, carrying capacity, and surface growth rate on population diversification are tested.

Plasticity

The fourth objective is to study the evolution of adhesion when encoded as a plastic trait with continuous distribution. By inspecting the trait distribution, we aim to investigate the evolution of niche specialists and generalists. Moreover, the spatial and temporal dynamics of the system will be reviewed to comprehend the cell-cell interactions and the cyclic patterns taking place in the evolution of adhesiveness during ecological succession.

Environmental change

Our last objective is to understand the effect of environmental instability on the evolution of adhesion. To this end, we will test the influence of systematic nutrient depletion and random disruption events. We expect that low surface turnover (i.e., under prosperous starting conditions) will generate reliable cues. Therefore, we predict high levels of plasticity in response to nutrient level changes. For surfaces with high turnover, we expect to find a selection regime typically found in young biofilm populations.

A chaotic system characterized by frequent disruption is hypothesized to generate less

reliable cues, thus resulting in low plastic responses to surface cues but higher receptiveness for environmental cues coming from the bulk. Additionally, high disruption is expected to go hand in hand with systematic selection in favor of new colonizers. Hence, we hypothesize that adhesion levels will rise in the bulk population compared to the adhesiveness in environmentally more stable scenarios.

Materials and methods

Model choice

As already touched on briefly, numerous factors, such as species composition and environmental characteristics, determine the evolutionary trajectory of a biofilm, and depending on the research goals, different approaches are used to study this.

In vitro experiments can arguably be called the foundation of our current knowledge of biofilm micro-ecology. Static biofilm models allow us to study spatial heterogeneity created within biofilms ex-situ without compromising simplicity. Flow models, on the other hand, allow for a more dynamic system in which changes over time can be captured. Flow cells simulate the shear forces and constant renewal of nutrients naturally occurring in most biofilms. Moreover, growing conditions, such as physical gradients, nutrient availability, and flow rate, can easily be manipulated (Steenackers et al., 2016; Zhang et al., 2011). The bead transfer model is an elegant approach to incorporating dispersion as a component of the experiment. In this test, planktonic cells can adhere to plastic beads and accumulate under gentle flow conditions until those beads are transferred to new test tubes. Then, cells must disperse to reiterate the cycle. As such, insights into the evolutionary dynamics during ecological succession can be unveiled (Poltak & Cooper, 2011).

However elegant, this technique, nor any other *in vitro* model for that matter, allows for high-throughput screening of multiple variables. To efficiently explore a large set of hypothetical scenarios, we can best shift to *in silico* models (van Loosdrecht et al., 2002). These models also provide the flexibility to simplify systems – and, if desired, gradually incorporate more complexity – to understand intricate webs of relationships. Moreover, computational models allow us to manipulate environmental variables meticulously and simulate evolutionary processes over thousands of generations. To answer the research questions presented in this work, we opted for an individual-based *in silico* model in Python (version 3.9.13). The project was supported by the computing power of a high-performance research computing environment (i.e., provided by the Flemish Supercomputer Center).

Structure of the model

As illustrated in Figure 3, the model contains four surfaces each surrounded by a liquid bulk space. We begin the evolutionary experiment with an initial population circulating in the bulk areas. These cells are

characterized by a gene for adhesion, which, if expressed strongly, allows them to adhere to the surfaces with a high probability. On this substrate, colonies grow as more immigrants adhere and residents produce progeny (i.e., surface growth). Cells with low adhesion levels have a high probability of detaching from the surface and returning to the bulk. Planktonic cells can also reproduce (i.e., bulk growth) and go to other bulk spaces (i.e., movement). Moreover, environmental richness and disturbance are introduced to the system. The model repeats these processes for a predefined number of generations, and throughout the experiment, a maximum of 20000 cells is allowed to evolve due to practical limitations to the computational power (i.e., a carrying capacity of 2500 cells for each surface and bulk space).

Consistent with the objectives, the model is divided into five phases. In the first and simplest form, the model consists of a metapopulation of sessile cells populating four surfaces and planktonic cells residing in four bulk spaces around the surfaces. These individuals are characterized by high (i.e., 0.8) or low (i.e., 0.2) adhesion levels. This trait is discrete and not yet subject to plasticity. In case of mutation, the inherited allele is exchanged for the other allele. In this phase, the aim is to gain an understanding of the fundamental functioning of the model. That is done by studying how the adhesiveness of colonizers influences the available niches. Also, we examine the spatial association of ecotypes and how colonies are formed. Furthermore, we analyze how the evolutionary path of the trait deviates as a function of the initial alleles.
In the second phase, we studied the coexistence of different phenotypes. To this end, an invasion analysis is conducted by analyzing whether a cell with a mutated adhesion gene can spread in a resident population. That was tested for all combinations of mutant and resident alleles, ranging from an adhesion level of 0.0 to 1.0. The initial bulk population consisted of 100 cells, of which 99 carried the resident genotype P_r and one the mutant genotype P_m. Thus, there was a mutant starting concentration of 1%. After 25000 timesteps (i.e., T_{max}) the end frequency of the mutant allele (f_{end}) was calculated. Invasion fitness was defined as $\log_2(\frac{fend}{fstart})$. The methodology behind the evolutionary invasion analysis was based on van Gestel and Wagner (2021) and Otto and Day (2007).

For the third phase, we introduced continuous trait values and measured the effects of the surface growth rate, the initial population size in the bulk, and the bulk carrying capacity on diversification. To compare the diversity of the metapopulation in various demographic scenarios, the Gini-Simpson diversity index was measured. To do so, alleles were first binned into ranges of 1%, and the relative abundance of each (p_i) was calculated. Based on this, the allelic richness and Gini-Simpson index were calculated as the count of alleles present in the population and as $1 - \sum_{i=1}^{s} p_i^2$,

respectively. We chose to present these results using a triangular plot to limit computational and visual overload. However, there are several limitations to this compact illustration

Firstly, there are many factors at play. That can cause multicollinearity and indirectly change allelic richness through the impact on population sizes. Secondly, the effects of a single variable are not illustrated isolated from those of other variables, complicating the interpretation. Thirdly, the scaling of the variables is not proportional due to the computational cost of a high number of individuals associated with increased carrying capacities and initial population sizes. To mitigate these drawbacks, we quantified the effects of the demographic parameters on the Gini-Simpson diversity index using a beta regression (using R version 4.3.0). For completeness, the effects of these parameter combinations on allelic richness and population sizes are included in the addendum.

To achieve the last two objectives, plasticity and substrate turnover were added to the model. How these two concepts were integrated is explained in the following section. The evolutionary outcomes of the different scenarios were plotted as histograms and violin plots to visualize the gene and trait distribution in the population. Also, figures depicting the temporal and spatial dynamics are included. As such, the model aims to study the evolutionary dynamics of adhesion in a biofilm metapopulation. Each phase of the model consisted of the following eight modules:

Module 1: Movement

This model consists of four superficial surfaces surrounded by a liquid orb. To prevent edge effects, the edges are connected, forming a solid torus (i.e., a doughnut shape; Figure 3). As bulk cells are subjected to a flow regime, they are expected to circulate between bulk spaces at a high rate. Visualizing the bulk as a ball surrounding the surface (Figure 3), a cell located in the upper half of the bulk space can either move in a cardinal direction (towards bulk 2 or 3), diagonally (bulk 4) (Figure 4), or downwards (attempting attachment onto surface 1) (Figure 3). The same goes for cells positioned in the lower half of the bulk orb, with the exception that cells move upward to reach the surface (Figure 3).

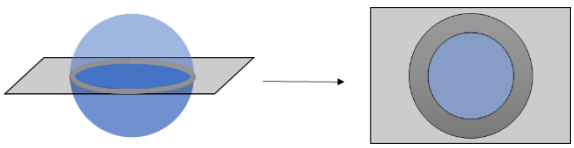

Figure 3: Edges of the surface are connected, forming a solid torus. Bulk space is not explicitly defined but can be visualized as a ball surrounding the surface. Left is the frontal view, and right the top view of the cross-section.

Movements in other directions are not possible as the model has a limited spatial extent. Hence why, each cell in the bulk has a total probability of 0.75 to migrate within the bulk spaces and a probability of 0.25 to attach to the surface. Migrators, in turn, have

a probability of $\frac{1}{2+\sqrt{2}}$ to make a cardinal movement, whereas the bulk situated diagonally to the focal cell is visited with a probability of $\frac{\sqrt{2}}{2+\sqrt{2}}$ (cf. Pythagoras; Figure 4). From this new starting point, settlers can attach to their new corresponding surface. Non-migrators, on the other hand, remain in the current bulk and are directly subjected to the next module.

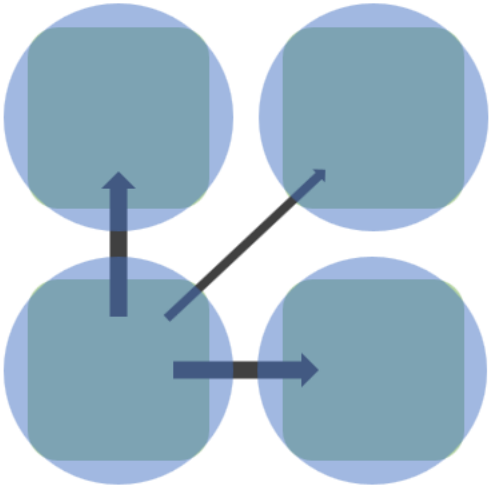

Figure 4: Movement of planktonic cells: cardinal movements span a shorter distance and occur more frequently than diagonal movement (cf. Pythagoras).

Module 2: Attachment

As previously established, the probability that a cell will attempt to attach to its corresponding surface is 0.25. Consider that only empty spots can be colonized, and thus, conquest attempts of occupied spots are unavoidably abortive. If an empty site is selected during the quest, the success of the focal cell will still depend on its own phenotype as well as that of its neighbors (Nadell & Bassler, 2011; Tai et al., 2022). More concretely, the cumulative probability that a cell manages to adhere is the sum of the adhesiveness of itself and that of all its direct neighbors present on the surface. The cut-off value of this sum is 100%, and thus, probabilities exceeding this value are reduced to the limit. Moreover, since a hexagonal cell-cell orientation is specified, each cell has a maximum of six neighbors (Figure 5). That also means that the competition for suitable spots increases under growing population pressure, while the individual chance of successfully adhering to the surface increases on account of sticky neighbors.

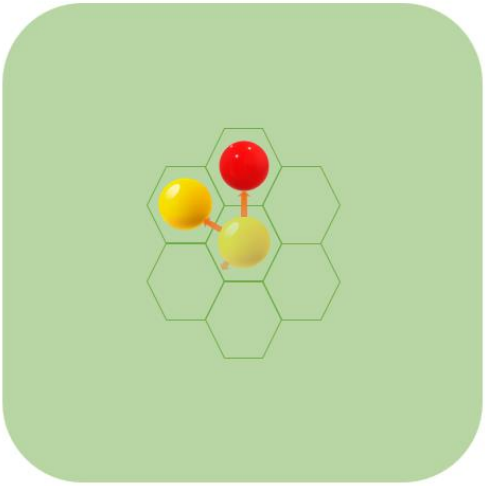

Figure 5: Attachment to the surface with a hexagonal grid. The probability of successful attachment is the sum of the own adhesiveness and that of all present neighbors (maximum six).

Module 3: Growth

Planktonic cells and sessile cells established on the surface both have an inherent growth probability of 0.1. However, the yield depends on the energy that is available for growth. Since cells pay a cost for adhesiveness and for plasticity (Achinas et

al., 2019; Nadell & Bassler, 2011; Yan et al., 2017), growth was reduced linearly as the level of these traits increased (i.e., a cost ranging from 0 for non-adhesive/non-plastic individuals to 0.25 for the maximally adhesive/plastic ones).

For adhesiveness, this cost is constitutive as maintaining the mechanisms in place to attach is also costly for those with a non-adhesive phenotype. Likewise, not only sessile cells but also free-living individuals have to lower growth outputs to compensate for increased adhesiveness (e.g., developing/maintaining pili and flagella; Achinas et al., 2019). Additionally, population pressure is incorporated in the growth formula: solitary cells grow maximally (i.e., log phase), whereas growth opportunities shrink as the surface becomes populated (i.e., stationary phase). In the case of surface cells, the energy available for growth also depends on the existing nutrient availability (Achinas et al., 2019). In the bulk, on the contrary, nutrients are constantly replenished by the existent flow. Therefore, bulk growth is not impaired by nutrient scarcity in this model. The carrying capacity is 2500 cells both for bulk and surface population. We make this simplifying assumption of a small bulk population, which has the same growth constraint as surface cells experience, to limit the computational costs and to be able to compare the population structure in the bulk and on the surface. That results in a growth equation including an inherent growth probability multiplied by the abovementioned costs for adhesiveness, plasticity, population pressure, and nutrient depletion (Addendum, Formula A.1).

Daughter cells of planktonic cells have a chance of 1 * 10-11 to carry a mutated genotype (adhesion gene or gene(s) for plasticity; Watford & Warrington, 2023). Because research shows that the mutation rate is elevated in biofilms, for each trait applies that 0.01% of the divided sessile cells have a different genotype compared to the mother cell (Coenye et al., 2022). In the first section, where adhesion is treated as a discrete trait, a mutation results in an altered allele. When mutations occur in continuous traits introduced in later sections of the model, the new genotype is drawn randomly from a normal (Gaussian) distribution around the genotype of the mother cell with a standard deviation of 0.1.

Module 4: Plasticity

Previously, the phenotype was entirely determined by the genotype. In this section, plasticity is introduced to the model. The initial population shows a uniformly distributed plasticity ranging from zero to one. In general terms, the phenotype is computed as a baseline, provided by the genotype, from which the cell can deviate by reacting plastically to one or more of the environmental cues (Addendum, Formula A.2). The plastic response depends on the plastic sensitivity to the cue and the information it transfers. These cues are factored in stepwise, starting with the individual effects and finally combining all cues.

First, the number of cohabitants of the bulk or surface can be perceived as an environmental cue. In other words, opportunistic cells can escape an overpopulated habitat in the search for a new niche (Nadell et al., 2008). Highly plastic planktonic cells can display phenotypic plasticity, which enables them to produce alternative adhesin levels (i.e., higher levels in case the bulk population approaches carrying capacity and vice versa). The same goes for sessile cells: under high population pressure, cells can detach by expressing a lower adhesion level relative to their genetic background. Cells can, however, not assess foreign habitats and are, thus, only driven by local demographics.

Secondly, the local population size is no longer evaluated. In contrast, surface cells can pick up the nutrient level of their habitat (Kimkes & Heinemann, 2019) and adjust adhesin production accordingly. As such, they have the possibility to detach from the surface when nutrients are nearly depleted and vice versa. Bulk cells cannot monitor this cue.

In the third stage of plasticity, both environmental cues - population sizes and nutrient levels - are functional. While, in the previous steps, plasticity was encoded as a common gene, three plasticity genes can now evolve independently (Van Gestel & Weissing, 2016). The first weighting factor corresponds to a plastic reaction to bulk population sizes, the second to surface population sizes, and the third to nutrient levels. Here, the combined effects of the plasticity in response to each cue determine the deviation from the genetic baseline.

Module 5: Nutrients

Initially, each surface is provided with a similar nutrient level, drawn from a normal (Gaussian) distribution around the initial concentration and with a standard deviation of 0.25. Here, the nutrient level is modeled as a relative measure. Specifically, starting from a nutrient level of one, nutrients on a maximally covered grid would be depleted after 1000 generations. When surface nutrients are depleted, all cells that have remained on the surface disappear together with the surface. Then, a new surface appears, stocked with nutrients.

Module 6: Detachment

Differing from attachment, the probability that a cell detaches from the surface is the complement of its attachment probability. As previously discussed, the latter equals the sum of the focal cell's adhesion and that of its neighbors. Furthermore, to mimic biofilm sloughing, detachment probabilities of cells with a detaching neighbor are recalculated within the same generation (Kaplan, 2010). For illustration, if a cell's only neighbor detaches, its probability of remaining on the surface is reevaluated. If this cell produces too few adhesins to be self-sufficient, it too will be removed from the surface. The ecosystem returns to a stable state - and continues with the next module - when no more (clumps of) cells are losing grip.

Module 7: Death

In each generation, 0.01% of the bulk and surface population dies. The perished cells are chosen at random.

Module 8: Dilution

Comparable to chemostat regimes, the bulk is diluted until it reaches carrying capacity at the end of each generation cycle (van Gestel & Wagner, 2021). Cells that are removed from the loop are again chosen at random.

Results

Niche modification and adhesion

We first examined the evolution of genes encoding adhesins in the absence of nutrient depletion or disruption events. Figure 6 shows the demographic characteristics of systems with varying specialization over the first 25000 generations. In the system with two generalists (top row), the more strongly adhesive ecotype has an adhesion level of 0.65 and the other of 0.35. Here, surfaces are maximally covered (i.e., up to 2500 cells per surface), as are the bulk spaces (Figure 6: population size curve in blue and red tones align). The right column demonstrates that the strongly adhesive genotype (in red) is relatively abundant in the early stages of biofilm development but is gradually replaced by less adhesive cells (in yellow).

The middle row presents a system with intermediate ecotypic differentiation: one has an adhesion level of 0.2 (yellow) and the other of 0.8 (red). Here, more stochasticity is present in the demographic evolution. That is, some surfaces reach a durable coexistence between both ecotypes at maximal surface coverage (e.g., surface 2), while others do not (e.g., surface 1). As ecotypic differentiation increases (Figure 6: descending), biofilm populations destabilize. More specifically, in the design with the most differentiation, not only the relative abundance of highly adhesive cells but also the total population size shrinks considerably after a period of fast growth in the young biofilm. Overall, both the maximal population size (reached at variable times) and the cell count at an adult stage (after 25000 generations) decline markedly as ecotypic differentiation increases (population sizes are shown on a logarithmic scale). Bulk growth is maximal in all presented cases. The genotypic abundances of bulk populations are not included since these show a largely uniform pattern throughout time, consisting almost exclusively of the least adhesive ecotype.

In each instance, adhesion levels are defined in such a manner that the bond between two ecotypes is unbreakable, unless by death. We selected levels whose sum is one to limit the number of contributory factors in this first representation of the model functions. Considering this, two generalist ecotypes yield greater biofilm output than two niche specialists. Note that by making this simplifying representation we do not allude that ecotypic differentiation *an sich* boosts the biofilm output. Rather, the specific strategy combinations of colonizers and successors will influence population productivity.

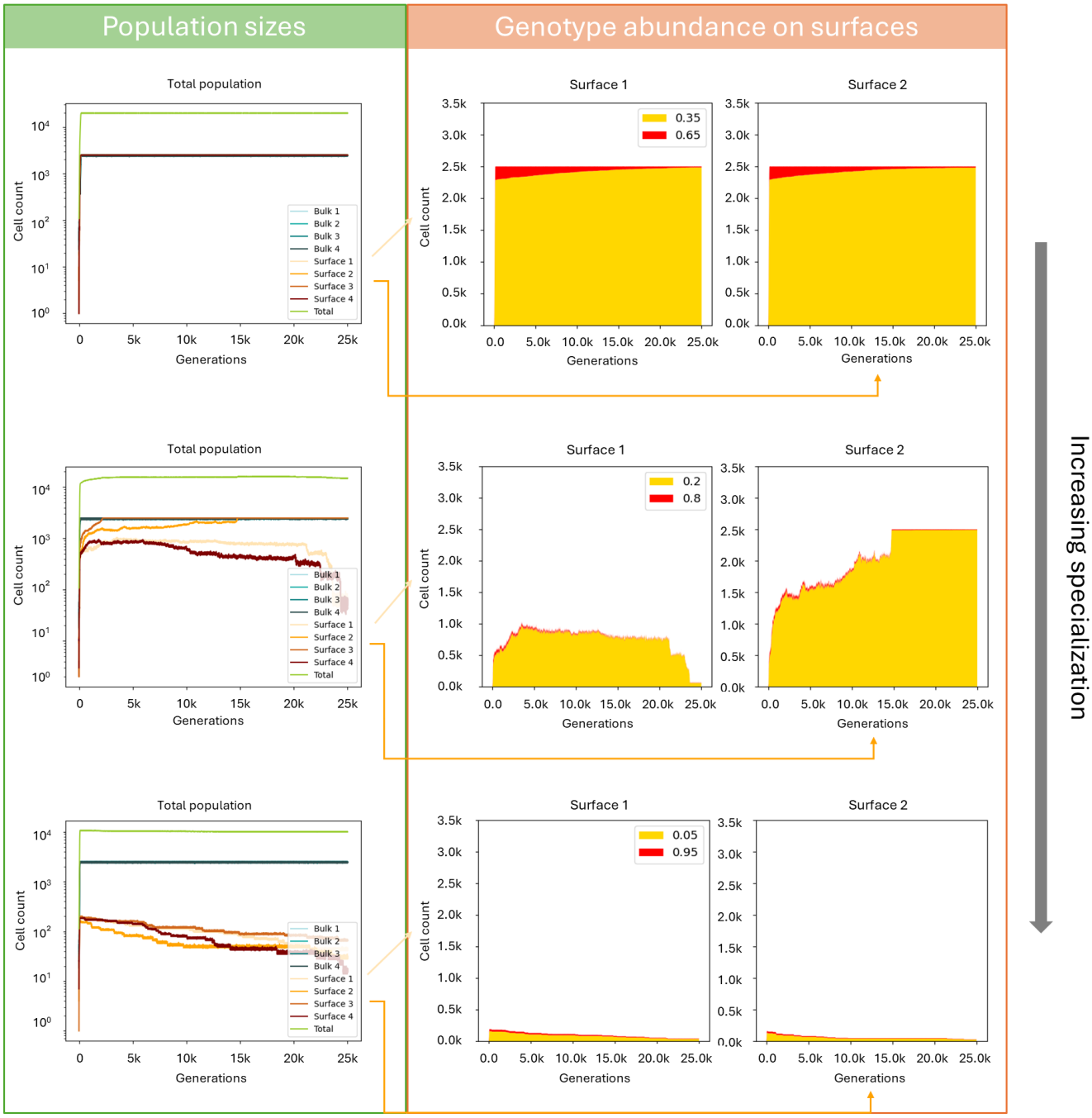

Figure 6: Demographics of the biofilm population for different levels of specialization. More specifically, in the rows, the adhesion levels 0.35 and 3.65, 0.2 and 0.8, and 0.05 and 0.95 are shown consecutively. In the left column (green), the population sizes of cells on the surfaces (i.e., red tones) and in the corresponding bulk spaces (i.e., blue tones), as well as the total population size (i.e., green graph) are quantified in time. It should be pointed out that population sizes are shown on a logarithmic scale. The right column (orange) presents the genotype abundances found in the population of surface 1 (left) and surface 2 (right), selected to paint a general picture of the biofilm community dynamics. Adhesion levels are mirrored around 0.5, and therefore, the link between two ecotypes can only be broken by death.

Figure A.1 is added to the addendum as an illustration of this. Moreover, Figure A.2 shows the yields of mono- and di-ecotypic biofilms. That gives more insights into the way bulk and surface specialists interact. Figure 7 shows how the adhesion alleles (with levels 0.2 and 0.8) evolve through time, as well as their spatial distribution on the surface. The temporal dynamics (left bottom) demonstrate that the bulk populations are initiated with approximately equal amounts of both ecotypes, as imposed by the model. After 100 generations of evolution, however, the planktonic population has already become minimally adhesive (i.e., mean adhesion level of 0.2). Surfaces, on the other hand, are colonized nearly exclusively by the strongly adhesive ecotype. That is indicated by the red curves starting close to the maximum (i.e., 0.8) and squares A and B displaying the bacterial population on surface 1 after one and ten generations, respectively. After 100 generations, the less adhesive cells have started surrounding the adhesive colonizers, forming little florets. Mean adhesion levels are lowering rapidly at this stage. Henceforth, empty spaces are padded by the slightly adhesive cells, and a mean adhesion level close to 0.2 is reached.

We see that adhesive pioneers are the first to colonize the surface, followed by the less adhesive cells that capitalize on the adhesins of neighbors. The latter form rosettes around the colonizers and start filling up the space. Colonizers rarely expand as they have a double disadvantage. Firstly, producing adhesins is energetically demanding, and therefore, biofilm output is 15% lower for highly adhesive individuals (for this combination of genotypes). Secondly, the empty spots around colonizers are rapidly occupied by poorly adhering cells from the bulk. As the successor cells grow much faster, dividing colonizers risk not finding an adjacent spot that is still vacant.

In the bulk, cells instantly evolve lower adhesion levels in response to selective pressures imposed by their ecological niche. More specifically, producing adhesins has no added value for planktonic cells but does entail energetic costs. Over time, highly adhesive cell lineages will either migrate to the surface, evolve genetically (i.e., mutated cells giving rise to novel adhesion phenotypes will proliferate), or be selected out through natural selection.

To summarize, in this first step, we explored the interactions between ecotypes. Figure 6 shows that high levels of specialization are often not favorable: two generalists show higher productivity than a highly adhesive biofilm specialist combined with a slightly adhesive successor. Figure 7 indicates that the average adhesion level of surface populations declines sharply after being nearly maximal in the colonizing phase, followed by a long phase of gradual reduction. Additionally, Figure 7 shows that slightly adhesive cells depend on the colonizers to attach. First, successors form little rosettes around colonizers and later pad the remaining openings.

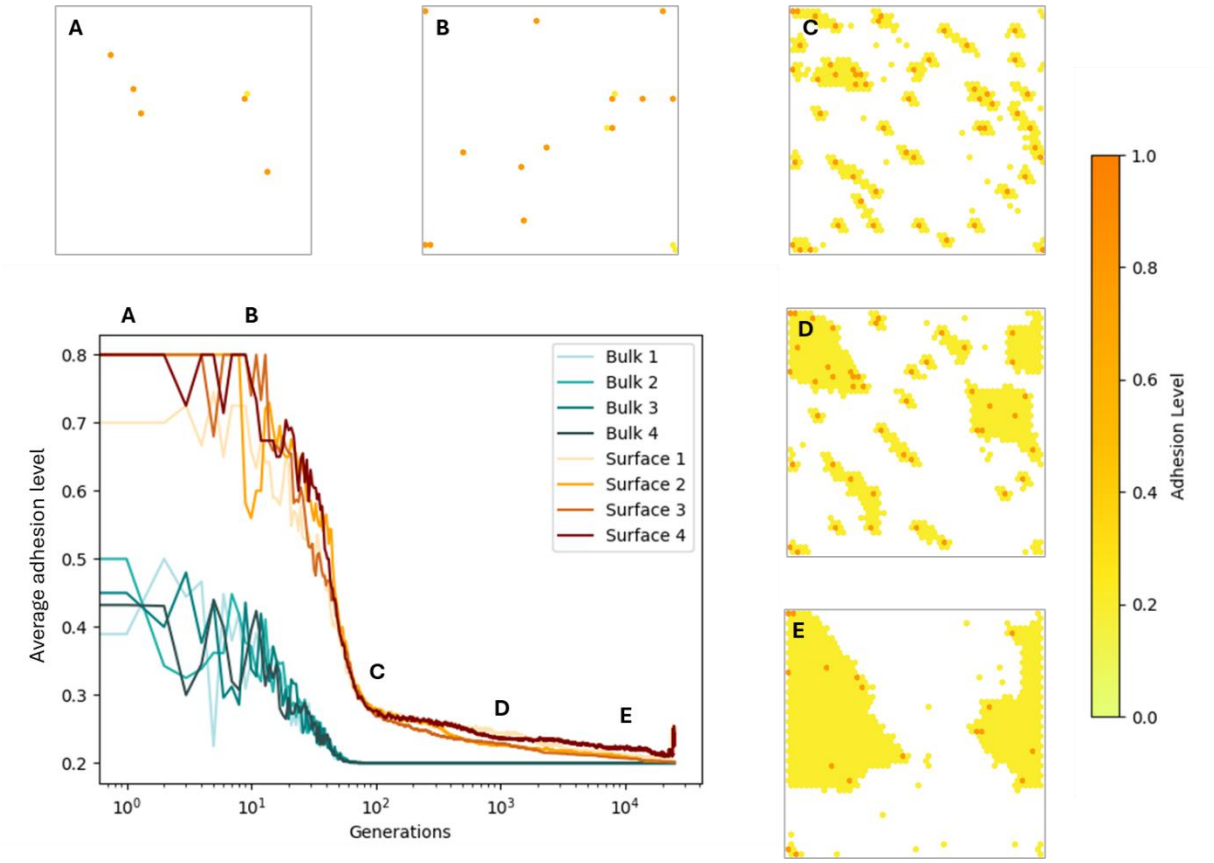

Figure 7: Spatial and temporal dynamics of the adhesion alleles in a model with intermediate ecotypic differentiation (i.e., adhesion level of 0.2 and 0.8). Squares (top row and right column) show the spatial distribution of bacterial cells on surface 1 at specified time frames (A. generation 1; B. generation 10; C. generation 100; D. generation 1000; E. generation 10000). Orange cells have a high adhesion level, and yellow cells are less adhesive. Curves (left bottom) show the average adhesion levels on the surfaces (red tones) and in the bulk spaces (blue tones) over 25000 generations. Data are collected from one simulation.

Coexistence

In the previous section, we established that highly and slightly adhesive cells can co-occur in a young biofilm, where the relative abundance of highly adhesive lineages decreases as the population ages. For ecotypes with little to intermediate genetic differentiation, this partnership can become a durable coexistence. In this part, we want to unravel this long-term evolutionary process. Why do we observe that different adhesion strategies coevolve in biofilms? Indeed, research shows that the biofilm growth cycle is characterized by coexisting cells with various levels of bacterial adhesion (Garret et al., 2008), and therefore, it would be interesting to develop a method that allows a range of attainable alleles, each encoding different adhesion levels. As such, we can address:

1) Which mutant alleles can invade a resident population?

2) Is there an evolutionarily stable state, and is this state convergence stable?

Figure 8 is the result of the evolutionary invasion analysis. This pairwise invasibility plot (PIP) shows the invasion fitness of a mutant with an adhesion level ranging from zero to one in a population of residents with adhesion levels in the same range. The black circle approaches the evolutionarily stable strategy (ESS) around 0.225, and the black square delineates the area around the ESS with higher resolution created for clarity purposes. Mutants carrying the allele encoding for this adhesion level can, thus, invade a resident population. We speak of an ESS because, once this equilibrium is reached, no other mutant strategy would be more successful (Otto & Day, 2007). In other words, the system is stable. The point is also convergence stable, meaning that a resident population removed from the ESS can be invaded by mutants closer to it. Blue and light orange squares represent phenotype combinations that coexist after 25000 generations of evolution.

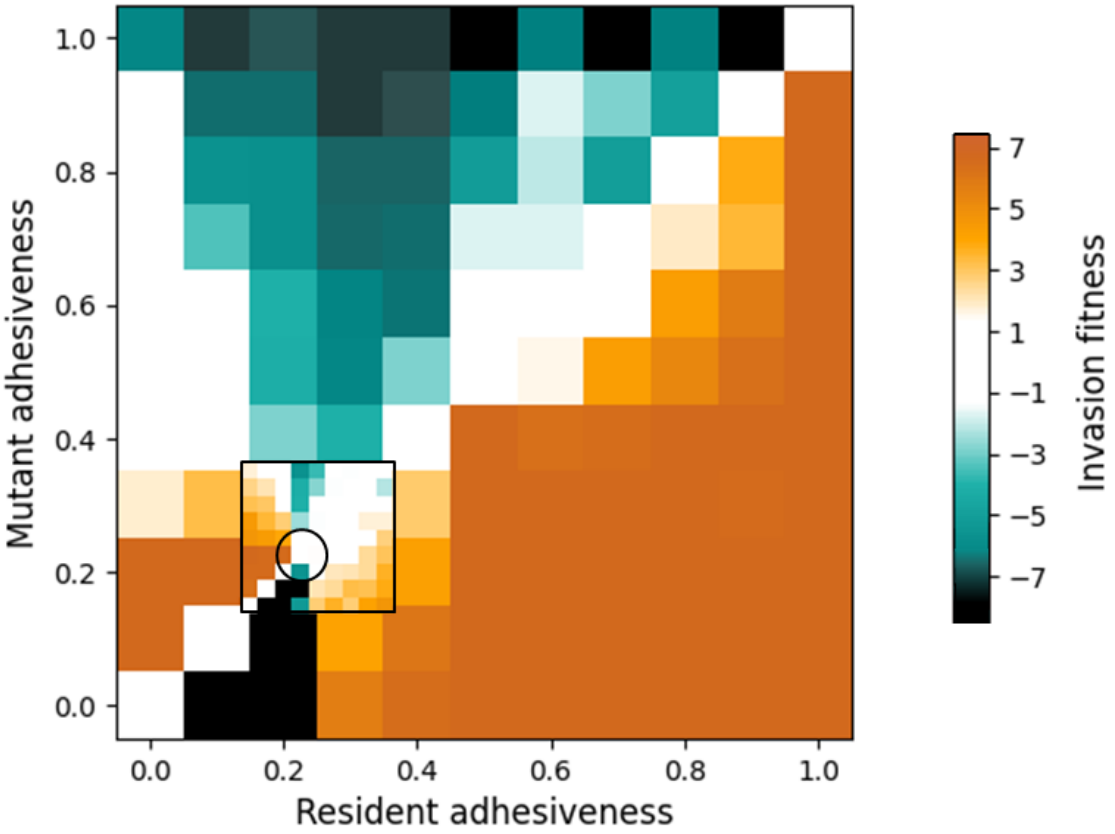

Figure 8: PIP of the model with adhesion as the evolving trait. Resident and mutant strategies include adhesion levels ranging from 0.0 to 1.0. Mutants manage to invade when invasion fitness is positive (orange shades). If the relative abundance of the mutant is unchanged, invasion fitness becomes zero (white). If it decreases, invasion fitness is negative (blue shades). Black cells show parameter combinations where the mutant genotype disappears. The uncolored diagonal represents neutral cases, as mutant and resident strategies are equivalent. The black box is a close-up of the region around the EES at mutant adhesion of 0.225, indicated with a circle. The figure includes data from ten simulations.

Diversity

The previous phase of the model demonstrated that the stable coexistence of cells with different adhesion strategies is possible under certain circumstances. Now, we want to determine how demographic parameters influence population diversification. As starting conditions, the adhesion levels in the initial population showed a normal (Gaussian) distribution around zero with a standard deviation of 0.1, where negative values were replaced by zero. The effects of surface growth rate, initial population size, and carrying capacity are examined, and we calculated the Gini-Simpson index to compare diversity estimates. These relationships were also described with a beta regression model and further illustrated in the addendum (Figure A.3). The test statistics of this model are included in the addendum (Table A.1). All model assumptions were met. The beta regression for the Gini-Simpson diversity index does not include interactive effects since the main effect models had lower Akaike information criterion (AIC) values. We had too little data to draw a firm conclusion regarding statistics. Yet, note that this model functions merely as a clarification of the triangular visualization. Finally, the effects of these demographic parameters on allelic richness and population sizes are added to the addendum for comparison (Figure A.4).

Figure 9 shows the results of the analysis of the Gini-Simpson diversity index, with initial population sizes increasing by a factor of 5 from left to right. Carrying capacity is presented on the right side of the large triangle. Here, each elevation is equivalent to an increment of 500 cells. Surface growth increases by a factor of two for each step towards the bottom left angle beginning from the top of the large triangle. The intermediate levels shown in this figure are used as the standard parameters throughout the rest of the work.

Similar patterns are found for both diversity measures. For this parameter combination, diversity is highest when the initial population size is maximized, with the peak situated in the right-bottom corner. The lowest diversity level lies across the maximum. For allelic richness, all combinations with low initial population sizes are species-poor. In contrast, the Gini-Simpson index indicated a diversity valley around an initial population size of four, an intermediate surface growth rate of 0.1, and a bulk carrying capacity of 2500 (i.e., matching the surface carrying capacity). This proportional effect of initial population size can be related to the fact that - when a population originates from a few initial colonizers - genetic drift can lead to the fixation of some alleles (i.e., founder effect). That relates to the priority effects associated with surface colonization.

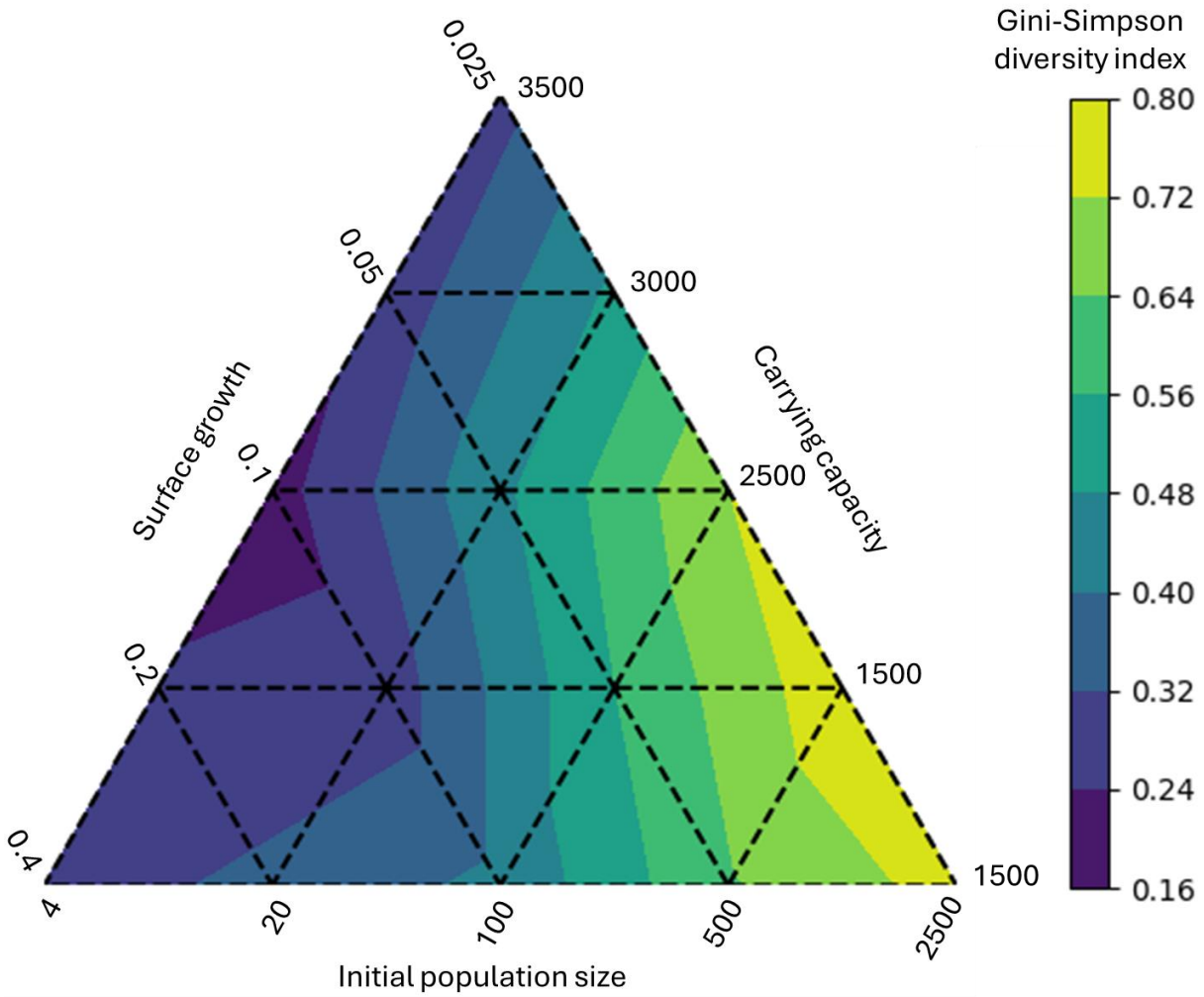

Figure 9: Diversity triangles expressed as the Gini-Simpson diversity index. From left to right, the initial population size increases with a factor of five for each side length of a dashed triangle. From the right bottom to the top of the triangle, the carrying capacity climbs five steps with an increment of 500 individuals per rise. The left side of the large triangle aligns with the axis, indicating surface growth levels beginning with 0.025 at the top and increasing with a factor of two per step downwards. Yellow shades depict relatively high diversity and blue shades stand for the less diversified populations. Data from ten simulations were used for this figure.

Plasticity

In this phase, the model gradually increases in complexity. Firstly, we want to test whether the population would evolve towards the evolutionary stable adhesion level of circa 0.225 - as indicated in the previous phase - if adhesiveness is encoded as a continuous trait. Next, using this model as the new baseline, we test the effects of nutrient depletion and plasticity on the genotypic and phenotypic distribution of adhesiveness (and plasticity, if applicable)

Figure 10.1 shows the results of the baseline model after running for 50000 generations. The blue histogram shows the genetic distribution of adhesion alleles in the bulk populations, and the orange bars indicate those present in the surface populations. Only genotypes (i.e., the baseline levels) are shown since plasticity is not yet included. Bulk genotypes exhibit a high peak at adhesion level zero and a smaller rise around 0.225. For biofilm cells, the opposite applies. That indicates a bifurcation in the evolutionary path of adhesiveness, resulting in two emergent ecotypes.

Figure 10.2 displays the resulting genotype distribution after 50000 generations in bulk (blue) and surface populations (orange). Here, the biofilm stays relatively young as the surface is refreshed every time nutrients are depleted. That results in an allelic distribution similar to the one for the aging biofilm (cf. Figure 10.1), with a tall peak near an adhesion level of 0.225 and a low elevation at no adhesion. The bulk, however, now also shows a high peak around the level 0.225 apart from the rise at the non-adhesive state. To sum up, in this system where substrates are refreshed periodically, we find continued selection in favor of new generations of colonizers (in the bulk and the surface) and in favor of planktonic cells (in the bulk).

In the next stage of the model, we start again from the baseline but include plasticity instead of nutrient depletion. Hence, biofilms can reach a mature state. In contrast to the precedent, we allow the evolution of phenotypic plasticity based on a single gene. This plasticity gene plays a role in the organism's ability to adapt to changing environmental conditions and starts with a uniform distribution between zero and one. The expression of the plasticity gene is regulated in response to environmental cues, and in this step, we set local population size as the signaling cue. The resulting genotypic and phenotypic distributions of adhesiveness, as well as the occurrence of plasticity in the bulk (i.e., blue tints) and on the surface (i.e., red tints), are illustrated in Figure 11. In both populations, nearly all individuals carry the allele that gives rise to minimal adhesion. For the phenotypes, the elevation has a less steep slope, with a single peak for the bulk at level zero and an additional one around 0.280 for the surface populations. The plasticity distribution shows a peak around zero for bulk populations. Surface populations display one peak at low plasticity levels, another between levels of 0.30 and 0.40, and most other cells fall between both rises.

As the bulk population expands, highly plastic planktonic cells become more adhesive in order to escape competition for bulk space. When these adhesive cells colonize the surface, they can stay attached because their plastic response will still support an adhesive phenotype. That explains the second peak in phenotype and plasticity distributions of surface cells. The other elevation in the trait distributions consists of successors that do not invest in adhesin production (neither by evolving highly adhesive genotypes nor by

responding plastically) but instead stick to other cells and grow fast. After 50000 generations, adhesive alleles got lost in bulk populations, and low levels of plasticity were fixed as this was sufficient for bulk cells to exploit the other niche in the succession stage. All cells carry alleles that express low levels of adhesion. In other words, it is more favorable to evolve plasticity than to have a high-adhesion genotype as a way to express adhesion (second peak) despite the fact that energetic costs for adhesion and plasticity are equal.

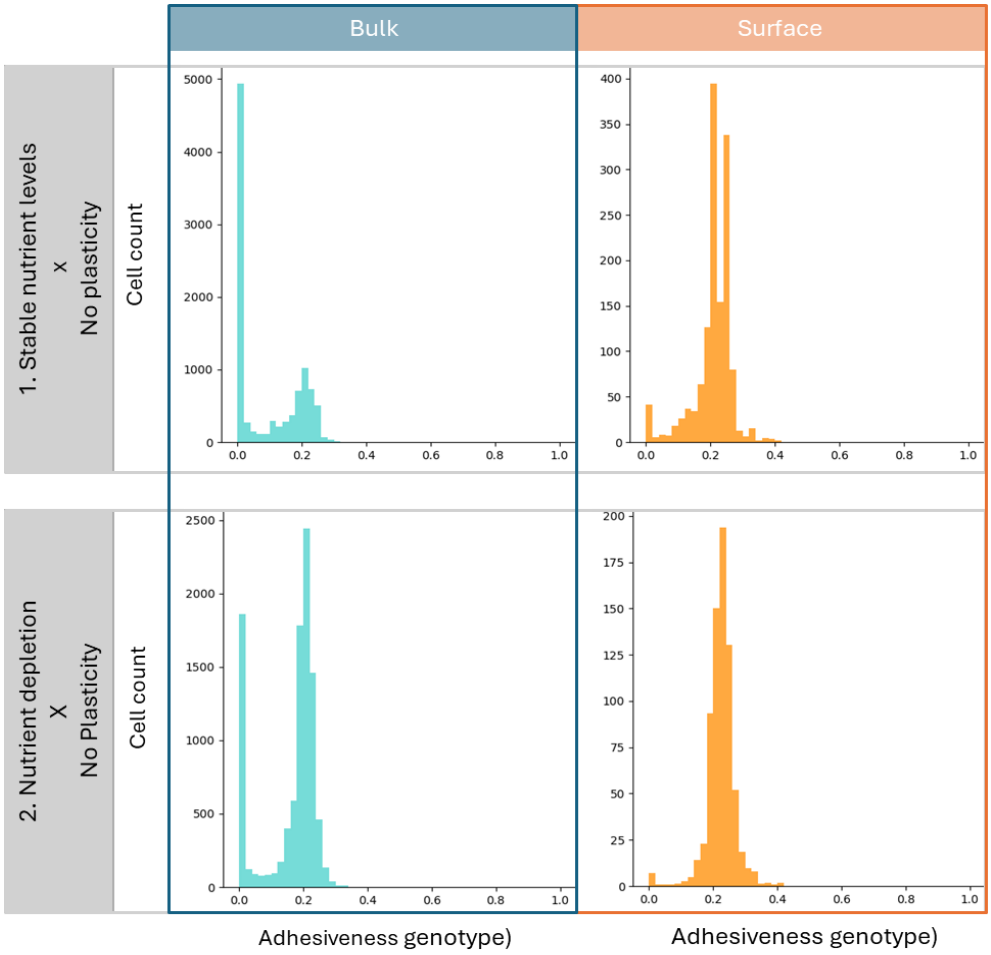

Figure 10: Adhesion levels in the basic model – without plasticity.

Figure 10.1: Histograms show the distribution of genotypes (absolute counts) of all bulks (left) and all surfaces (right) combined and averaged over 100 simulations after 50000 generations in the simplest version of the model. Note that absolute counts are displayed for a bulk population of 9823 cells and a biofilm population of 1375.

Figure 10.2: Idem as 10.1, but now nutrient depletion is introduced. The average combined bulk population counts 9826 cells, and the four surfaces jointly are, on average, occupied by 717 individuals.

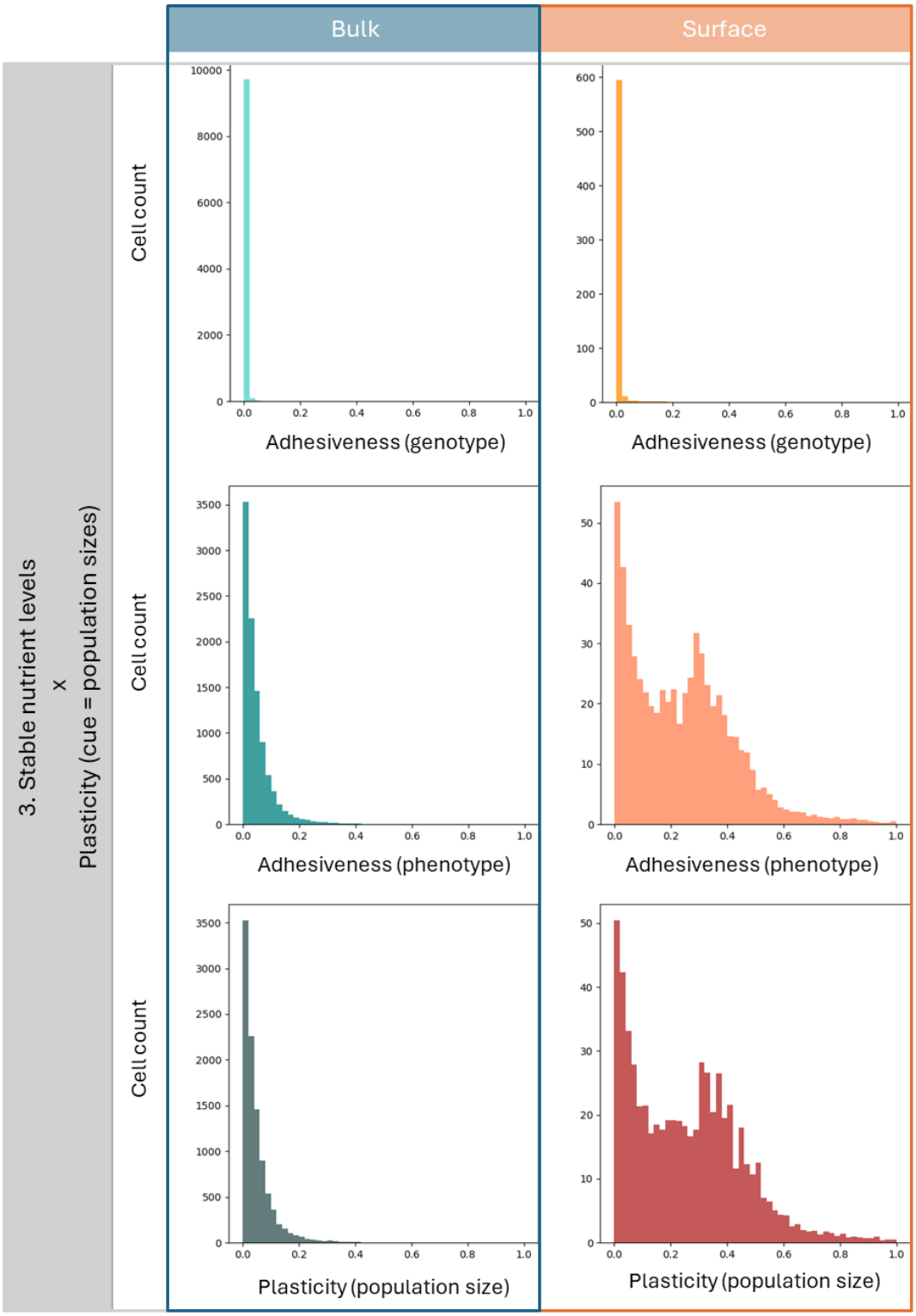

Figure 11: Trait distributions of the model including a stable nutrient regime and plasticity, with the population size of the cell's habitat as the cue. Histograms show the absolute count of the cell's adhesion (top) genotypes and (middle) phenotypes, as well as their relative (bottom) plasticity levels in the four bulk (left) and surface (right) populations. These counts are averaged over 100 simulations and measured after 50000 generations. The average total bulk population reaches 9828 individuals, and the average occupation of the four surfaces counts 618 cells.

After testing the effects of cyclicity and plasticity separately, both are combined. Here, the expression of the plasticity gene is not modulated based on the local population size but on the nutrient level of the inhabited surface. That means that only surface cells can sense and respond to the environmental cue, allowing them to adapt to the present resource state of the surface. After 50000 generations, the descendants' genotypes mainly encode for a non-adhesion cell state, with an additional low elevation around level 0.2 (Figure 12). For surface cells, this second rise in the phenotypic distribution reaches relatively larger counts and higher levels of adhesiveness. Bulk phenotypes are analogous to genotypes. The plasticity gene aligns with a left-tailed distribution for cells in the bulk and on the surface.

Bearing in mind that the environmental cue is not valuable for bulk cells in this system, while it is costly, plasticity is expected to be selected against in the bulk populations. In surface cells, it can be beneficial to spend energy on phenotypic plasticity, and thus, higher plasticity levels can be expected. However, as the surface population is continuously washed away and new populations can only be founded by bulk cells, plasticity levels cannot reach high levels on the surface either. Instead, adhesion is brought to expression by evolving higher genotypic adhesion levels. For surface populations, we find a peak around zero and one around the ESS. The second of the two is represented by more cells since surface coverage is low, and therefore, more adhesive cells are needed to secure the microcolonies. In the bulk, there is selection for a non-adhesive cell state, which is most fit for the planktonic lifestyle. Yet, they are not exclusively non-adhesive, and consequently, they safeguard the possibility of adhering. Note that the low-adhesion genotype is less abundant than in the model including nutrient depletion but excluding plasticity. That could be related to the fact that, here, the biofilm does not reach maturity.

As histograms only give a detailed view of the endpoints, the mean adhesion phenotypes of the previous four steps are plotted through time in Figure 13. That shows temporal variation, albeit small enough to assume that the histograms provide a representative picture. At the end of the experiment, the 95% confidence intervals (CI) of the mean phenotype in the models without nutrient depletion do not overlap, while in the cyclic models, they do. That is because, in the latter two, surface populations are regularly washed away to be reinitiated by founders from the bulk, and therefore, there is no time for evolutionary branching. The 95% CI in the third step of the model (left bottom) is broad for the surface cells since their high plasticity levels allow for fast changes.

In the final and most detailed phase, nutrient depletion and plasticity are applied. Yet, this part of the model allows three genes to evolve independently in response to specific environmental cues. For the first plasticity

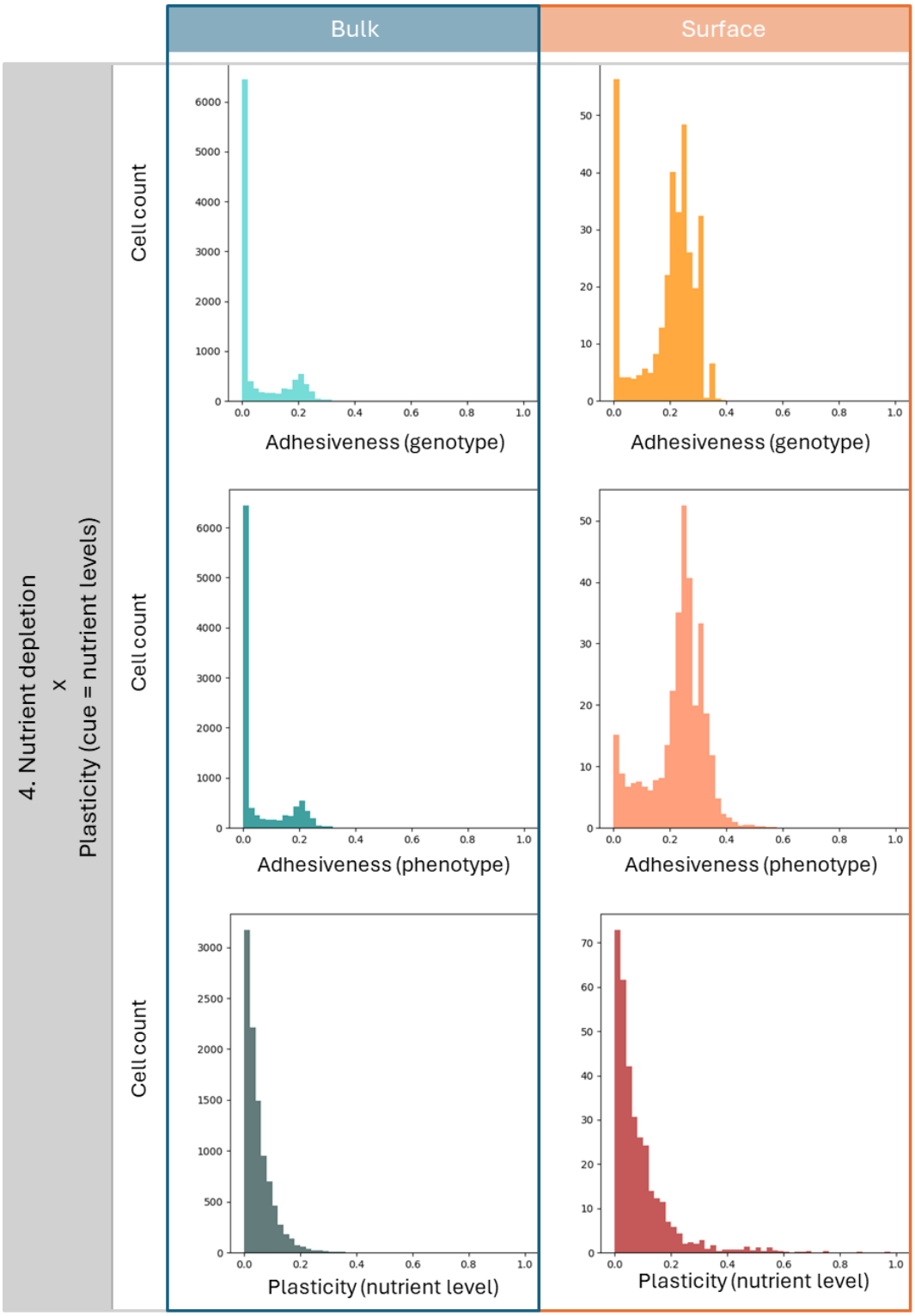

Figure 12: Trait distributions for the model including a dynamic nutrient regime and plasticity, with the nutrient level on the surface as the cue. Histograms show the absolute count of the cell's adhesion genotypes (top) and phenotypes (middle) as well as their relative plasticity levels (bottom) in the four bulk (left) and surface (right) populations. These counts are averaged over 100 simulations and measured after 50000 generations. Total cell counts in the bulk spaces and on the four surfaces reach 9836 and 333 individuals, respectively.

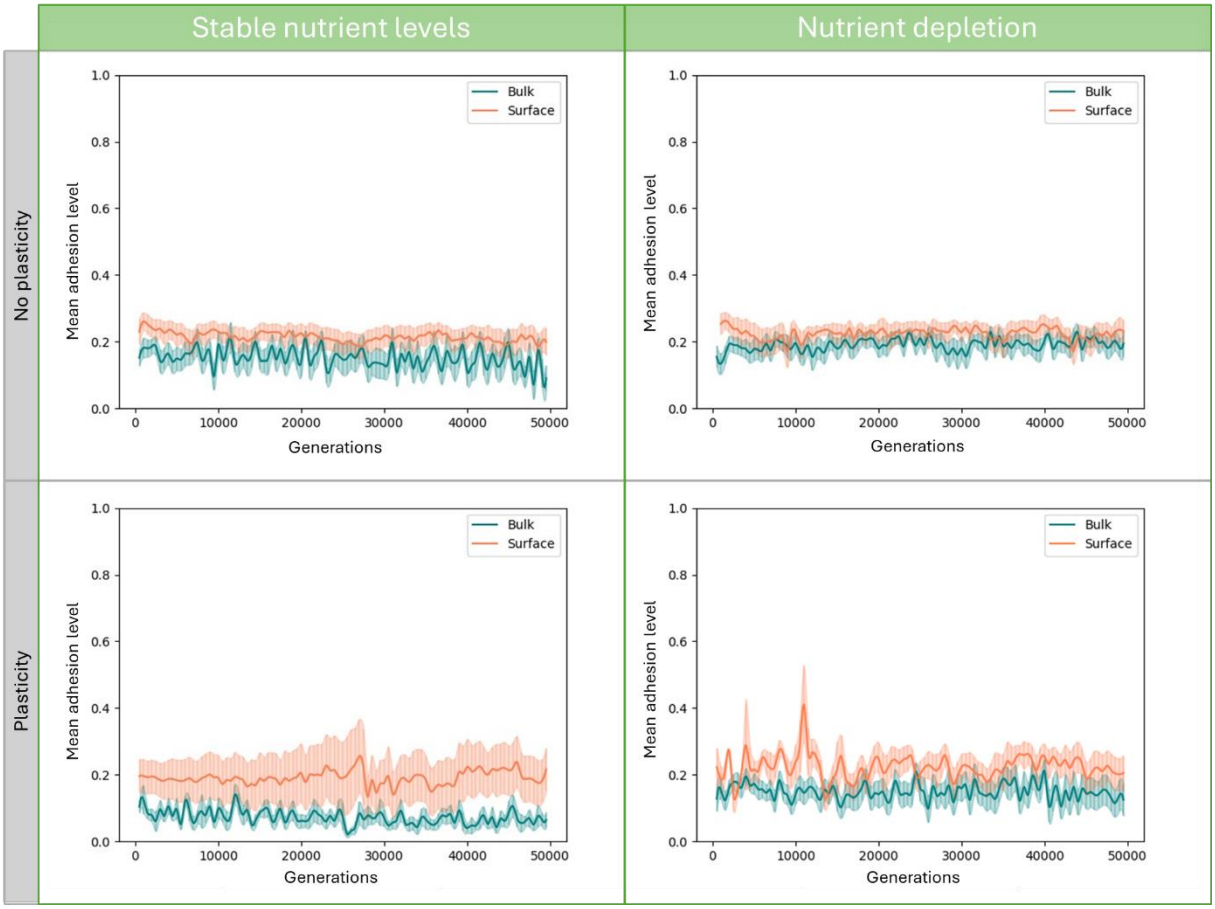

Figure 13: Exploratory illustration of evolutionary dynamics of the mean adhesion phenotype through time. The upper-left graph shows the design without plasticity or nutrient depletion (cf. Figure 10.1). The upper-right graph shows the mean phenotypes of cells subjected to cyclic nutrient depletion that are unable to respond plastically to the environment (cf. Figure 10.2). In the lower-left corner, a system without nutrient depletion is depicted where cells can have a plastic reaction as a result of perceived cell abundance (cf. Figure 11). Finally, in the lower-right figure, nutrients deplete cyclically, and cells can react plastically to this (cf. Figure 12). Vertical stripes show the 95% CI. Averages are taken over 20 simulations.

gene, the signal is the population size of the cell's bulk space. Biofilm cells, on the other hand, can pick up the surface occupation signal, and the second plasticity gene responds accordingly. Thirdly, there is a plasticity gene whose expression is influenced by the nutrient level of the focal cell's surface.

Figure 14.1 and Figure 14.2 show the evolutionary outcomes of this regime. Bulk and surface cells nearly all carry a genotype with adhesion level zero. The expressed phenotype of bulk cells follows a left-tailed distribution with a peak at adhesion 0.08. Surface cells display adhesion traits aligning with a two-tailed distribution with a maximum cell count of 0.18. The first

plasticity gene takes a similar evolutionary path in the bulk as on the surface, resulting in a left-tailed distribution reaching the high point around a plasticity level of 0.08. A bimodal pattern can be observed when displaying plasticity levels for the second plasticity gene in the bulk spaces and the surfaces; namely, there is a rise around 0.02 and 0.08 and an absolute maximum at levels 0.16 and 0.24, respectively. Most bulk cells have a level of between 0.0 and 1.2 for the last plasticity gene, whereas for surface cells, the mode lies around 0.1.

As was the case for the third step, evolving the ability to react plastically has proven more favorable than maintaining high-adhesion genotypes. That is because, in this system, where the environment changes gradually and predictably, the environmental cue can be picked up in time to react to

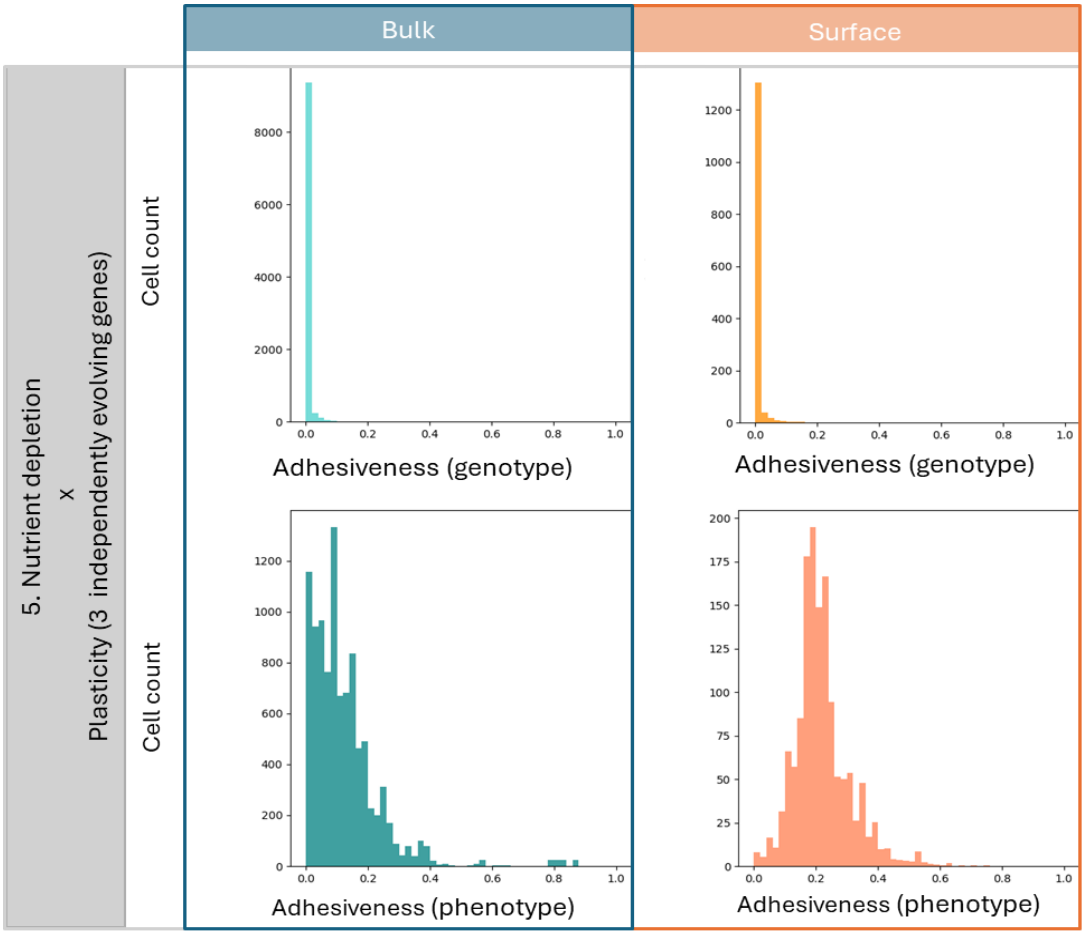

Figure 14: Dynamic nutrient regime with plasticity encoded in three genes that can evolve independently. These counts are averaged over 100 simulations and measured after 50000 generations. The average bulk metapopulation reaches a total size of 9814 cells, and the four surfaces, on average, sum up to 1384.

Figure 14.1: Histograms show the absolute count of the cell's adhesion (top) genotypes and (bottom) phenotype in the four bulk (left) and surface (right) populations.

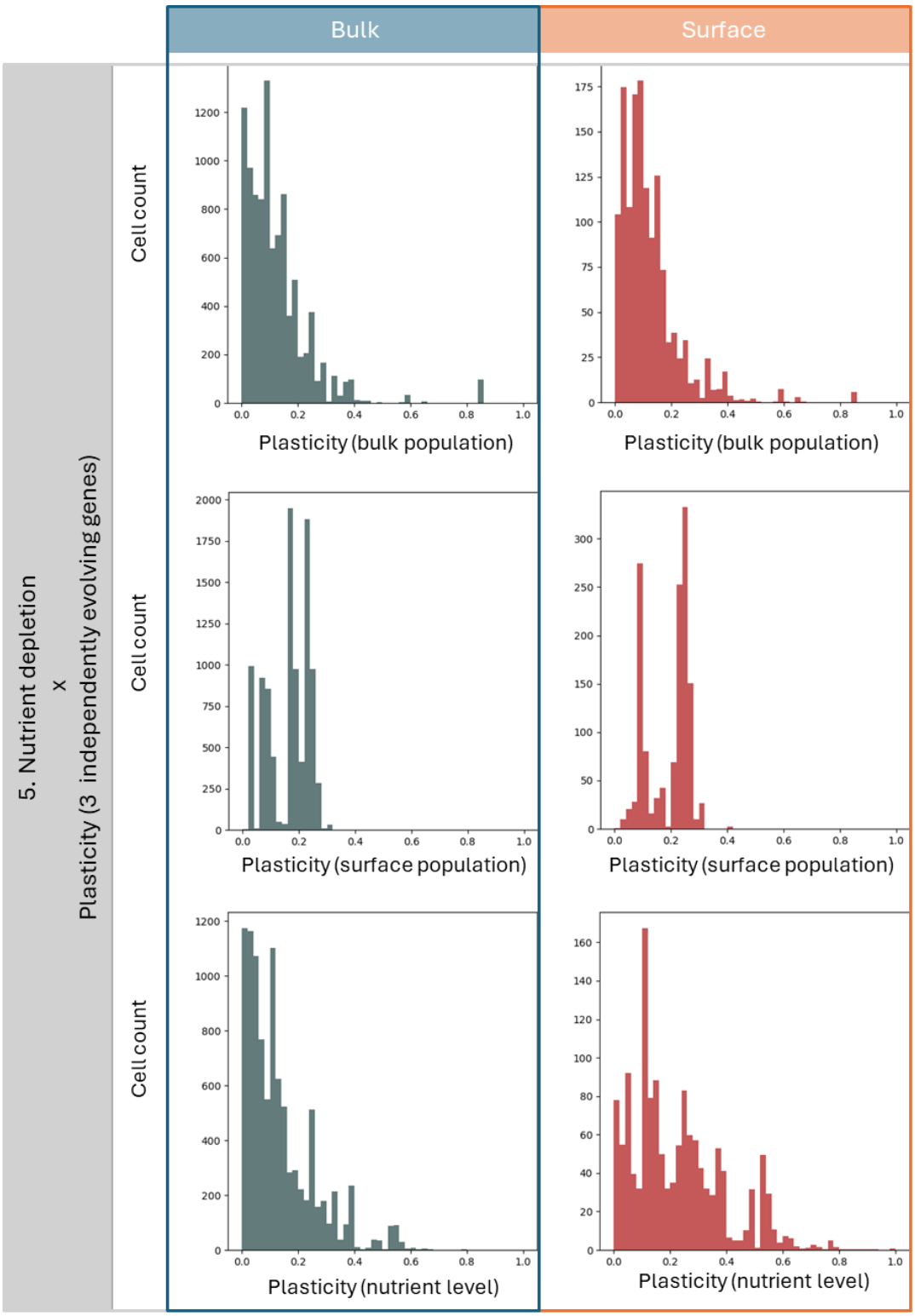

Figure 14.2: Histograms show the weighting factors corresponding to the plastic reactions to (top) population sizes of the bulk space, (middle) surface demographics, and (bottom) nutrient availability on the surface, respectively.

fluctuations. Consequently, the surface and bulk populations evolve low to intermediate plasticity to all cues, while the adhesion genotype evolves to minimal levels. The resulting phenotype of the bulk population is a reflection of the first plasticity gene. The other two genes do not affect bulk phenotypes. In surface populations, the phenotype is similar to that in other surface populations under nutrient stress (i.e., model steps two and four). Figures correlating these distribution patterns are included in the addendum (Figure A.5 – Figure A.7). For the total population, the phenotype is positively correlated with the plastic responses to bulk and surface population sizes ($r^2 = 0.72$, $p < .001$ and $r^2 = 0.01$, $p < .001$, respectively). These two plastic traits are negatively correlated with the third (i.e., plastic responsiveness to nutrient levels; $r^2 = 0.03$, $p < .001$ and $r^2 = 0.01$, $p < .001$, respectively). The bulk population shows similar correlations between traits, with the exception of the third plastic trait being negatively correlated with the phenotype ($r^2 = 0.04$, $p < .001$). The phenotype is again positively correlated with the plasticity in response to bulk population sizes ($r^2 = 0.99$, $p < .001$), and the third plastic trait is negatively correlated to the other two plastic traits (bulk population: $r^2 = 0.04$, $p < .001$, and surface population: $r^2 = 0.01$, $p < .001$). For the surface population, more trait correlations were found. The phenotype is positively correlated with the genotype ($r^2 = 0.01$, $p < .001$) and plastic responsiveness to surface cues (surface coverage: $r^2 = 0.11$, $p <.001$, and nutrient levels: $r^2 = 0.31$, $p < .001$), while for bulk cues this association is negative ($r^2 = 0.02$, $p < .001$). Similarly to bulk populations, there is a negative association between responsiveness to nutritional cues and demographic cues (bulk: $r^2 = 0.03$, $p < .001$; surface: $r^2 = 0.08$, $p < .001$) for surface cells.

In order to get a clearer picture of the dynamics through time, Figure 15 is included. That shows the evolutionary path of the adhesion phenotype (left) and the first plasticity gene (right) followed by the planktonic cells of simulation one. High phenotypes slowly disappear from the stage, while lineages with lower phenotypes generally display higher survival rates. For the plasticity gene - the only one of the three that is influenced by a cue that can be interpreted by bulk cells - a similar pattern as for the phenotypes can be observed, with the exception that the plasticity trait follows a less continuous distribution and less temporal oscillations (i.e., a pattern that was not picked up by the histogram as that is only a snapshot).

Similarly, Figure 16 shows the evolution of the adhesion phenotype and the second and third plasticity genes for cells on the surface in simulation one. Here, a rhythmic pattern can be observed for the phenotypes but not for the two plasticity genes. The periodic branching is likely related to the life cycle of the biofilm. That is, each time the resources on the surface become scarcer, lineages with a highly plastic response to local energy sources may decrease adhesiveness to

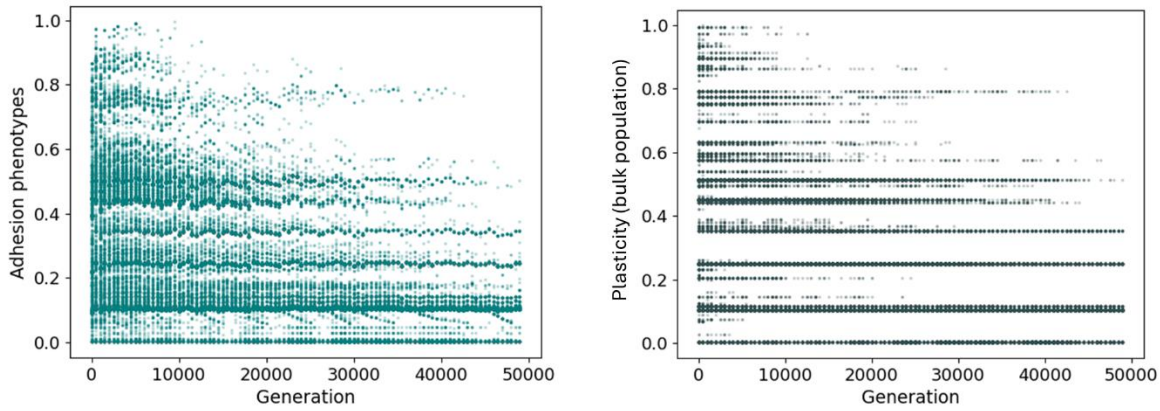

Figure 15: Dynamic nutrient regime with plasticity (environmental cues = population sizes of own habitat and, if applicable, nutrient level on the surface) over time (i.e., 50000 generations). Plasticity is encoded in three genes that can evolve independently. Dots represent the individual data from bulk cells over time for one simulation. Adhesion phenotypes are shown on the left, and the evolution of the first plasticity gene – corresponding to plasticity in response to bulk population – is shown on the right.

prepare for detachment. In other words, cells with a strong plastic response to nutrient levels (3+) and a weak reaction to surface population sizes (2) correspond to the steeply descending branch (following exponential decay).

Individuals with lower levels of the third plasticity gene can react less swiftly to dropping resource levels, and therefore, the cyclic phenotypic decline is less steep. This results in a ribbon at the bottom of the figure consisting of cells that react weakly to nutrient levels. Based on the plastic behavior related to population sizes, three abundant lineages (in dark orange) can be distinguished within this zone. Lineages with high plastic sensitivity to surface coverage (2+, 3-) will express relatively high adhesiveness since population pressure is a minor stressor in this disturbed system. For cells that are less equipped to react to low competition on the surface (i.e., lineages with lower levels of this plasticity gene), expressing low levels of the trait may be more cost-efficient (i.e., the lower band of adhesion phenotypes). Hence, a slightly weaker response to surface coverages (2, 3-) will show a similar pattern at lower values for the y-axis. Finally, cells with low plastic responsiveness to both cues will start a biofilm cycle at relatively low adhesion phenotypes (2-) and show a gentle slope (3-).

To investigate this pattern further, we tested the correlation between phenotypes and the plasticity genes associated with surface cues for this case specifically (addendum, Figure

A.8). Indeed, the cells on the correlation plots align with the endpoints shown in Figure 16, supporting the hypothesis that relates 1) the steepness of the phenotypic decline with the plasticity in response to nutrients becoming scarcer, and 2) the position on the y-axis with the plastic response to surface coverage. Note that the exact pattern that is formed varies among simulations and that this illustration only functions to explain the system dynamics.

Figure 17 is another representation of the biofilm process through time based on the last phase of the model, but these snapshots capture the spatial dynamics taking place on the surface. Figure 17.A depicts a surface population at generation 25000. In this young biofilm, most cells express a highly adhesive phenotype. A few less adhesive cells have settled around the colonizers. During maturation, empty spaces are filled

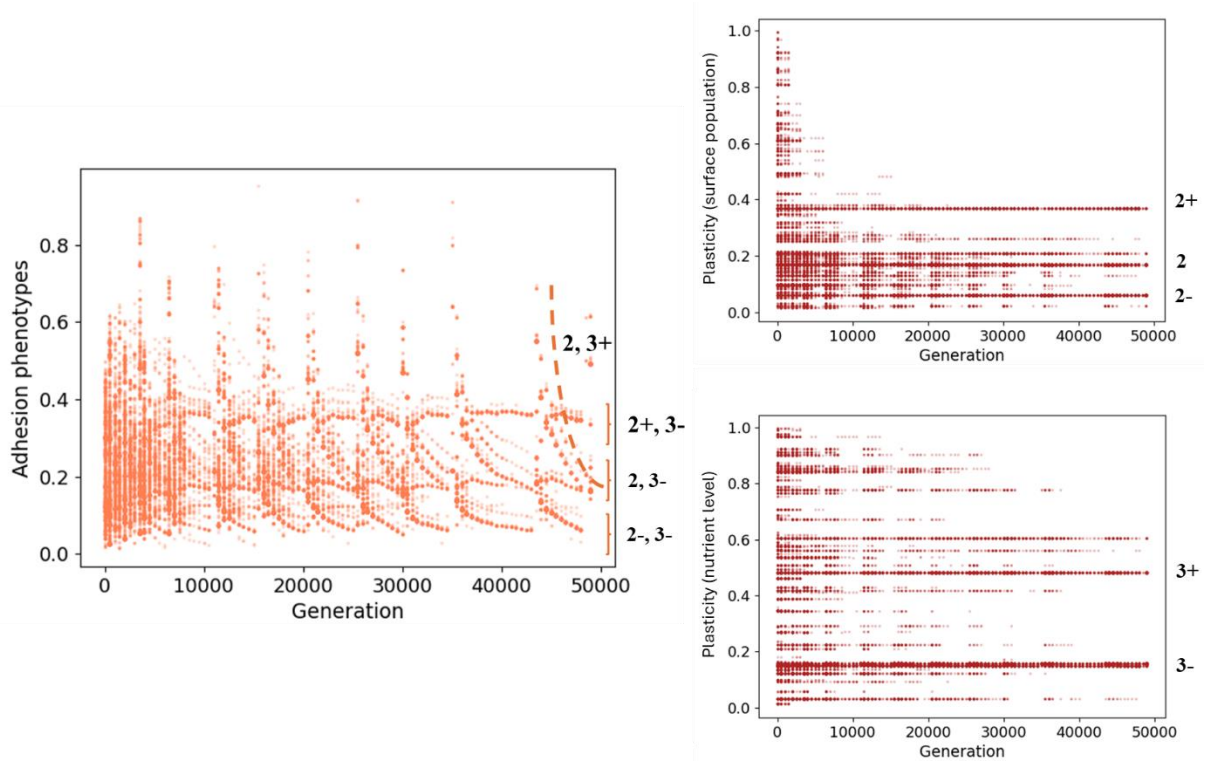

Figure 16: Dynamic nutrient regime with plasticity (environmental cues = population sizes of own habitat and, if applicable, nutrient level on the surface) over time (i.e., 50000 generations). Plasticity is encoded in three genes that can evolve independently. Dots represent the individual data from surface cells over time for one simulation. Adhesion phenotypes are shown on the left, and the evolution of plasticity in response to surface coverage (top) and nutrient availability (bottom) are displayed on the right. The dotted line marks the exponentially decreasing phenotypes associated with high plasticity in response to (exponentially decreasing) nutrient levels (i.e., 2, 3+). Braces indicate lineages with – from top to bottom – decreasing plasticity in response to surface coverage (i.e., 2+, 2, and 2-, respectively) and low plasticity in response to nutrient levels (i.e., 3-).

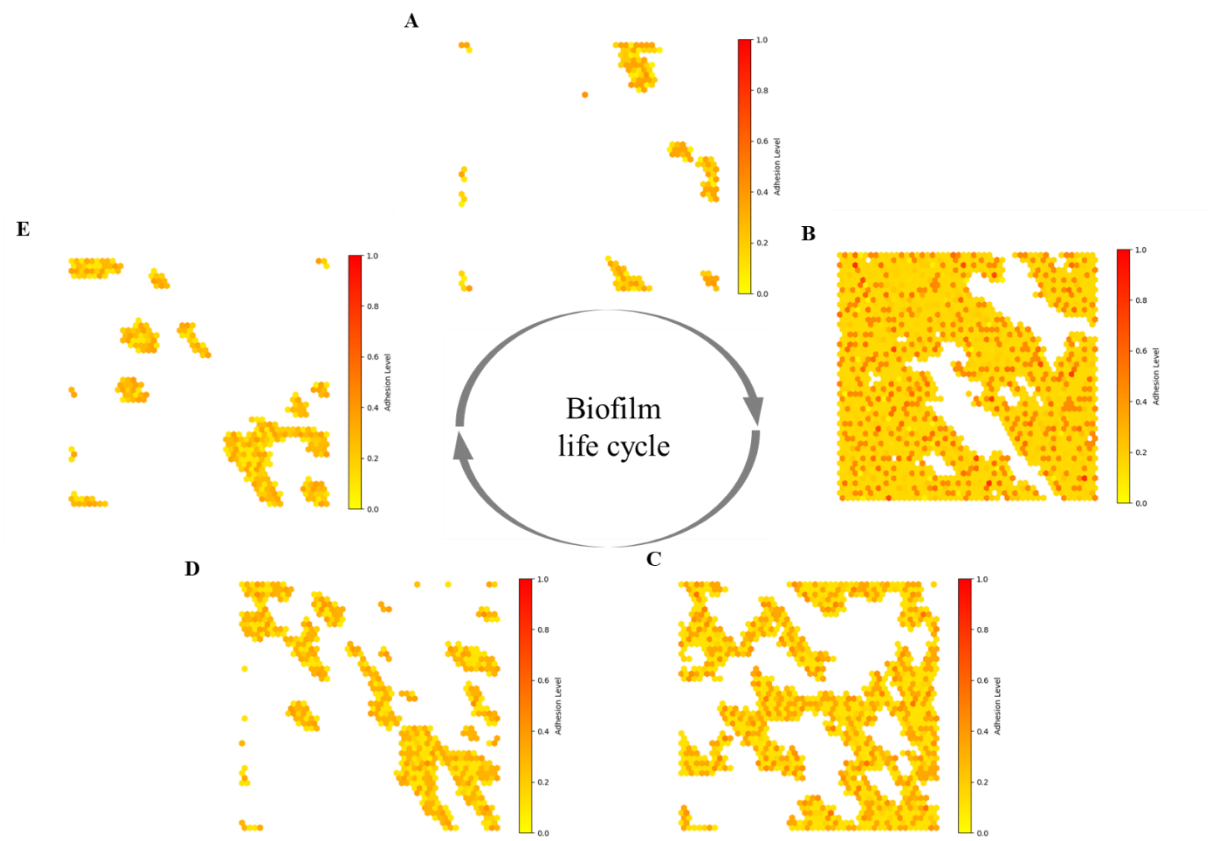

Figure 17: Succession cycle on the surface. Adhesion phenotypes of the cells are shown in red tones: slightly adhesive individuals are yellow, and this color progressively darkens as the adhesiveness rises. Figures A-E show the spatial distribution of cells on a surface at generation 25000 until generation 27000.

with poorly adhesive cells, and the surface grid gets crowded (Figure 17.B at generation 25500). However, due to severe energy consumption at high population sizes, nutrients are depleting rapidly, and thus, many cells leave the surface (Figure 17.C at generation 26000 to Figure 17.E at generation 27000). Also cells that previously produced high quantities of adhesins are now expressing lower levels of adhesion (i.e., the color intensity of the most adhesive cells drops). This gradual decay continues until the nutrients are depleted, and the cycle is repeated on a freshly stocked surface

Environmental change

In the fifth and final phase, the central aim is to unravel the effects of environmental instability on the system. That is, how will the evolutionary paths of population members be influenced by the repeated discontinuation of biofilm development as a result of nutrient depletion? And does the predictability of the stressor matter? In other words, will an increase in abrupt, fast changes influence population composition differently than an increase in gradual and predictable fluctuations? To examine this, we measured the attained adhesion phenotypes after 50000 generations of

development in a system with differing initial nutrient levels. The more resources, the older a biofilm can become before being fully depleted, and therefore, the longer a succession cycle will last. Additionally, disruption events were added to the model, with a probability of zero (control) or 0.01 per generation. When such an event strikes, all biofilm cells die, the surface is replaced and colonization by bulk cells can start over.

Figure 18 shows the results of this test on bulk (blue) and surface (orange) cells. Impoverishing or enriching the nutrient regime did not cause consistent changes in the phenotype distribution, suggesting no monotonic relation between both. However, we can observe a trend of lower inter-niche differentiation and, overall, a broader phenotypic range for cells experiencing slower surface turnover. This pattern is caused by the underlying plasticity genes (i.e., those responding to surface cues) having a more uniform distribution for high initial nutrient levels. For biofilms with a fast turnover, nutrient levels will become a less reliable cue compared to population sizes, and therefore, these populations peak at high levels for the second plasticity gene and at low levels for the third. For bulk populations, the adhesion likely reaches higher levels when surfaces have more resources as a result of selection for biofilm growth. In contrast, bulk populations show a selection regime that is typical for the association with young biofilms (cf. bimodal pattern Figure 10.2) when turnover is high.

The bottom row of each figure shows the evolution of adhesion and plasticity in a system with high disruption rates. Due to the unpredictable character of this stressor, plastic responsiveness to surface cues decreases, while levels of genotypic adhesion and plasticity based on bulk cues increase. On the surface, few cells express the successor phenotype as the populations do not reach a mature state. Expressed bulk adhesion levels are higher as a result of this increased ability to react plastically to bulk population stress. This way, bulk cells can easily attach to the surface. Once they have reached this new niche, cells can profit from the lower population pressure to expand, especially when (initial) nutrient levels are elevated. When there is a high probability of surface disruption, cells ideally only remain attached for a limited time. Having a weak plastic response to surface cues enables cells to detach readily. As such, a part of the cells that display this ‘risky’ strategy can successfully attach, grow, and detach again before a disruption event takes place.

Combining both stressors gives rise to intricate responses, and more analyses on the spatial and temporal dynamics are needed to fully comprehend this. For instance, stress caused by disruptions and nutrient deficiencies seemingly have an antagonistic effect on the plastic response to nutrient levels, which could be an indirect effect of the other plastic reactions being affected more negatively. Nutrient levels are, thus, not necessarily a more reliable cue in

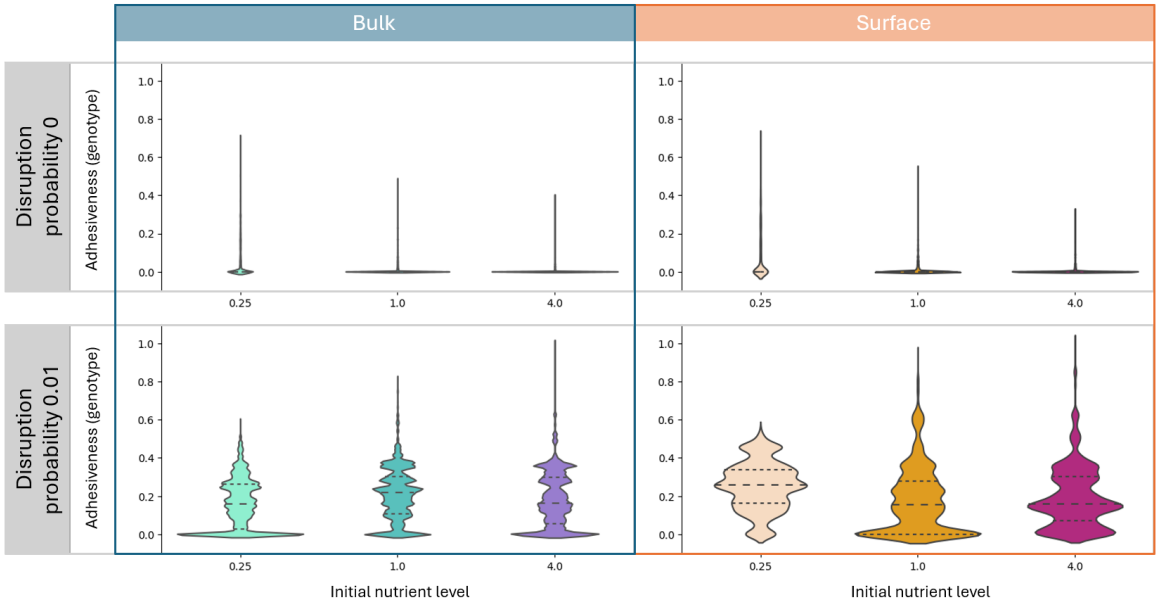
Bulk
Surface
Disruption probability 0
Disruption probability 0.01
Adhesiveness (genotype)
1.0
0.8
0.6
0.4
0.2
0.0
0.25
1.0
4.0
Initial nutrient level

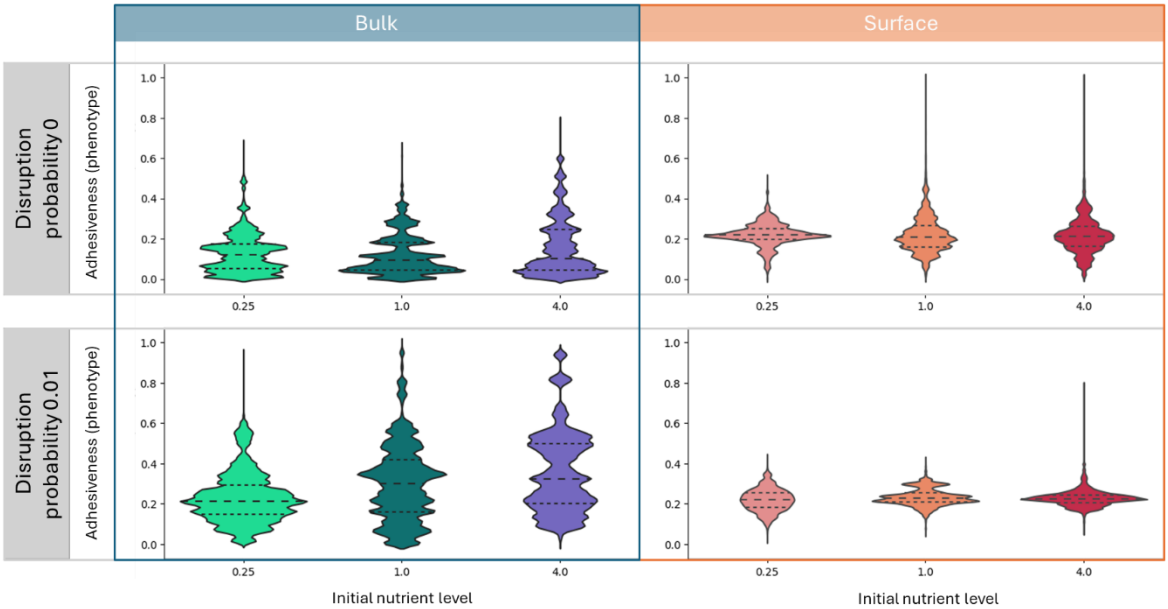
Bulk
Surface
Disruption probability 0
Disruption probability 0.01
Adhesiveness (phenotype)
1.0
0.8
0.6
0.4
0.2
0.0
0.25
1.0
4.0
Initial nutrient level

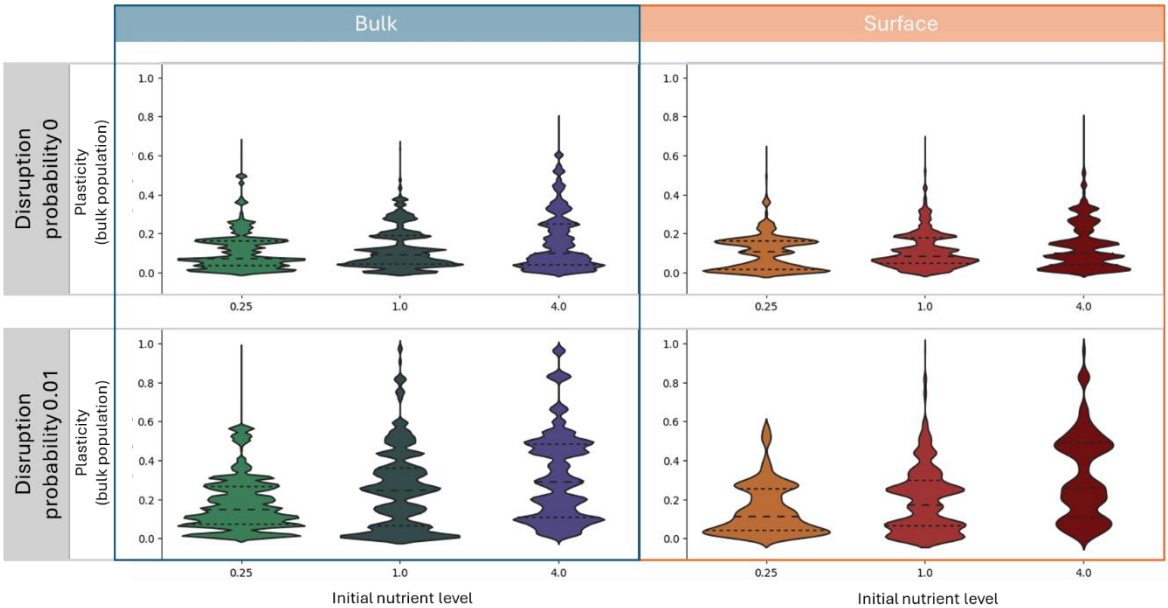
Bulk
Surface
Disruption probability 0
Disruption probability 0.01
Plasticity (bulk population)
1.0
0.8
0.6
0.4
0.2
0.0
0.25
1.0
4.0
Initial nutrient level

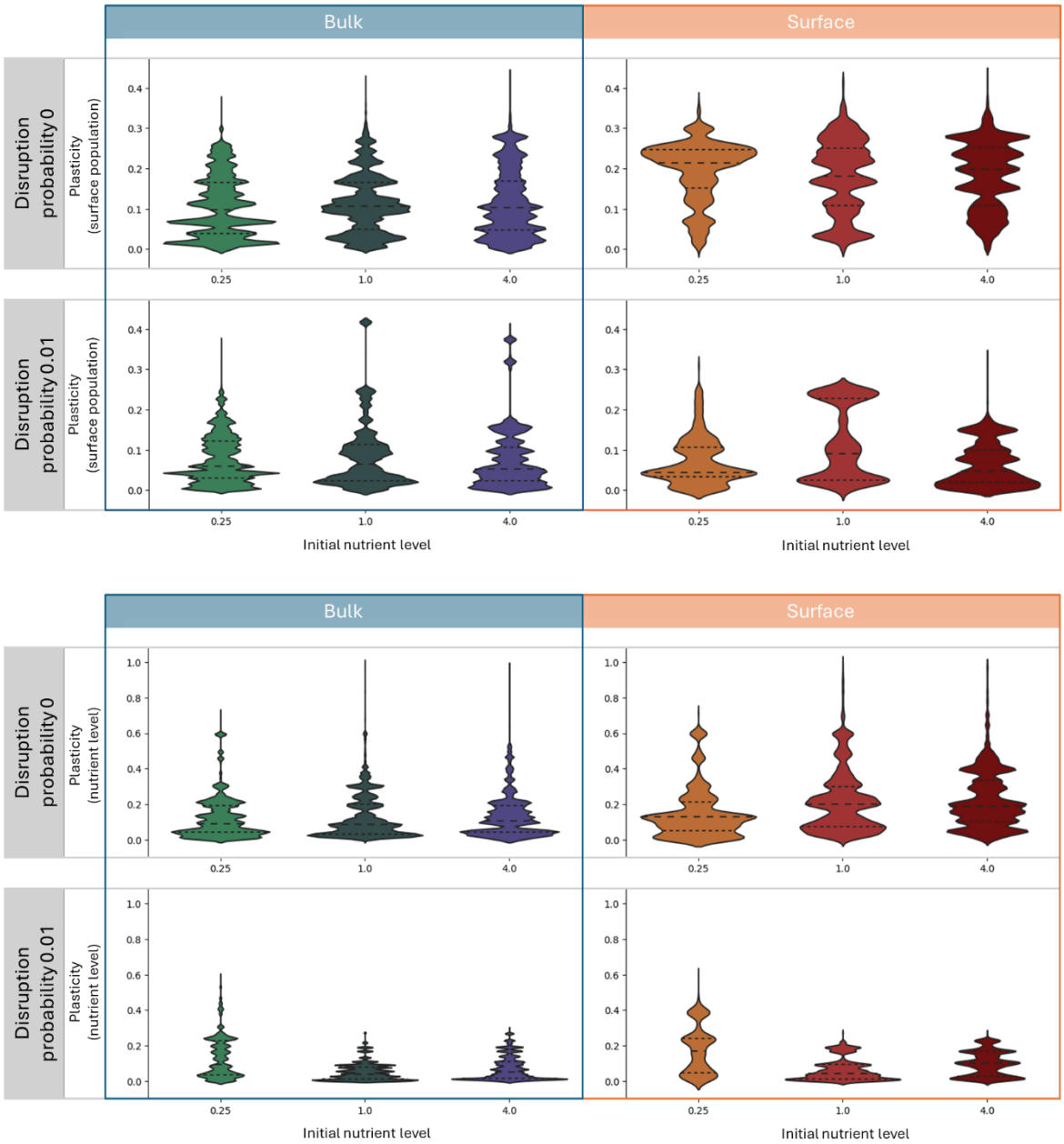

Figure 18: Violin plots show the distribution of adhesion genotypes (top), adhesion phenotypes (middle), and the three plasticity genes (bottom) in the bulk (blue) and the surface (orange) after 50000 generations for varying initial nutrient levels (vertically) and disruption probabilities (horizontally). Dashed lines show the median, and the dotted lines show the boundaries of the interquartile range. Data from 20 simulations are plotted.

frequently disrupted systems, yet cells that disperse from surfaces with few resources effectively escape disruption events. Test statistics were added to the addendum (Table A.2 and Table A.3).

Discussion

Biofilm growth is characterized by an ecological succession of different ecotypes, of which adhesion ecotypes are the focus of this work. Our model showed that when starting with a non-adhesive bulk population, some lineages will evolve increased adhesive potential. As these lineages become more adhesive, the probability that some members will manage to attach increases. Successful colonizers can exploit a vacant niche and, as such, outrun competition with the bulk population (i.e., niche partitioning). Furthermore, early colonizers provide anchors for less adhesive cells to attach to and, hence, facilitate the growth of successor cells (i.e., niche modification). This newly formed population is relatively resistant to environmental fluctuations. However, when more detrimental environmental stresses strike, cells are often forced to disperse or undergo apoptosis. The succession cycle is reiterated when the surviving lineages colonize a new substrate. In this work, we reviewed the abovementioned stages with individual-based simulations, tracking the evolution of adhesion and plasticity under various circumstances.

Successional stages

As a first step, we examined the successional stages in more detail. To specify, we studied how ecotypes interact and how eco-evolutionary feedback mechanisms shape the population. Beginning with surface colonization, we found that microcolonies are nearly exclusively founded by strongly adhesive cells. That was expected, bearing in mind that even though, in every generation, a fourth of the planktonic cells attempt to adhere, cells are still completely self-dependent at this stage. To clarify, candidates have a chance of attaching to an empty surface that is proportional to their adhesion level. Failing cells return to the bulk space, and successful cells attach reversibly. As found in natural biofilms (Saur et al., 2002), cells bind irreversibly once bonds are consolidated; or in this model, when the sum of their adhesion level and that of adjacent neighbors reaches one. Subsequently, slightly adhesive cells can also start attaching to the surface by finding a spot next to adhesive individuals. As such, adhesive cells modify the available niches, facilitating the rise of less adhesive lineages. Like van Gestel and Nowak, we found that incoming cells indeed surround adhesive colonizers (2016). Later, successors start padding empty spaces between the microcolonies. In conclusion, colonizers fuel ecological succession characterized by a beginning stage of high average adhesion followed by declining levels, and by extent, they drive diversification in adhesion genes, as found in various natural systems and computer simulations (Flynn et al., 2016; Odling-Smee et al., 2013; Poltak & Cooper, 2011; Rainey & Travisano, 1998; Spiers et al., 2002; Traverse et al., 2013; van Gestel & Nowak, 2016)

Diversification and demographics

This diversification process was influenced by the demographic properties of the population. More specifically, we found a diversity valley for populations with the

lowest initial population sizes. The beta regression also shows a positive trend between initial population sizes and Gini-Simpson diversity indices ($p = 0.068$). Note that this trend becomes significant when the parameter combinations with limited sample sizes are omitted ($p < 0.001$). This idea is known as the founder effect, introduced by Mayr for cases where the isolated introduction of a limited number of founders gives rise to a genetically uniform population (Provine, 2004). In contrast, when the simulation is initiated with high population sizes, genetically distinct colonizers can establish microcolonies. As such, the founder population starts with more standing variation, which results in higher diversity among cells after 50000 generations. Similarly, allelic richness rises with increasing numbers of founders.

Also, high-adhesion phenotypes are favored under these conditions, as more new migrants can come in before descendants of the fast-growing, slightly adhesive cells have spread over the entire surface. That adds to the total Gini-Simpson diversity since high adhesiveness is rare in this system. Contrarily, van Gestel et al. have reported the opposite. Their experimental and mathematical study showed that highly adhesive cells are disfavored in systems with high initial cell densities because, as spatial segregation decreases, their competitive potential does so too. It is worth considering that sample sizes affect allelic richness, and that bulk populations are relatively low at this diversity peak, whereas surface populations have intermediate sizes (Leberg, 2002).

Furthermore, we found that diversity was lowest at intermediate levels of surface growth. Note, however, that the carrying capacity also influences the site of the valley, as, in the triangular representation we employed, the maximum of one variable is always combined with minima for the other studied variables. The beta regression indicated that surface growth rates have a negative effect on the Gini-Simpson index levels ($p = 0.025$). A reason for that could be that high surface growth rates confer a disproportionately high growth advantage to the competitive phenotype. Allelic richness did not show a clear pattern in relation to surface growth.

The Gini-Simpson diversity peak also aligns with low to intermediate carrying capacity. Consider that this partly happens because of overruling influences. The beta regression shows that the main effect of carrying capacity on the Gini-Simpson diversity is not significant ($p = 0.78$). Likely, it is not positive because the selection in favor of colonizers in the bulk space decreases over time. Thus, after the colonization stage, the bulk population will reach a point where non-adhesive cells fill all remaining empty spots. Hence why the rare alleles decline in relative terms.

Similarly, the effect of the carrying capacity on the allelic richness is unclear. However, we would expect that this relationship is

strictly positive because the absolute allele count cannot be lowered as more individuals are added to the population. The fact that the effect is not strong enough to cause a clear pattern likely has to do with the limited data range for this variable (due to computational limits). It can also partly be caused by the high selection pressure for non-adhesive planktonic cells. Therefore, when bulk populations grow, nearly no new alleles will be added to the gene pool. It is again critical to consider that carrying capacity positively affects population sizes and, therefore, affects the interpretation of allelic richness (Leberg, 2002).

Overall, these results highlight the importance of priority effects. As the initial population size rises, more founders can colonize the surface, increasing the overall diversity of the future population. Adhesive cells modify the niche and, as such, facilitate the establishment of successor lineages. The carrying capacity influences the abundance and arrival timing of new immigrants. In other words, their ecological opportunity depends on the niche occupation upon arrival (Brockhurst et al., 2006). Invading a population with higher fitness (closer to the ESS) is unachievable. However, these later-arriving cells often have a fitness advantage since bulk selection favors low-adhesion phenotypes (like in older biofilms). Therefore, the pre-adapted invader can win the evolutionary race from the early-arrived colonizer (De Meester et al., 2016). Lastly, as surface growth rates increase, the adaptational process of the colonizer population is accelerated, which can confer fitness advantages to the colonizers and hinder the establishment of new immigrants (Svoboda et al., 2018). However, if slightly adhesive cells accompany adhesive colonizers early on, these will spread disproportionately fast. Increased surface growth rates can, thus, affect the genetic profile of the population in various ways. In short, this experiment shows the importance of diversification rates and the chronology of immigration events, as studied by e.g., Fukami et al. (2007) and Gómez & Buckling (2013).

Note that the Gini-Simpson diversity index measures the probability that two randomly selected individuals belong to different groups (e.g., alleles) (Roswell et al., 2021). More specifically, it compliments Simpson's D, which is higher for low diversity, and therefore, the Gini-Simpson index is perceived as less counterintuitive. The Gini-Simpson index is, however, not popular in microbiology (Feranchuk et al., 2018). Accordingly, we recognize that the simplicity of this measure often does not match the complexity of microbial populations, and extremely high levels of inequality are found in microbiological studies compared to those conducted in human societies (where it is used most). Therefore, more elegant measures are often preferred over the traditional diversity indices (i.e., allelic richness, Shannon diversity index, and Gini-Simpson diversity index). Nevertheless, bearing these drawbacks in mind, we argue that the Gini-

Simpson diversity index can still be useful for us since we compare diversity results between simulations performed with a strongly simplified computational model, and especially because in this work, measuring the trait distribution is of great interest.

Another problem arises when choosing between these traditional measures since they each measure different ecological population traits (Roswell et al., 2021). The allelic richness is the mean number of alleles present in the population. To compare, the Shannon index, which measures the uncertainty regarding the allele identification of the sample, is more frequently used in microbiological research (Feranchuk et al., 2018). However, to prevent an overload of information, we chose to omit Shannon diversity from the analysis because this measure gives more weight to rareness than the Gini-Simpson diversity index but less than the allelic richness. Allelic richness was included in the addendum since it provides information on long-term adaptability and persistence opportunities (Greenbaum et al., 2014). In order to obtain this count, we binned the alleles in 100 intervals of 1% each. This binning process is highly artificial. In more advanced models representing populations of specific model organisms, the alleles should be encoded using more realistic and sophisticated systems (e.g., discussed in Idury & Cardon, 1997).

Diversification and productivity

Previously, we have established that demographic parameters influence population diversity. Here, we discuss how diversification, in turn, affects biofilm productivity. Depending on how ecotypes interact, they will show gains or losses in growth when coinhabiting a biofilm compared to living isolated (Tan et al., 2017). As expressed by van Nadell et al., biofilm populations are built on a harmony of cooperative and competitive associations (2009). On the one hand, population productivity is expected to advance with diversity in biofilms formed by positively interacting members (i.e., mutualism or commensalism). Indeed, Poltak & Cooper showed augmented biofilm yields in mixed compared to homogeneous biofilms because of the facilitative effects of adhesive colonizers on less adhesive successors (2011). Comparably, we found that certain niche specialists complement each other and reach higher total population sizes when grown together. Aside from biofilm induction and mass, additional forms of synergisms have been found, including cases of nutrient cross-feeding, transfer of genetic material, and enhanced resistance (Joshi et al., 2021; Sadiq et al., 2023). Ren et al. demonstrated that synergies have a widespread presence in natural biofilms (2014). Yet, according to Madsen et al, their prevalence is strongly influenced by the joint evolutionary history of strains (2016). While local cooperation is found in many instances, global cooperation across all biofilm cells is rare (Nadell et al., 2009). Instead, many cells

interact antagonistically through competition for resources and space or by producing inhibitory compounds (Nadell et al., 2016). In this model, resource competition was included on the surface by reducing nutrient levels proportionately to the number of consumers. Bulk population pressure was implemented by imposing a carrying capacity of 2500 cells, like for surface populations. Also, the number of empty spots adjacent to the focal cell limits division by sessile individuals. Especially for adhesive cells, that hinders growth because they quickly become surrounded by less adhesive cells that arrive in great numbers from the booming bulk populations and spread rapidly on the surface. Therefore, biofilm specialists can often expand more when growing isolated.

Furthermore, we found that, depending on the level of specialization, different biofilm output is obtained. We found that high degrees of specialization resulted in reduced yields. That is caused by the trade-off between the energetic costs of high adhesion and instability at low adhesion levels (Schluter et al., 2015). To understand around what point balancing selection operates, we performed an invasion analysis on biofilm populations that evolved for 25000 generations. The PIP indicated that the ESS approximates an adhesion level of 0.225 in this model, meaning that no mutant can invade a resident population that has reached this equilibrium. Conversely, mutants lying closer to this point than the established population will invade as the ESS is convergence stable. This analysis also illustrated that many ecotypes can coexist, especially relatively highly adhesive ones. It is likely that NFDS sustained the long-term coexistence in this model.

Cyclicity and plasticity

Poltak & Cooper found that long-term selection for adhesion to the surface induces ecological succession, even in the absence of standing genetic variation in the initial population (2011). Similarly, in this work, we wanted to investigate the eco-evolutionary dynamics that occur when a new niche becomes obtainable for a - formerly only - planktonic population. Hence why, our starting population was characterized by non-adhesive cells. However, to accelerate the evolutionary process for computational reasons, the initial population had a standing variation, i.e., a normal (Gaussian) distribution around zero with a standard deviation of 0.1. Negative values were replaced by zero. Moreover, we analyzed whether the same ESS would be reached when employing continuous trait levels instead of discrete levels.

For the simplest model with continuous traits (but no nutrient depletion or plastic responses), we found that most planktonic cells were non-adhesive and most sessile cells carried a genotype around the ESS, as predicted earlier. These two ecotypes arose after a bifurcation in their respective evolutionary tracks, driven by the trade-off between bulk and surface growth (Østman et al., 2014). A smaller proportion of both populations carried a genotype typically found in the other niche. Adhesive genotypes

can be found in the bulk since, in every generation, approximately 400 to 500 cells detach from the surface. That number can be explained by taking into account that the average surface cover amounts to less than 14%, which signifies that cells have a probability of 82.3% to have at least one neighbor, after which the probabilities rapidly decrease (i.e., 11.3% for two or more neighbors, 2% for at least three and so on). Given that the focal cell and its neighbors have average adhesion levels, each cell has a probability of around 50% to detach. However, since cells are clustered in microcolonies, the detachment probability drops to around a third per generation. The non-adhesive subpopulation on the surface is likely formed by successor cells from the bulk that have seized the opportunity to attach to a microcolony, making the adhesion of the newcomer redundant.

In the model with nutrient depletion, non-adhesive cells can less easily invade since there are fewer cells to stick to in biofilms that are continuously reinitiated compared to aged populations. Similarly, Jayathilake et al. showed that low coverage enhances the competitional advantage of adhesive cells (2017). Also, hydrodynamic factors affect the interaction between cooperators and cheaters by influencing spacing patterns in the biofilm (Rossy et al., 2019). For the bulk populations, we observe even more change compared to the previous step of the model. Here, the peak with adhesive cells is taller and broader than the elevation with non-adhesive cells. That happens because, in this regime, where surfaces are refreshed cyclically, there is selection in favor of colonizers in the bulk population. Compared to the previous model, there is less detachment in absolute counts (i.e., several dozen across all surfaces per generation), as the surface contains little cells to let go of in the first place (i.e., coverage of around 7%). Yet, adhesive cells from the bulk can attach to the surface for a couple of generations, during which they can expand as there is very little competition for space. Later, cells can detach again. If they do so before the surface renews, lineages can bypass growth limitations in the bulk at carrying capacity.

In the third phase, cells could react plastically in response to their population sizes. Comparably, the perceivable environmental cue was the nutrient level of the - gradually impoverishing - surface in phase four, and the last phase combined the two. That is, three genes could evolve independently of which two were coupled to the respective population sizes and the other to resource levels. These cues affect dispersal through altered adhesion levels, as found in biofilm-producing bacteria such as *Vibrio cholerae* (Nadell et al., 2008) and *Pseudomonas putida* (Gjermansen et al., 2005), respectively. There are multiple reasons why it may be more beneficial for a population to develop plastic responsiveness as opposed to maintaining a diverse array of adhesion alleles. Firstly, and mainly, a flexible strategy confers more fitness benefits than a static one in systems subjected to environmental change (Yan et

al., 2017). Another contributory factor can be that the initial population starts with minimal adhesion (as cells are planktonic) but with standing variation for plasticity. A third explanation could be that cells with high adhesion and low plasticity leave the bulk fast since they can adhere independently of others. Contrarily, individuals with low adhesion and high plasticity express only slightly adhesive phenotypes as long as bulk populations are relatively small and, thus, they generally remain in the bulk space for longer. Cells not yet attached to colonizers will increase their adhesion levels plastically and form new colonies on the surface once bulk spaces become more populated. By this time, the plastic planktonic cell will have grown more than the adhesive colonizers. That is because bulk spaces are more favorable for growth at intermediate population sizes since growth opportunities of planktonic daughter cells are unrestricted by the number of neighboring cells. Non-plastic cells with a low-adhesion genotype (first peak) are fast growers and can join the biofilm if others accommodate their lack of adhesion. Having both a high-adhesion and a high-plasticity allele would be redundant, and thus, this combination is not present in the population after 50000 generations of evolution.

Generally, there is a higher selection pressure for phenotypic plasticity in fluctuating regimes (Yan et al., 2017). Yet, we observed the opposite. The population in phase three evolved to higher plasticity levels than the fourth phase populations did, while the former did not include a regime with cyclical nutrient depletion. It is, however, worth calling to attention that in the combined phase, which also includes environmental fluctuations and three independently evolving plasticity genes, the gene whose expression is regulated in response to surface coverage reaches relatively high levels compared to the other two plasticity genes. That indicates that, in this system, surface coverage is the best predictor of the optimal strategy for surface cells.

The fact that these levels are higher than the levels of the plasticity gene related to bulk population sizes indicates that surface coverage transfers relatively more valuable information to individuals than bulk population sizes. That would result in the observed differentiation between both genes when independent evolution is included in the model. Monitoring surface populations is likely more efficient since these follow a succession cycle characterized by different growth conditions, whereas bulk populations stagnate once having reached the carrying capacity. Compared to nutrient levels, surface coverage may also be the preferred cue. That is because – aligned with the resource levels – the plastic reactions decrease (approximately) exponentially in magnitude and, therefore, phenotypic adhesion levels can be altered with far less than 0.5 on average for maximum plasticity. Contrarily, the average adhesion boost in response to surface coverage (i.e., 14%) would continually account for over 0.86 for

maximum plasticity. The latter, thus, results in a fiercer plastic response for an equivalent energetic cost. This dynamic is expected in all cases where surface coverage is less than 50%. Moreover, because of this cyclical pattern, nutrient levels have a broader range compared to surface coverages, and, therefore, the level range of the third plasticity gene is more widespread than that of the second. The analysis of the correlations between these traits per cell confirmed this hypothesis.

Another noteworthy result is that, in the fifth phase, there is less differentiation between bulk and surface subpopulations. Instead, under the fifth regime, cells evolve plasticity, enabling them to thrive in both niches. In other words, even though the bulk genotypes approximate those on the surface, generalist cells can match the environment due to their plastic characteristics. Logically, bulk phenotypes are the strongest correlated with the expression of plasticity gene one, and for surface phenotypes, levels of plasticity genes two and three are the most defining. The plastic response to nutrient conditions is negatively correlated to the responsiveness to surface coverage ($r^2 = 0.08$, $p < .001$), likely because investing in both cues is energetically too costly compared to the added advantage. van Gestel and Weissing showed that this limitation plays a lesser role in more mechanistic gene regulatory network models compared with classical reaction norm models like we used (2016).

When comparing the temporal dynamics, we found that cyclic nutrient depletion gives rise to populations with less inter-niche differentiation. Plasticity in response to surface coverage likely caused the cyclic phenotypic differentiation in phase five. Illustrations of the spatial dynamics showed strong inter-colony phenotypic differentiation. However, as global environmental cues are assessed by cells, phenotypic differences are indicative of genetic diversity within microcolonies.

Adapting to instability

In the final part of the model, we introduced varying degrees of environmental stability by manipulating initial nutrient levels and the probability of disruption events. The interpretation of these results is not straightforward, and tests of the spatial and temporal dynamics are needed to come to firm conclusions. Nevertheless, some general trends can be observed. More specifically, surface cells showed a more powerful plastic response to surface coverage when turnover was high. That is likely because population sizes are kept small in this system, resulting in a plastic response that enables them to remain attached. For low turnover, we found higher levels of plasticity associated with nutrient levels. That means cells are highly adhesive when nutrients are abundant, and growth conditions are extra beneficial on the surface. As nutrient supplies decrease – and by extension, growth opportunities drop – these cells can respond by gradually lowering adhesion, and eventually, they can

detach before the surface is replaced. As such, these generalists can exploit both niches (i.e., bulk and surface) and match the successional stages.

In populations subjected to high probabilities of surface disruption, the selection pressure on colonizers increased in bulk populations. As these disruption events were entirely unpredictable, sensitivity to surface cues decreased (Reed et al., 2010), whereas responsiveness to bulk population sizes increased. Therefore, cells respond to bulk population stress with increased adhesiveness and attach to the surface. Once there, the production of adhesins goes down because cells are less sensitive to surface cues. Cells that remain attached long enough to divide but detach before a disruption event occurs can successfully evade the growth limitation in overpopulated bulk spaces. In other words, generalists who adopt this 'risky' strategy can balance growth with the risk of disruption events by speeding up the biofilm life cycle. Importantly, we found that increasing disruption probabilities is associated with genetic diversification. Diversifying the array of phenotypes may, namely, enhance the long-term survival of a population in the face of unpredictable changes (Donaldson-Matasci et al., 2013), as seen in bet-hedging populations, for instance.

Alternative frameworks

Not addressed in the model was the effect of kin selection. As discussed by McNally and Brown, in the case of secretion of a public good, behavior is regarded as mutually beneficial at low cell densities, whereas, at high densities, it is altruistic (2015). Here, direct (return of product) and indirect (product available to kin) gains for the producer are density-dependent. The rationale behind the former is that producers have less access to the diffused public good at high population densities (Ross-Gillespie et al., 2009). Secondly, the relatedness of a producer to the population as a whole decreases, and hence, altruistic behavior is less likely to evolve (cf. Hamilton's rule: r*b>c; where r is relatedness, b is the benefit to the recipient, and c is the cost to the altruist; Hamilton, 1964). Xavier & Foster incorporated kin selection into an individual-based model, where cells act altruistically toward kin. That is, by secreting adhesins, they push descendants to the upper layers with more suitable oxygen conditions while neighboring lineages are suffocated (2007). In contrast to their model, this model only included two dimensions, and consequently, cells cannot give preferential treatment to kin through adhesin production. As a result, in 2D models, there is less incentive to produce adhesins. It is also important to note that the strength and direction of selection for these bacterial interactions depend on numerous parameters, such as relatedness, cell diffusion, and public goods confinement (Dobay et al., 2014; Drescher et al., 2014; Xavier & Foster, 2007).

Providing resources to non-kin is, in most cases, not beneficial. Therefore, cells will develop strategies to prevent this. Adhesive

cells can react to cheaters by increasing adhesion and broadening the phenotypic gap between ecotypes (Martin et al., 2020). However, this anti-cheat strategy is not sustainable in the long run and will shift into a case of "the tragedy of the commons", where cheaters take over. In contrast, other studies found that cells that react by lowering their adhesiveness can successfully prevent invasion by cheaters (Diard et al., 2013; Kümmerli et al., 2015; O'Brien et al., 2017). That can be achieved through several mechanisms (Rankin et al., 2007), such as diminishing returns (associated with decreasing effects of competition; Foster, 2004) and policing (c.f., worker policing in eusocial honeybee colonies; Ratnieks & Helanterä, 2009), and kinship. Other types of cheater control found in microbial populations and communities are discussed by Smith and Schuster (2019). None of these mechanisms were included in this study but could function as alternative frameworks.

Conclusion

To conclude, we assembled an evolutionary model with which we inspected the successional cycle of adhesion and plasticity levels. First, we only combined two discrete levels of adhesion and no plasticity. That provided insights into the principal mechanisms of the model. Most importantly, we found that highly adhesive cells decreased in relative and absolute numbers as biofilms aged. Furthermore, spatial illustrations of the biofilm showed how florets of slightly adhesive cells surrounding more adhesive individuals are formed. As a result, the growth of colonizers is spatially restricted. The invasion analysis revealed that the ESS of this model is found at an adhesion level of approximately 0.225. Next, instead of discrete trait levels, adhesion was encoded as a continuous trait. Also now, populations evolved towards the adhesiveness equilibrium of 0.225. Moreover, demographic parameters, including carrying capacity, initial population size, and surface growth rate, affected the population diversity. That highlights the importance of priority effects when studying ecological succession in biofilms. Subsequently, the effects of cyclicity and plasticity were investigated by comparing the distribution of the genes carried in the population and the resulting phenotypes for different combinations of model functions. Here, we found that cyclicity was associated with less phenotypic inter-niche differentiation. Furthermore, while genetic variation was minimized, a considerable part of the population was plastically responsive to population sizes and nutrient levels after 50000 generations of evolution. Finally, the model was completed by adding predictable and unpredictable system instability. We found that the evolutionary reaction to different degrees of instability depended on the type of stress. More specifically, populations subjected to high surface turnover showed signs of less phenotypic differentiation, as was found previously in rejuvenating biofilms with the introduction of cyclicity. Increased probabilities of chaotic disruptions, in

contrast, were coupled with increased genetic diversity.

Ultimately, this study shows that bacteria are highly adaptable to their biofilm environment, where niches are partitioned and modified. In the absence of nutrient depletion or plasticity, a generalist evolved. When plasticity was included in the model (i.e., phases three and four), two specialists evolved in the surface population, occupying a different niche. More specifically, among cells that sense population sizes, successor ecotypes are more abundant because of biofilm aging. In contrast, when we added system cyclicity and perception of nutrient levels, more cells expressed the colonizer ecotype. That is because only cells with adhesion alleles can colonize the surface if bulk cells cannot react plastically. When combining these plasticity traits, a generalist evolved again. Being able to respond plastically to multiple cues enabled this generalist to become highly successful, reaching double and quadruple population sizes compared to phases four and three, respectively. Moreover, demographic parameters and system instability affected the diversification processes. For instance, at high disruption probabilities, we observed genetic diversification, which can broaden the niche of the population as a whole. These results highlight the importance of the evolution of genetic diversity and/or phenotypic plasticity for populations to thrive under a wide range of ecological conditions.

A valuable addition to the model would be a parameter quantifying the relatedness of cells. As such, we could assess the role of kin selection as a driver of cooperation. It would then also be engaging to incorporate vertical growth. In a 3D biofilm model including kin selection, we could capture the altruistic effects of cells pushing daughter cells into layers with better conditions (Xavier & Foster, 2007). Here, cheaters are negatively affected by colonizers, while in our model, colonizers merely had a facilitating role. This trade-off may be a worthwhile addition when delving further into the eco-evolutionary aspects since the position that a biofilm cell takes up has been shown to have considerable effects on its competitional potential (Kim et al., 2014). Also, sporulation is a factor we did not account for, although it may influence the dynamics we observed (Van Gestel et al., 2012). Furthermore, by encoding the bulk in a spatially explicit model where all surface patches are integrated into one bulk space, we could gain insights into the spatial relationships between patches (DeAngelis & Yurek, 2016). Also, in the future, we could add variations in the number of surfaces between simulations and within runs (Ebrahimi et al., 2022). As such, we could grasp an understanding of the patch dynamics in a more realistic system where substrate availability fluctuates. Apart from the initial nutrient levels, directly manipulating the turnover speed of surfaces may help us unravel the effects of gradual changes. Also to this end, nutrient depletion could occur on a more local scale (Hunt et

al., 2004). Consequently, heterogeneity within the biofilm is introduced. Studying different heterogeneity patterns (gradual, predictable changes versus abrupt, unforeseeable changes) could clarify how environmental fluctuations affect the biofilm population. The extent to which populations evolve plastic responses to cues may also be affected by the rate of change, predictability, and cue reliability (Burton et al., 2022; Donaldson-Matasci et al., 2013; Reed et al., 2010). Hence, these factors could be taken into account. Moreover, how plasticity is incorporated into the model is improvable. For instance, we could explore using gene regulatory networks instead of our reaction norm model (Van Gestel & Weissing, 2016). Horizontal gene transfer may also be a useful addition as this could affect the genetic composition of established populations that would otherwise be genetically relatively stable. Lastly, running a larger number of simulations would improve the statistical power of the results.

More broadly speaking, many areas of biofilm literature require more research. Yet, these days we have the major advantage that experimental and computational studies can complement each other to clarify biofilm functioning. The main challenges today are, firstly, extending fundamental research, for which these individual-based models provide the opportunity to simulate long-term evolutionary processes. Apart from adhesion research, our understanding of topics – such as the interactions between biofilm members, spatial dynamics, and the evolution of resistance and persistence in the face of antibiotics – is developing. These insights can then be incorporated into strategic basic research. The second challenge is, namely, to develop new strategies to combat biofilm infections in a range of settings, such as health care and industry. Coupling back to this work, by studying biofilm adhesion in an eco-evolutionary context, we gain knowledge that may eventually lead to lowered health hazards and economic costs while tapping into the full potential of the beneficial application of biofilm systems (Philipp et al., 2023).

References

Achinas, S., Charalampogiannis, N., & Euverink, G. J. W. (2019). A brief recap of microbial adhesion and biofilms. *Applied Sciences*, *9*(14), 2801. https://doi.org/10.3390/app9142801

Allouche, O., Kalyuzhny, M., Moreno-Rueda, G., Pizarro, M., & Kadmon, R. (2012). Area-heterogeneity tradeoff and the diversity of ecological populations. *Proceedings of the National Academy of Sciences of the United States of America*, *109*(43), 17495–17500. https://doi.org/10.1073/pnas.1208652109

Alotaibi, G. F. (2021). Factors influencing bacterial biofilm formation and development. *American Journal of Biomedical Science & Research*, *12*(6), 617–626. https://doi.org/10.34297/ajbsr.2021.12.001820

Bazzaz, F., & Catovsky, S. (2001). Resource Partitioning. *Encyclopedia of Biodiversity (Second Edition)*, 429-437. https://doi.org/10.1016/B978-0-12-384719-5.00123-4

Berlanga, M., & Guerrero, R. (2016). Living together in biofilms: the microbial cell factory and its biotechnological implications. *Microbial Cell Factories*, *15*(1). https://doi.org/10.1186/s12934-016-0569-5

Bjedov, I., Tenaillon, O., Gérard, B., Souza, V., Denamur, E., Radman, M., Taddei, F., & Matic, I. (2003). Stress-induced mutagenesis in bacteria. *Science (New York, N.Y.)*, *300*(5624), 1404–1409. https://doi.org/10.1126/science.1082240

Brislawn, C. J., Graham, E. B., Dana, K., Ihardt, P., Fansler, S. J., Chrisler, W. B., Cliff, J. B., Stegen, J. C., Moran, J. J., & Bernstein, H. C. (2019). Forfeiting the priority effect: turnover defines biofilm population succession. *The ISME journal*, *13*(7), 1865–1877. https://doi.org/10.1038/s41396-019-0396-x

Brockhurst, M. A., Colegrave, N., Hodgson, D. J., & Buckling, A. (2007). Niche occupation limits adaptive radiation in experimental microcosms. *PloS one*, *2*(2), e193. https://doi.org/10.1371/journal.pone.0000193

Brockhurst, M. A., Hochberg, M. E., Bell, T., & Buckling, A. (2006). Character displacement promotes cooperation in bacterial biofilms. *Current biology: CB*, *16*(20), 2030–2034. https://doi.org/10.1016/j.cub.2006.08. 068

Bucci, V., Nadell, C. D., & Xavier, J. B. (2011). The evolution of bacteriocin production in bacterial biofilms. *The American naturalist*, *178*(6), E162–E173. https://doi.org/10.1086/662668

Burton, T., Ratikainen, I. I., & Einum, S. (2022). Environmental change and the rate of phenotypic plasticity. *Global Change Biology*, *28*(18), 5337–5345. https://doi.org/10.1111/gcb.16291

Callahan, B. J., Fukami, T., & Fisher, D. S. (2014). Rapid evolution of adaptive niche construction in experimental microbial populations. *Evolution; international journal of organic evolution*, *68*(11), 3307–3316. https://doi.org/10.1111/evo.12512

Cámara, M., Green, W., MacPhee, C. E., Rakowska, P. D., Raval, R., Richardson, M. C., Slater-Jefferies, J., Steventon, K., & Webb, J. S. (2022). Economic significance of biofilms: a multidisciplinary and cross-sectoral challenge. *NPJ biofilms and microbiomes*, *8*(1), 42. https://doi.org/10.1038/s41522-022-00306-y

Chappell, C. R., Dhami, M. K., Bitter, M. C., Czech, L., Herrera Paredes, S., Barrie, F. B., Calderón, Y., Eritano, K., Golden, L. A., Hekmat-Scafe, D., Hsu, V., Kieschnick, C., Malladi, S., Rush, N., & Fukami, T. (2022). Wide-ranging consequences of priority effects governed by an overarching factor. *eLife*, *11*, e79647. https://doi.org/10.7554/eLife.79647

Cheong, J. Z. A., Johnson, C. J., Wan, H., Liu, A., Kernien, J. F., Gibson, A. L. F., Nett, J. E., & Kalan, L. R. (2021). Priority effects dictate population structure and alter virulence of fungal-bacterial biofilms. *The ISME journal*, *15*(7), 2012–2027. https://doi.org/10.1038/s41396-021-00901-5

Christie, M. R., & McNickle, G. G. (2023). Negative frequency dependent selection unites ecology and evolution. *Ecology and Evolution*, *13*(7), e10327. https://doi.org/10.1002/ece3.10327

Coenye, T., Bové, M., & Bjarnsholt, T. (2022). Biofilm antimicrobial susceptibility through an experimental evolutionary lens. *NPJ biofilms and microbiomes*, *8*(1), 82. https://doi.org/10.1038/s41522-022-00346-4

Connell, J.H. and Slatyer, R.O. (1977). Mechanisms of Succession in Natural Populations and Their Role in Population Stability and Organization. *The American Naturalist*, *111*, 1119-1143. http://dx.doi.org/10.1086/283241

Costerton, J. W., Geesey, G. G., & Cheng, K. J. (1978). How bacteria stick. *Scientific American*, *238*(1), 86–95. https://doi.org/10.1038/scientificamerican0178-86

Costerton, J. W., Lewandowski, Z., Caldwell, D. E., Korber, D. R., & Lappin-Scott, H. M. (1995). Microbial biofilms. *Annual review of microbiology*, *49*, 711–745. https://doi.org/10.1146/annurev.mi.49.100195.003431

De Meester, L., Vanoverbeke, J., Kilsdonk, L. J., & Urban, M. C. (2016). Evolving Perspectives on Monopolization and Priority Effects. *Trends in ecology & evolution*, *31*(2), 136–146. https://doi.org/10.1016/j.tree.2015.12.009

de Souza Júnior, M. B. , Ferreira, F. F. , & de Oliveira, V. M. (2014). Effects of the spatial heterogeneity on the diversity of ecosystems with resource competition. *Physica A: Statistical Mechanics and Its Applications*, *393*, 312–319. 10.1016/j.physa.2013.08.045

DeAngelis, D. L., & Yurek, S. (2016). Spatially Explicit Modeling in Ecology: A review. *Ecosystems*, *20*(2), 284–300. https://doi.org/10.1007/s10021-016-0066-z

Debray, R., Herbert, R. A., Jaffe, A. L., Crits-Christoph, A., Power, M. E., & Koskella, B. (2021). Priority effects in microbiome assembly. *Nature Reviews Microbiology*, *20*(2), 109–121. https://doi.org/10.1038/s41579-021-00604-w

Diard, M., Garcia, V., Maier, L., Remus-Emsermann, M. N., Regoes, R. R., Ackermann, M., & Hardt, W. D. (2013). Stabilization of cooperative virulence by the expression of an avirulent phenotype. *Nature*, *494*(7437), 353–356. https://doi.org/10.1038/nature11913

Dmitrijs, F., Guo, J., Huang, Y., Liu, Y., Fang, X., Jiang, K., Zha, L., Cai, J., & Fu, X. (2022). Bacterial Succession in Microbial Biofilm as a Potential Indicator for Postmortem Submersion Interval Estimation. *Frontiers in Microbiology*, *13*, 951707–951707. https://doi.org/10.3389/fmicb.2022.951707

Donaldson-Matasci, M. C., Bergstrom, C. T., & Lachmann, M. (2013). When unreliable cues are good enough. *the American Naturalist*, *182*(3), 313–327. https://doi.org/10.1086/671161

Donlan, R. M., & Costerton, J. W. (2002). Biofilms: survival mechanisms of clinically relevant microorganisms. *Clinical microbiology reviews*, *15*(2), 167–193. https://doi.org/10.1128/CMR.15.2.167-193.2002

Drescher, K., Nadell, C. D., Stone, H. A., Wingreen, N. S., & Bassler, B. L. (2014). Solutions to the public goods dilemma in bacterial biofilms. *CB/Current Biology*, *24*(1), 50–55. https://doi.org/10.1016/j.cub.2013.10.030

Ebrahimi, A., Goyal, A., & Cordero, O. X. (2022). Particle foraging strategies promote microbial diversity in marine environments. *eLife*, *11*. https://doi.org/10.7554/elife.73948

Ellis, C. N., Traverse, C. C., Mayo-Smith, L., Buskirk, S. W., & Cooper, V. S. (2015). Character displacement and the evolution of niche complementarity in a model biofilm population. *Evolution; international journal of organic evolution*, *69*(2), 283–293. https://doi.org/10.1111/evo.12581

Evans, C. R., Kempes, C. P., Price-Whelan, A., & Dietrich, L. E. P. (2020). Metabolic Heterogeneity and Cross-Feeding in Bacterial Multicellular Systems. *Trends in microbiology*, *28*(9), 732–743. https://doi.org/10.1016/j.tim.2020.03.008

Feranchuk, S., Belkova, N., Potapova, U., Kuzmin, D., & Belikov, S. (2018). Evaluating the use of diversity indices to distinguish between microbial populations with different traits. *Research in Microbiology*, *169*(4–5), 254–261. https://doi.org/10.1016/j.resmic.2018.03.004

Flemming, H. C., & Wingender, J. (2010). The biofilm matrix. *Nature reviews. Microbiology*, *8*(9), 623–633. https://doi.org/10.1038/nrmicro2415

Flemming, H. C., Neu, T. R., & Wozniak, D. J. (2007). The EPS matrix: the "house of biofilm cells". *Journal of bacteriology*, *189*(22), 7945–7947. https://doi.org/10.1128/JB.00858-07

Flemming, H. C., Wingender, J., Szewzyk, U., Steinberg, P., Rice, S. A., & Kjelleberg, S. (2016). Biofilms: an emergent form of bacterial life. *Nature reviews. Microbiology*, *14*(9), 563–575. https://doi.org/10.1038/nrmicro.2016.94

Flynn, K. M., Dowell, G., Johnson, T. M., Koestler, B. J., Waters, C. M., & Cooper, V. S. (2016). Evolution of Ecological Diversity in Biofilms of Pseudomonas aeruginosa by Altered Cyclic Diguanylate Signaling. *Journal of bacteriology*, *198*(19), 2608–2618. https://doi.org/10.1128/JB.00048-16

Foster, K. R. (2004). Diminishing returns in social evolution: the not-so-tragic commons. *Journal of Evolutionary Biology*, *17*(5), 1058–1072. https://doi.org/10.1111/j.1420-9101.2004.00747.x

Fowler, S. J., Torresi, E., Dechesne, A., & Smets, B. F. (2023). Biofilm thickness controls the relative importance of stochastic and deterministic processes in microbial population assembly in moving bed biofilm reactors. *Interface focus*, *13*(2), 20220069. https://doi.org/10.1098/rsfs.2022.0069

Frank, S. A. (2011). Natural selection. II. Developmental variability and evolutionary rate*. *Journal of Evolutionary Biology*, *24*(11), 2310–2320. https://doi.org/10.1111/j.1420-9101.2011.02373.x

Fukami, T. (2015). Historical Contingency in Population Assembly: Integrating Niches, Species Pools, and Priority Effects. *Annual Review of Ecology, Evolution, and Systematics*, *46*(1), 1-23. https://doi.org/10.1146/annurev-ecolsys-110411-160340

Fukami, T., Beaumont, H. J., Zhang, X. X., & Rainey, P. B. (2007). Immigration history controls diversification in experimental adaptive radiation. *Nature*, *446*(7134), 436–439. https://doi.org/10.1038/nature05629

Galié, S., García-Gutiérrez, C., Miguélez, E. M., Villar, C. J., & Lombó, F. (2018). Biofilms in the Food Industry: Health Aspects and Control Methods. *Frontiers in microbiology*, *9*, 898. https://doi.org/10.3389/fmicb.2018.00898

Garrett, T. R., Bhakoo, M., & Zhang, Z. (2008). Bacterial adhesion and biofilms on surfaces. *Progress in Natural Science/Progress in Natural Science*, *18*(9), 1049–1056. https://doi.org/10.1016/j.pnsc.2008.04.001

Geesey G. G., Mutch R., Costerton J. W., Green R. B. (1978). Sessile bacteria: an important component of the microbial population in small mountain streams. *Limnology and Oceanography*, *23*(12), 14-23.

Gelderblom, H., Diddens, C., & Marin, A. (2022). Evaporation-driven liquid flow in sessile droplets. *Soft matter*, *18*(45), 8535–8553. https://doi.org/10.1039/d2sm00931e

Gjermansen, M., Ragas, P., Sternberg, C., Molin, S., & Tolker-Nielsen, T. (2005). Characterization of starvation-induced dispersion in *Pseudomonas putida* biofilms. *Environmental Microbiology*, *7*(6), 894–904. https://doi.org/10.1111/j.1462-2920.2005.00775.x

Gómez, P., & Buckling, A. (2013). Real-time microbial adaptive diversification in soil. *Ecology letters*, *16*(5), 650–655. https://doi.org/10.1111/ele.12093

Gómez, J.M., González-Megías, A., Armas, C., Narbona, E., Navarro, L. & Perfectti, F. (2023) T he role of phenotypic plasticity in shaping ecological networks. Ecology *Letters*, *26*(Suppl. 1), S47–S61. https://doi.org/10.1111/ele.14192

Greenbaum, G., Templeton, A. R., Zarmi, Y., & Bar-David, S. (2014). Allelic Richness following Population Founding Events – A Stochastic Modeling Framework Incorporating Gene Flow and Genetic Drift. *PloS One*, *9*(12), e115203. https://doi.org/10.1371/journal.pone.0115203

Hall-Stoodley, L., Costerton, J. W., & Stoodley, P. (2004). Bacterial biofilms: from the natural environment to infectious diseases. *Nature reviews. Microbiology*, *2*(2), 95–108. https://doi.org/10.1038/nrmicro821

Hamilton W. D. (1964). The genetical evolution of social behaviour. I. *Journal of theoretical biology*, *7*(1), 1–16. https://doi.org/10.1016/0022-5193(64)90038-4

Høiby, N., Ciofu, O., Johansen, H. K., Song, Z., Moser, C., Jensen, P. Ø., Molin, S., Givskov, M., Tolker-Nielsen, T., & Bjarnsholt, T. (2011). The clinical impact of bacterial biofilms. *International Journal of Oral Science/International Journal of Oral Science*, *3*(2), 55–65. https://doi.org/10.4248/ijos11026

Hunt, S. M., Werner, E. M., Huang, B., Hamilton, M. A., & Stewart, P. S. (2004). Hypothesis for the role of nutrient starvation in biofilm detachment. *Applied and environmental microbiology*, *70*(12), 7418–7425. https://doi.org/10.1128/AEM.70.12.7418-7425.2004

Idury, R. M., & Cardon, L. R. (1997). A simple method for automated allele binning in microsatellite markers. *Genome research*, *7*(11), 1104–1109. https://doi.org/10.1101/gr.7.11.1104

Jablonski D. (2017). Approaches to Macroevolution: 2. Sorting of Variation, Some Overarching Issues, and General Conclusions. *Evolutionary biology*, *44*(4), 451–475. https://doi.org/10.1007/s11692-017-9434-7

Jayathilake, P. G., Jana, S., Rushton, S., Swailes, D., Bridgens, B., Curtis, T., & Chen, J. (2017). Extracellular Polymeric Substance Production and Aggregated Bacteria Colonization Influence the Competition of Microbes in Biofilms. *Frontiers in microbiology*, *8*, 1865. https://doi.org/10.3389/fmicb.2017.01865

Jensen, P. Ø., Givskov, M., Bjarnsholt, T., & Moser, C. (2010). The immune system vs.Pseudomonas aeruginosabiofilms. *FEMS Immunology and Medical Microbiology*, *59*(3), 292–305. https://doi.org/10.1111/j.1574-695x.2010.00706.x

Jo, J., Price-Whelan, A., & Dietrich, L. E. P. (2022). Gradients and consequences of heterogeneity in biofilms. *Nature Reviews. Microbiology*, *20*(10), 593–607. https://doi.org/10.1038/s41579-022-00692-2

Joshi, R. V., Gunawan, C., & Mann, R. (2021). We Are One: Multispecies Metabolism of a Biofilm Consortium and Their Treatment Strategies. *Frontiers in microbiology*, *12*, 635432. https://doi.org/10.3389/fmicb.2021.635432

Kaplan, J. B. (2010). Biofilm dispersal: mechanisms, clinical implications, and potential therapeutic uses. *Journal of Dental Research*, *89*(3), 205–218. https://doi.org/10.1177/0022034509359403

Kim, W., Racimo, F., Schluter, J., Levy, S. B., & Foster, K. R. (2014). Importance of positioning for microbial evolution. *Proceedings of the National Academy of Sciences of the United States of America*, *111*(16), E1639–E1647. https://doi.org/10.1073/pnas.1323632111

Kimkes, T. E. P., & Heinemann, M. (2019). How bacteria recognise and respond to surface contact. *FEMS Microbiology Reviews*, *44*(1), 106–122. https://doi.org/10.1093/femsre/fuz029

Klotz, M., Kretschmer, M., Goetz, A., Ezendam, S., Lieleg, O., & Opitz, M. (2019). Importance of the biofilm matrix for the erosion stability of *Bacillus subtilis* NCIB 3610 biofilms. *RSC advances*, *9*(20), 11521–11529. https://doi.org/10.1039/c9ra01955c

Kostakioti, M., Hadjifrangiskou, M., & Hultgren, S. J. (2013). Bacterial biofilms: development, dispersal, and therapeutic strategies in the dawn of the postantibiotic era. *Cold Spring Harbor perspectives in medicine*, *3*(4), a010306. https://doi.org/10.1101/cshperspect.a010306

Koza, A., Moshynets, O., Otten, W., & Spiers, A. J. (2010). Environmental modification and niche construction: developing O2 gradients drive the evolution of the Wrinkly Spreader. *the ISME Journal*, *5*(4), 665–673. https://doi.org/10.1038/ismej.2010.156

Kümmerli, R., Santorelli, L. A., Granato, E. T., Dumas, Z., Dobay, A., Griffin, A. S., & West, S. A. (2015). Co-evolutionary dynamics between public good producers and cheats in the bacterium Pseudomonas aeruginosa. *Journal of evolutionary biology*, *28*(12), 2264–2274. https://doi.org/10.1111/jeb.12751

Lane N. 2015 The unseen world: reflections on Leeuwenhoek (1677) 'Concerning little animals'. *Philosophical Transactions Royal Society B*, *370*, 20140344. http://dx.doi.org/10.1098/rstb.2014.0344

Leberg, P. L. (2002). Estimating allelic richness: Effects of sample size and bottlenecks. *Molecular Ecology*, *11*(11), 2445–2449. https://doi.org/10.1046/j.1365-294x.2002.01612.x

Lee, K. W. K., Yam, J. K. H., Mukherjee, M., Periasamy, S., Steinberg, P. D., Kjelleberg, S., & Rice, S. A. (2015). Interspecific diversity reduces and functionally substitutes for intraspecific variation in biofilm populations. *the ISME Journal*, *10*(4), 846–857. https://doi.org/10.1038/ismej.2015.159

Lewandowski, Z. (2000). Structure and function of biofilms. In L. V. Evans (ed.), *Biofilms: recent advances in their study and control.* (pp. 1–17). Harwood Academic Publishers, Amsterdam, The Netherlands.

Li, L., Zhu, J., Yang, K., Xu, Z., Liu, Z., & Zhou, R. (2014). Changes in gene expression of *Actinobacillus pleuropneumoniae* in response to anaerobic stress reveal induction of central metabolism and biofilm formation. *Journal of Microbiology*, *52*(6), 473–481. https://doi.org/10.1007/s12275-014-3456-y

Longdon, B., Hadfield, J. D., Day, J. P., Smith, S. C., McGonigle, J. E., Cogni, R., Cao, C., & Jiggins, F. M. (2015). The causes and consequences of changes in virulence following pathogen host shifts. *PLoS pathogens*, *11*(3), e1004728. https://doi.org/10.1371/journal.ppat.1004728

MacArthur, R. H. (1958). Population ecology of some warblers of Northeastern coniferous forests. *Ecology*, *39*(4), 599–619.

Madsen, J. S., Røder, H. L., Russel, J., Sørensen, H., Burmølle, M., & Sørensen, S. J. (2016). Coexistence facilitates interspecific biofilm formation in complex microbial populations. *Environmental Microbiology*, *18*(8), 2565–2574. https://doi.org/10.1111/1462-2920.13335

Martin, M., Dragoš, A., Otto, S. B., Schäfer, D., Brix, S., Maróti, G., & Kovács, Á. T. (2020). Cheaters shape the evolution of phenotypic heterogeneity in Bacillus subtilis biofilms. *the ISME Journal*, *14*(9), 2302–2312. https://doi.org/10.1038/s41396-020-0685-4

Matz, C., & Kjelleberg, S. (2005). Off the hook--how bacteria survive protozoan grazing. *Trends in microbiology*, *13*(7), 302–307. https://doi.org/10.1016/j.tim.2005.05.009

McCarty, S., Woods, E., & Percival, S. L. (2014). Biofilms. In *Elsevier eBooks* (pp. 143–163). https://doi.org/10.1016/b978-0-12-397043-5.00009-8

McDougald, D., Rice, S. A., Barraud, N., Steinberg, P. D., & Kjelleberg, S. (2011). Should we stay or should we go: mechanisms and ecological consequences for biofilm dispersal. *Nature Reviews. Microbiology*, *10*(1), 39–50. https://doi.org/10.1038/nrmicro2695

McNally, L., & Brown, S. P. (2015). Building the microbiome in health and disease: niche construction and social conflict in bacteria. *Philosophical transactions of the Royal Society of London. Series B, Biological sciences*, *370*(1675), 20140298. https://doi.org/10.1098/rstb.2014.0298

Morawska, L. P., Hernandez-Valdes, J. A., & Kuipers, O. P. (2021). Diversity of bet-hedging strategies in microbial populations-Recent cases and insights. *WIREs mechanisms of disease*, *14*(2), e1544. https://doi.org/10.1002/wsbm.1544

Nadell, C. D., & Bassler, B. L. (2011). A fitness trade-off between local competition and dispersal in Vibrio cholerae biofilms. *Proceedings of the National Academy of Sciences of the United States of America*, *108*(34), 14181–14185. https://doi.org/10.1073/pnas.1111147108

Nadell, C. D., Drescher, K., & Foster, K. R. (2016). Spatial structure, cooperation and competition in biofilms. *Nature Reviews. Microbiology*, *14*(9), 589–600. https://doi.org/10.1038/nrmicro.2016.84

Nadell, C. D., Xavier, J. B., & Foster, K. R. (2009). The sociobiology of biofilms. *FEMS Microbiology Reviews*, *33*(1), 206–224. https://doi.org/10.1111/j.1574-6976.2008.00150.x

Nadell, C. D., Xavier, J. B., Levin, S. A., & Foster, K. R. (2008). The evolution of quorum sensing in bacterial biofilms. *PLoS Biology*, *6*(1), e14. https://doi.org/10.1371/journal.pbio.0060014

Nadezhdin, E., Murphy, N., Dalchau, N., Phillips, A., & Locke, J. C. W. (2020). Stochastic pulsing of gene expression enables the generation of spatial patterns in Bacillus subtilis biofilms. *Nature communications*, *11*(1), 950. https://doi.org/10.1038/s41467-020-14431-9

Naik, A. T., Kamensky, K. M., Hellum, A. M., & Moisander, P. H. (2023). Disturbance frequency directs microbial community succession in marine biofilms exposed to shear. *MSphere*, *8*(6). https://doi.org/10.1128/msphere.00248-23

Nijhout, H. F. (2013). *Stochastic gene expression: dominance, thresholds and boundaries*. Madame Curie Bioscience Database - NCBI Bookshelf. https://www.ncbi.nlm.nih.gov/books/NBK6366/

O'Brien, S., Luján, A. M., Paterson, S., Cant, M. A., & Buckling, A. (2017). Adaptation to public goods cheats in Pseudomonas aeruginosa. Proceedings - Royal Society. Biological Sciences/Proceedings - *Royal Society. Biological Sciences*, *284*(1859), 20171089. https://doi.org/10.1098/rspb.2017.1089

Odling-Smee, F. J., Laland, K. N., & Feldman, M. W. (2013). *Niche construction: the neglected process in evolution (MPB-37)*. Princeton university press.

Ophir, T., & Gutnick, D. L. (1994). A role for exopolysaccharides in the protection of microorganisms from desiccation. *Applied and environmental microbiology*, *60*(2), 740–745. https://doi.org/10.1128/aem.60.2.740-745.1994

Østman, B., Lin, R., & Adami, C. (2014). Trade-offs drive resource specialization and the gradual establishment of ecotypes. *BMC Evolutionary Biology*, *14*(1), 113. https://doi.org/10.1186/1471-2148-14-113

O'Toole, G., Kaplan, H. B., & Kolter, R. (2000). Biofilm formation as microbial development. *Annual review of microbiology*, *54*, 49–79. https://doi.org/10.1146/annurev.micro.54.1.49

Otto, S. P., & Day, T. (2007). A Biologist's guide to Mathematical Modeling in Ecology and Evolution. In *Princeton University Press eBooks*. https://doi.org/10.1515/9781400840915

Pahwa, R. (2023, August 7). *Chronic Inflammation*. StatPearls - NCBI Bookshelf. https://www.ncbi.nlm.nih.gov/books/NBK493173/#article-19530.s17

Patel, R. (2005). Biofilms and antimicrobial resistance. *Clinical Orthopaedics and Related Research*, *NA;*(437), 41–47. https://doi.org/10.1097/01.blo.0000175714.68624.74

Penesyan, A., Paulsen, I. T., Kjelleberg, S., & Gillings, M. R. (2021). Three faces of biofilms: a microbial lifestyle, a nascent multicellular organism, and an incubator for diversity. *Npj Biofilms and Microbiomes*, *7*(1). https://doi.org/10.1038/s41522-021-00251-2

Petrova, O. E., & Sauer, K. (2012). Sticky situations: key components that control bacterial surface attachment. *Journal of bacteriology*, *194*(10), 2413–2425. https://doi.org/10.1128/JB.00003-12

Philipp, L., Bühler, K., Ulber, R., & Gescher, J. (2023). Beneficial applications of biofilms. *Nature Reviews. Microbiology*. https://doi.org/10.1038/s41579-023-00985-0

Pickett, S. T. A. (1976). Succession: an Evolutionary Interpretation. *the American Naturalist*, *110*(971), 107–119. https://doi.org/10.1086/283051

Poltak, S., & Cooper, V. (2011). Ecological succession in long-term experimentally evolved biofilms produces synergistic populations. *ISME J, 5*, 369–378. https://doi.org/10.1038/ismej.2010.136

Preda, V. G., & Săndulescu, O. (2019). Communication is the key: biofilms, quorum sensing, formation and prevention. *Discoveries (Craiova, Romania)*, *7*(3), e100. https://doi.org/10.15190/d.2019.13

Provine, W. B. (2004). Ernst Mayr. *Genetics*, *167*(3), 1041–1046. https://doi.org/10.1093/genetics/167.3.1041

Rainey, P. B., & Travisano, M. (1998). Adaptive radiation in a heterogeneous environment. *Nature*, *394*(6688), 69–72. https://doi.org/10.1038/27900

Rankin, D. J., Bargum, K., & Kokko, H. (2007). The tragedy of the commons in evolutionary biology. *Trends in Ecology & Evolution*, *22*(12), 643–651. https://doi.org/10.1016/j.tree.2007.07.009

Ratnieks, F. L., & Helanterä, H. (2009). The evolution of extreme altruism and inequality in insect societies. *Philosophical transactions of the Royal Society of London. Series B, Biological sciences*, *364*(1533), 3169–3179. https://doi.org/10.1098/rstb.2009.0129

Reed, T. E., Waples, R. S., Schindler, D. E., Hard, J. J., & Kinnison, M. T. (2010). Phenotypic plasticity and population viability: the importance of environmental predictability. *Proceedings - Royal Society. Biological Sciences/Proceedings - Royal Society. Biological Sciences*, *277*(1699), 3391–3400. https://doi.org/10.1098/rspb.2010.0771

Ren, D., Madsen, J. S., Sørensen, S. J., & Burmølle, M. (2014). High prevalence of biofilm synergy among bacterial soil isolates in cocultures indicates bacterial interspecific cooperation. *the ISME Journal*, *9*(1), 81–89. https://doi.org/10.1038/ismej.2014.96

Ross-Gillespie, A., Gardner, A., Buckling, A., West, S. A., & Griffin, A. S. (2009). Density dependence and cooperation: theory and a test with bacteria. *Evolution; international journal of organic evolution*, *63*(9), 2315–2325. https://doi.org/10.1111/j.1558-5646.2009.00723.x

Rossy, T., Nadell, C. D., & Persat, A. (2019). Cellular advective-diffusion drives the emergence of bacterial surface colonization patterns and heterogeneity. *Nature communications*, *10*(1), 2471. https://doi.org/10.1038/s41467-019-10469-6

Roswell, M., Dushoff, J., & Winfree, R. (2021). A conceptual guide to measuring species diversity. *Oikos*, *130*(3), 321–338. https://doi.org/10.1111/oik.07202

Sadiq, F. A., De Reu, K., Burmølle, M., Maes, S., & Heyndrickx, M. (2023). Synergistic interactions in multispecies biofilm combinations of bacterial isolates recovered from diverse food processing industries. *Frontiers in microbiology*, *14*, 1159434. https://doi.org/10.3389/fmicb.2023.1159434

Sauer, K., Camper, A. K., Ehrlich, G. D., Costerton, J. W., & Davies, D. G. (2002). Pseudomonas aeruginosa displays multiple phenotypes during development as a biofilm. *Journal of bacteriology*, *184*(4), 1140–1154. https://doi.org/10.1128/jb.184.4.1140-1154.2002

Sauer, K., Stoodley, P., Goeres, D. M., Hall-Stoodley, L., Burmølle, M., Stewart, P. S., & Bjarnsholt, T. (2022). The biofilm life cycle: expanding the conceptual model of biofilm formation. *Nature Reviews Microbiology*, *20*(10), 608–620. https://doi.org/10.1038/s41579-022-00767-0

Schluter, J., Nadell, C. D., Bassler, B. L., & Foster, K. R. (2015). Adhesion as a weapon in microbial competition. *The ISME journal*, *9*(1), 139–149. https://doi.org/10.1038/ismej.2014.174

Smith, P., & Schuster, M. (2019). Public goods and cheating in microbes. *CB/Current Biology*, *29*(11), R442–R447. https://doi.org/10.1016/j.cub.2019.03.001

Spiers, A. J., Kahn, S. G., Bohannon, J., Travisano, M., & Rainey, P. B. (2002). Adaptive Divergence in Experimental Populations of *Pseudomonas fluorescens*. I. Genetic and Phenotypic Bases of Wrinkly Spreader Fitness. *Genetics*, *161*(1), 33–46. https://doi.org/10.1093/genetics/161.1.33

Steenackers, H. P., Parijs, I., Dubey, A., Foster, K. R., & Vanderleyden, J. (2016). Experimental evolution in biofilm populations. *FEMS microbiology reviews*, *40*(3), 373–397. https://doi.org/10.1093/femsre/fuw002

Stewart, P. S., & Franklin, M. J. (2008). Physiological heterogeneity in biofilms. *Nature reviews. Microbiology*, *6*(3), 199–210. https://doi.org/10.1038/nrmicro1838

Svoboda, P., Lindström, E. S., Ahmed Osman, O., & Langenheder, S. (2018). Dispersal timing determines the importance of priority effects in bacterial populations. *The ISME journal*, *12*(2), 644–646. https://doi.org/10.1038/ismej.2017.180

Tai, J. B., Mukherjee, S., Nero, T., Olson, R., Tithof, J., Nadell, C. D., & Yan, J. (2022). Social evolution of shared biofilm matrix components. *Proceedings of the National Academy of Sciences of the United States of America*, *119*(27), e2123469119. https://doi.org/10.1073/pnas.2123469119

Tan, C. H., Lee, K. W. K., Burmølle, M., Kjelleberg, S., & Rice, S. A. (2017). All together now: experimental multispecies biofilm model systems. *Environmental Microbiology*, *19*(1), 42–53. https://doi.org/10.1111/1462-2920.13594

Tilahun, A., Haddis, S., Teshale, A., & Hadush, T. (2016). Review on biofilm and microbial adhesion. *International Journal of Microbiological Research*, *7*(3), 63–73. https://doi.org/10.5829/idosi.ijmr.2016.63.73

Traverse, C. C., Mayo-Smith, L. M., Poltak, S. R., & Cooper, V. S. (2013). Tangled bank of experimentally evolved Burkholderia biofilms reflects selection during chronic infections. *Proceedings of the National Academy of Sciences of the United States of America*, *110*(3), E250–E259. https://doi.org/10.1073/pnas.1207025110

Turner, C. B., Buskirk, S. W., Harris, K. B., & Cooper, V. S. (2020). Negative frequency-dependent selection maintains coexisting genotypes during fluctuating selection. *Molecular ecology*, *29*(1), 138–148. https://doi.org/10.1111/mec.15307

Valentini, M., & Filloux, A. (2016). Biofilms and Cyclic di-GMP (c-di-GMP) Signaling: Lessons from Pseudomonas aeruginosa and Other Bacteria. *The Journal of biological chemistry*, *291*(24), 12547–12555. https://doi.org/10.1074/jbc.R115.711507

Vallespir Lowery, N., & Ursell, T. (2019). Structured environments fundamentally alter dynamics and stability of ecological populations. *Proceedings of the National Academy of Sciences of the United States of America*, *116*(2), 379–388. https://doi.org/10.1073/pnas.1811887116

van Gestel, J., & Nowak, M. A. (2016). Phenotypic Heterogeneity and the Evolution of Bacterial Life Cycles. *PLoS computational biology*, *12*(2), e1004764. https://doi.org/10.1371/journal.pcbi.1004764

Van Gestel, J., & Wagner, A. (2021). Cryptic surface-associated multicellularity emerges through cell adhesion and its regulation. *PLoS Biology*, *19*(5), e3001250. https://doi.org/10.1371/journal.pbio.3001250

Van Gestel, J., & Weissing, F. J. (2016). Regulatory mechanisms link phenotypic plasticity to evolvability. *Scientific Reports*, *6*(1). https://doi.org/10.1038/srep24524

Van Gestel, J., Nowak, M. A., & Tarnita, C. E. (2012). The evolution of Cell-to-Cell communication in a sporulating bacterium. *PLOS Computational Biology/PLoS Computational Biology*, *8*(12), e1002818. https://doi.org/10.1371/journal.pcbi.1002818

van Loosdrecht, M., Heijnen, J., Eberl, H. *et al.* (2002). Mathematical modelling of biofilm structures. *Antonie Van Leeuwenhoek, 81*, 245–256. https://doi.org/10.1023/A:1020527020464

Vasudevan, R. (2014). Biofilms: Microbial cities of scientific significance. *Journal of Microbiology & Experimentation*, *1*(3). https://doi.org/10.15406/jmen.2014.01.00014

Vestby, L. K., Grønseth, T., Simm, R., & Nesse, L. L. (2020). Bacterial Biofilm and its Role in the Pathogenesis of Disease. *Antibiotics (Basel, Switzerland)*, *9*(2), 59. https://doi.org/10.3390/antibiotics9020059

Wan, N., Wang, H., Ng, C. K., Mukherjee, M., Ren, D., Cao, B., & Tang, Y. J. (2018). Bacterial metabolism during biofilm growth investigated by 13C Tracing. *Frontiers in Microbiology*, *9*. https://doi.org/10.3389/fmicb.2018.02657

Watford, S., & Warrington, S. J. (2023, April 10). *Bacterial DNA mutations*. StatPearls - NCBI Bookshelf. https://www.ncbi.nlm.nih.gov/books/NBK459274/

Wilking, J. N., Zaburdaev, V., De Volder, M., Losick, R., Brenner, M. P., & Weitz, D. A. (2013). Liquid transport facilitated by channels in Bacillus subtilis biofilms. *Proceedings of the National Academy of Sciences of the United States of America*, *110*(3), 848–852. https://doi.org/10.1073/pnas.1216376110

Yan, J., Nadell, C. D., & Bassler, B. L. (2017). Environmental fluctuation governs selection for plasticity in biofilm production. *The ISME journal*, *11*(7), 1569–1577. https://doi.org/10.1038/ismej.2017.33

Zhang, W., Sileika, T. S., Chen, C., Liu, Y., Lee, J., & Packman, A. I. (2011). A novel planar flow cell for studies of biofilm heterogeneity and flow-biofilm interactions. *Biotechnology and bioengineering*, *108*(11), 2571–2582. https://doi.org/10.1002/bit.23234

Addendum

Formula A.1: Probability that a cell will divide with given adhesiveness and plasticity levels, with a standard growth rate of 0.1 and an energetic cost of 0.25 for adhesion and plasticity.

$$cell\_division_{probability} = growth_{rate} * (1 - cost_{adhesiveness} * genotype_{adhesiveness}) * (1 - cost_{plasticity\ wf1} * plasticity_{wf1}) * (1 - cost_{plasticity\ wf2} * plasticity_{wf2}) * (1 - cost_{plasticity\ wf2} * plasticity_{wf3})$$

Formula A.2: Definition of the plastic response, dependent on the cell's genotypic adhesiveness and plasticity, and the environmental variables. Bulk is a variable that becomes one if the cell lives in the bulk space and equals zero for biofilm cells. The phenotype is the sum of the genotypic baseline, a plastic response to the population stress in the bulk (for bulk = 1 and $plasticity_{wf1} \neq 0$), a plastic response to the surface coverage (for bulk = 0 and $plasticity_{wf2} \neq 0$), and a plastic response to the nutrient levels on the surface (for bulk = 0 and $plasticity_{wf3} \neq 0$). The resulting phenotype is a number between zero and one.

$$phenotype = genotype_{adhesiveness} + plasticity_{wf1} * bulk * \left(\frac{population\ size_{bulk} - carrying\ capacity)}{carrying\ capacity} + 1 - genotype_{adhesiveness} \right) + plasticity_{wf2} * (1 - bulk) * \left(\frac{carrying\ capacity - population\ size_{surface}}{carrying\ capacity} - genotype_{adhesiveness} \right) + plasticity_{wf3} * (1 - bulk) * (nutrient\ levels_{surface} - genotype_{adhesiveness})$$

Table A.1: Summary table of the beta regression model. It shows the effects of initial population size, carrying capacity, and surface growth on the Gini-Simpson diversity index. The significance codes are 0 '***' 0.001 '**' 0.01 '*' 0.05 '.' 0.1 ' ' 1.

	Estimate	**Std. Error**	**t value**	**Pr(>|t|)**	**Sig. Code**
(Intercept)	4.789e-01	7.932e-02	6.038	9.16e-08	***
Initial population size	4.949e-05	2.664e-05	1.858	0.0679	.
Carrying capacity	-8.657e-06	3.132e-05	-0.276	0.7832	
Surface growth	-3.708e-01	1.610e-01	-2.303	0.0246	*

Table A.2: Statistics table of the simulations with disruption probability 0 (top) and 0.01 (bottom). Means, lower and upper bounds of the 95% CI, and absolute counts are shown for bulk (left) and surface (right) populations at different nutrient levels.

	Bulk				**Surface**			
Nutrients (t0)	**Mean**	**[0.025**	**0.975]**	**Count**	**Mean**	**[0.025**	**0.975]**	**Count**
				Disruption probability 0				
0.25	0.03584183	0.03583042	0.03585323	9850	0.033336508	0.031817572	0.03485544	59
1	0.052370217	0.051280815	0.053459619	9758	0.129795026	0.122984914	0.13660514	1540
4	0.137542448	0.136631681	0.138453214	9883	0.270661579	0.250470537	0.29085262	242
				Disruption probability 0.01				
0.25	0.027417794	0.027056222	0.027779365	9802	0.034156225	0.022991341	0.045321109	40
1	0.013481576	0.013327743	0.013635410	9827	0.014938109	0.013283412	0.016592806	147
4	0.029875496	0.029835903	0.029915089	9830	0.029826	0.029826	0.029826	127

Table A.3: Test statistics comparing simulations with disruption probability 0 and 0.01. T-statistics and significance levels of the pairwise comparison are shown for bulk (left) and surface (right) populations at different nutrient levels.

	Bulk		**Surface**	
Nutrients(t0)	**t-stat**	**p-value**	**t-stat**	**p-value**
0.25	45.75121004	0	- 0.16961229	0.865668
1	69.51059545	0	10.20429309	9.16548 e-24
4	230.8532564	0	16.89009245	9.23739 e-48

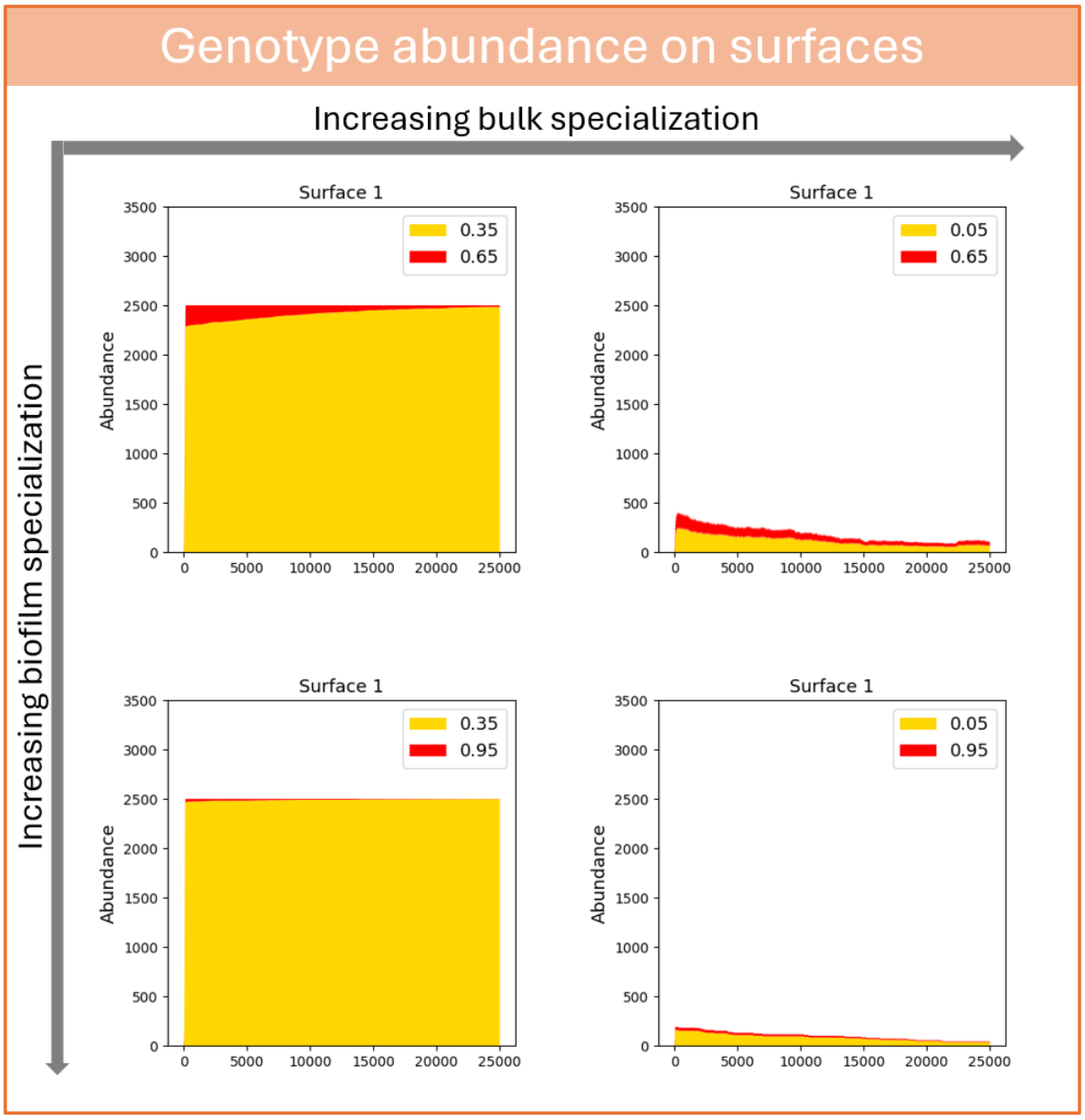

Figure A.1: Productivity of different combinations of generalists and specialists. Upper left: generalists (0.35 and 0.65) grow maximally in association. Lower left: as one ecotype becomes more specialized in surface growth, its relative abundance decreases; population productivity is still maximal. Upper right: when a generalist is combined with a bulk specialist, both are (approximately) equally fit, but population productivity declines. Lower right: high levels of specialization lead to reduced biofilm yields.

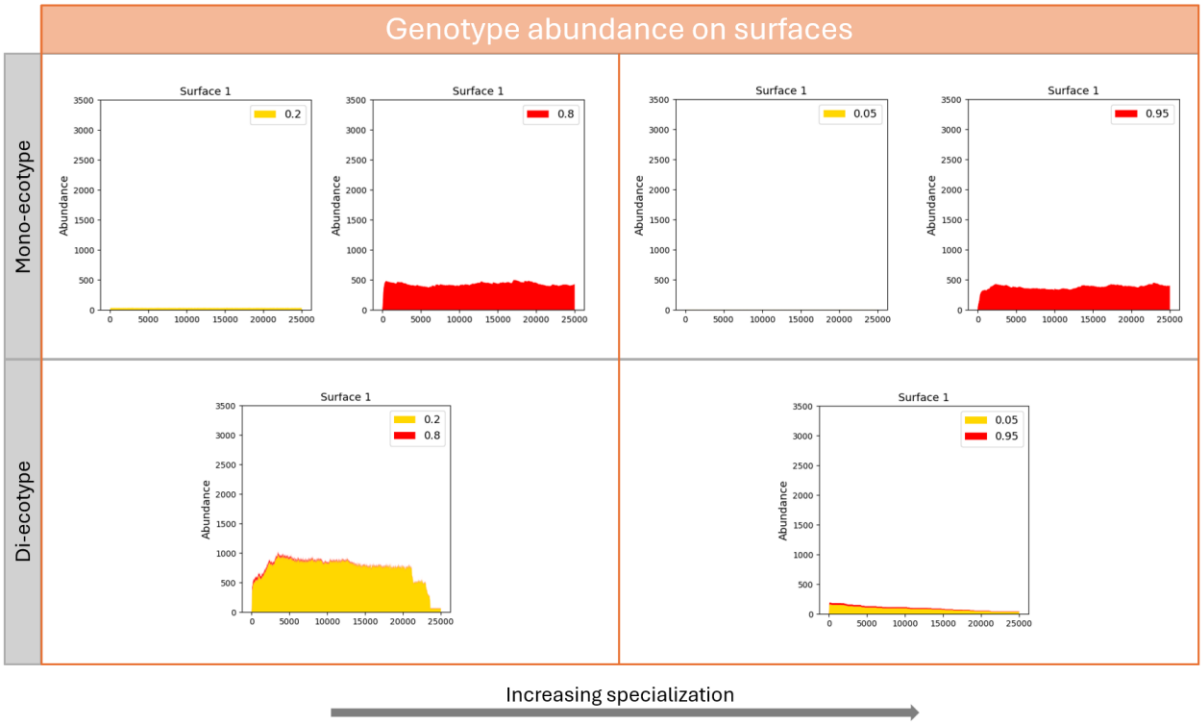

Figure A.2: Two examples of niche specialists forming a mono-ecotypic biofilm (top) or co-occur in a di-ecotypic biofilm (bottom). In both instances, biofilm specialists (red) reach higher population sizes when grown solitary, while bulk specialists (yellow) are facilitated by adhesive biofilm specialists, and therefore, they are more successful when grown in association. Left: Niche specialists (0.2 and 0.8) complement each other and reach higher total population sizes when grown together. Right: more highly specialized ecotypes (0.05 and 0.95) are less productive (cf. left) and grow antagonistically.

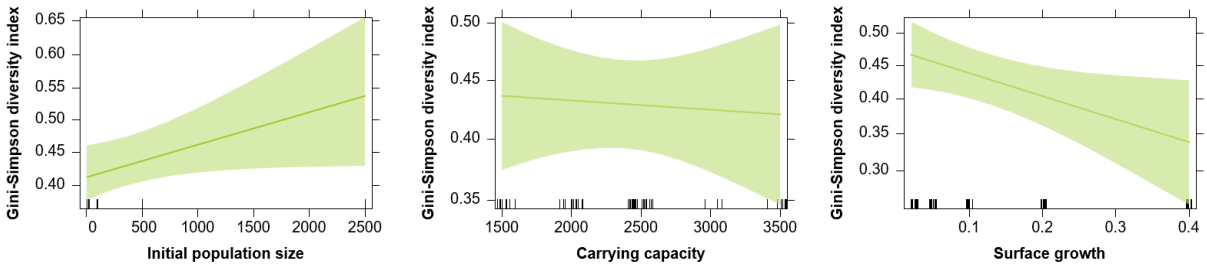

Figure A.3: Fit of the beta regression describing the Gini-Simpson diversity index as a function of initial population size (left), carrying capacity (middle), and surface growth (right). The green ribbon shows the 95% CI.

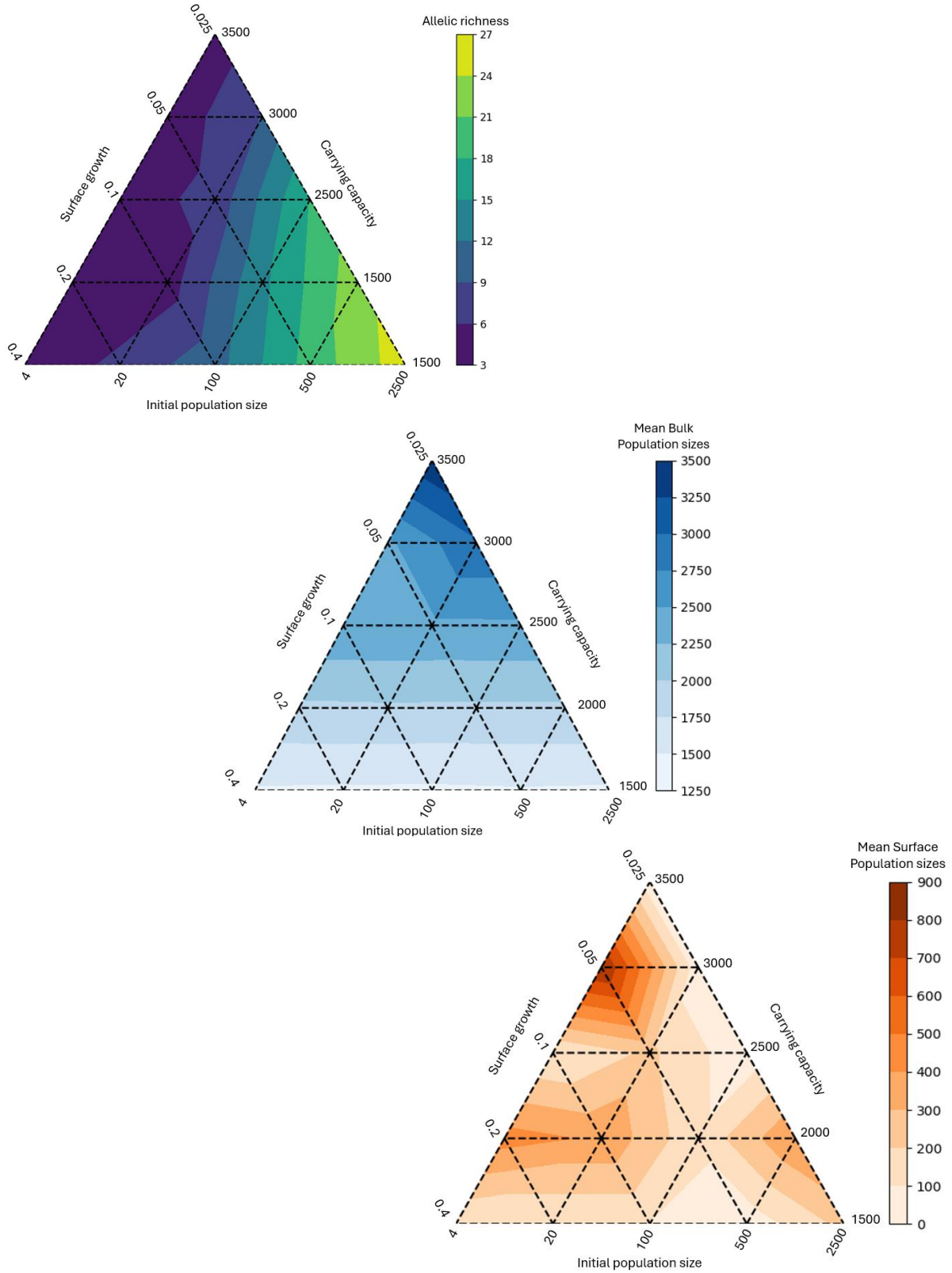

Figure A.4: Allelic richness and population sizes reached for different demographic scenarios. Allelic richness (top), bulk (middle), and surface (bottom) cell counts are shown in relation to initial bulk population size, bulk carrying capacity, and surface growth rate.

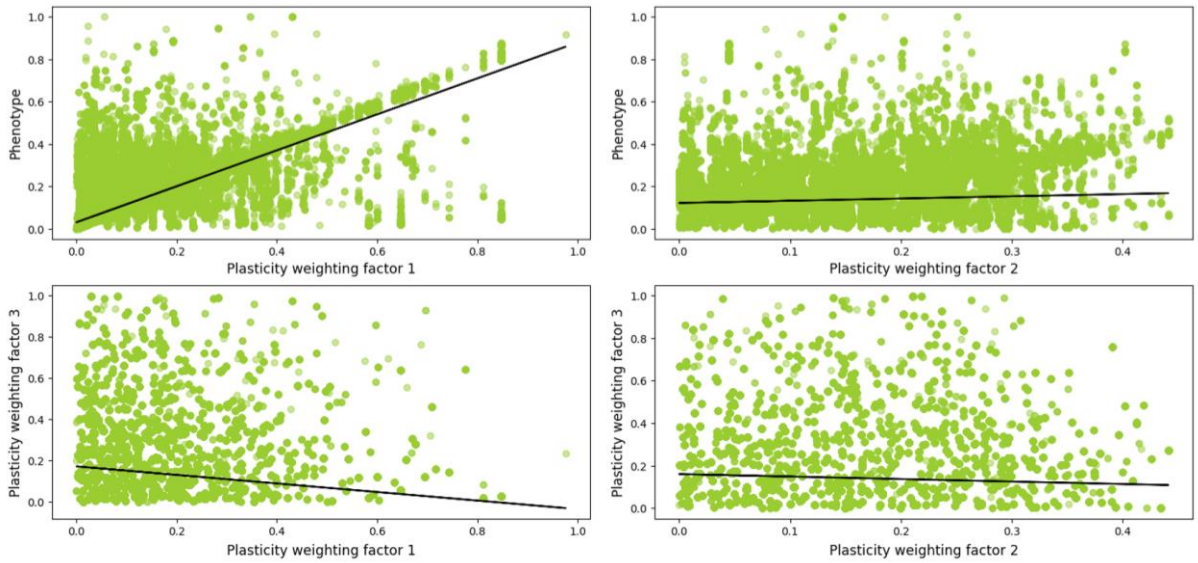

Figure A.5: Correlations between trait levels for the total populations. There is a positive association between the adhesiveness phenotype and the plastic response to population sizes in the bulk ($r^2 = 0.72$, $p < .001$) and – to a lesser extent – between the phenotype and surface coverage ($r^2 = 0.01$, $p < .001$). The correlation between the plastic response to nutrient levels and the two other plastic responses is slightly negative ($r^2 = 0.03$, $p < .001$; $r^2 = 0.01$, $p < .001$). All correlations between trait levels that were significantly different from zero are shown.

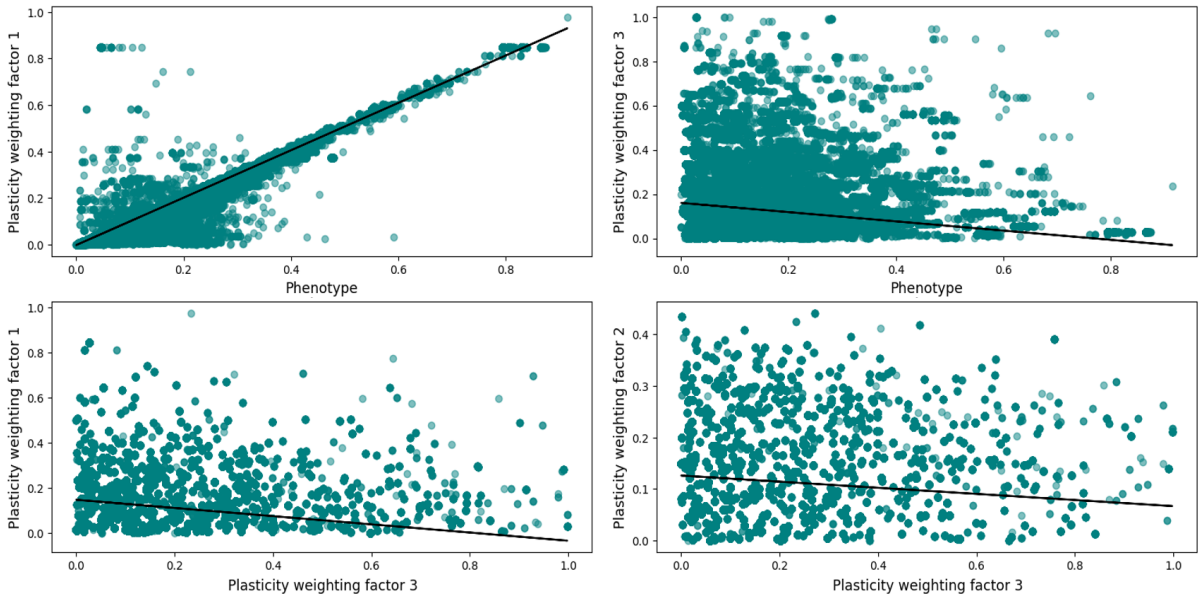

Figure A.6: Correlations between trait levels for the bulk populations. The phenotype is highly positively correlated to the plastic response to bulk population sizes ($r^2 = 0.99$, $p < .001$), while it is negatively correlated to the plasticity as a result of nutrient levels ($r^2 = 0.04$, $p < .001$). The plastic response to nutrient levels is negatively associated with the ability to react plastically to other environmental cues ($r^2 = 0.04$, $p < .001$; $r^2 = 0.01$, $p < .001$). All correlations between trait levels that were significantly different from zero are shown.

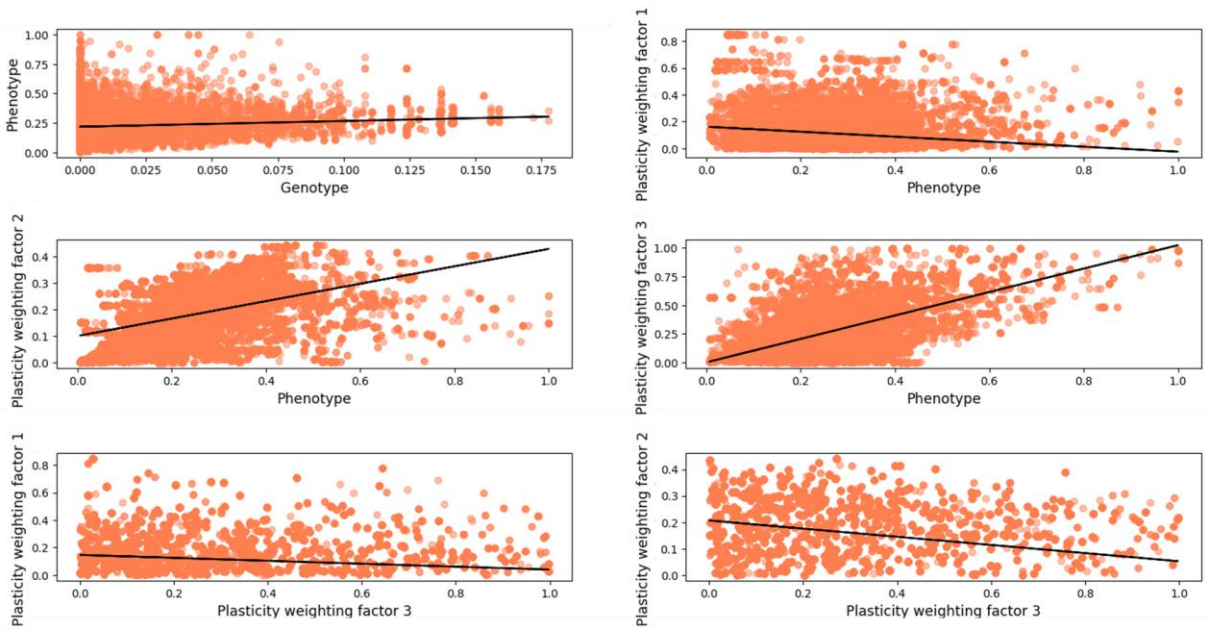

Figure A.7: Correlations between trait levels for surface populations. In contrast to the previous two, there is an effect of the adhesion genotype on the phenotype in surface populations yet be it only small ($r^2 = 0.01$, $p < .001$). Instead, most of the adhesiveness is a response to surface cues, i.e., surface coverage ($r^2 = 0.11$, $p < .001$) and nutrient levels ($r^2 = 0.31$, $p < .001$), whereas the other plastic response is negatively correlated to the phenotype ($r^2 = 0.02$, $p < .001$). The sensitivity to nutrient levels is negatively associated with sensitivity to other cues ($r^2 = 0.03$, $p < .001$; $r^2 = 0.08$, $p < .001$). All correlations between trait levels that were significantly different from zero are shown.

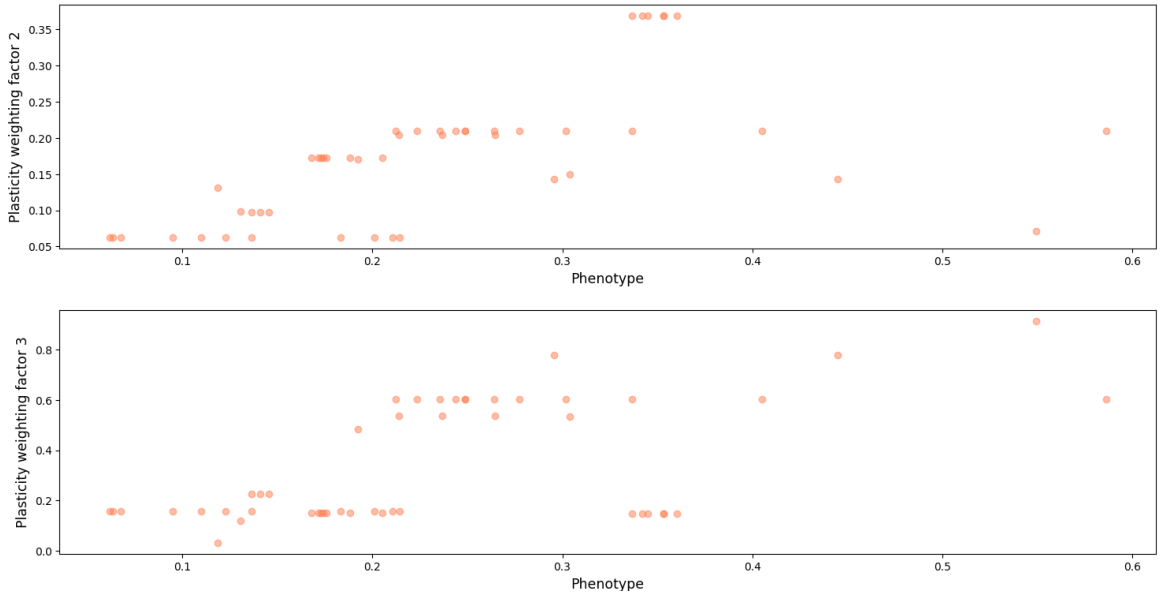

Figure A.8: Correlations between the traits levels for cells residing on surface 1 of simulation 1, specifically. This plot supports the hypothesis related to Figure 16, which illustrates the relationship between the adhesion phenotype and the ability to react plastically.

AFDELING
Straat nr bus 0000
3000 LEUVEN, BELGIË
tel. + 32 16 00 00 00
fax + 32 16 00 00 00
www.kuleuven.be